Thèse

présentée pour obtenir le grade de docteur

de l'École Nationale Supérieure des Télécommunications

Spécialité : Electronique et Communications

Christian Fischer

PATHWISE INTERFERENCE CANCELLATION FOR A DS-CDMA UPLINK

Soutenance: Vendredi 26 Avril 2002 devant le jury composé de

Pierre Comon (I3S, Sophia Antipolis)	Rapporteurs
Philippe Forster (Paris X, Paris)	
Joseph Boutros (ENST, Paris)	Examinateurs
Pierre Chevillat (IBM Research, Zurich)	
Jean-François Diouris (IRCCyN, Nantes)	
Dirk Slock (EURECOM, Sophia Antipolis)	Directeur de Thèse

École Nationale Supérieure des Télécommunications

Acknowledgment

Firstly, I would like to express my gratitude to my thesis supervisor, Prof. Dirk Slock. He has been a source of inspiration and help throughout the time spent at Eurecom and I am grateful for having had a chance to work with him. The time with him was a learning experience in the best sense of the term not many a supervisor could have provided.

I would also like to thank the Swiss National Science Foundation (SNF) in Bern and AKB, Aarau for their financial support that allowed me to pursue my doctoral studies.

Many thanks also to the Eurecom Institute and its staff for hosting me during my thesis time. In particular, I would like to thank my fellow doctoral students for the good time that we spent together, also off work.

A special thank you goes to my family in Switzerland for their support throughout my studies, first in Southampton and then in Sophia-Antipolis. In particular, I am greatly indepted to my parents whose open-mindedness and support have made it possible for me to go 'off the beaten student track' and leave for England for my undergraduate studies, with my doctoral studies in Sophia-Antipolis almost a consequence. Both professionally and personally, the experience of living and working nearly eight years abroad in two different countries has been very enriching. Without a doubt, this experience would not have been possible without the support of my parents, which is why I would like to dedicate this thesis to them.

Last but not least, I would like to thank all the members of my thesis committee for their efforts and constructive comments.

Christian Fischer, April 2002

Résumé en français

Cette thèse concerne l'application de l'annulation d'interférence pour une liaison montante DS-CDMA et en particulière, le traitement par trajet. Il y a essentiellement deux manières de traiter l'annulation d'interférence, soit après ou avant que les divers composants du signal (trajets multiple, antenne multiples) ont été recombinées. Ces méthodes sont connues comme étant respectivement "precombining interference cancellation" et "postcombining interference cancellation". On montrera que le signal reçu peut être factorisé en deux composantes, une composante se basant sur les paramètres variant lentement et l'autre sur les paramètres variant rapidement. Cette observation a motivé l'annulation d'interference par trajet qui nécessite uniquement la connaissance des paramètres variant lentement. L'avantage évident d'une telle approche sont les critères adaptatifs moins contraignant puisque la fréquence de mise à jour du filtre est proportionelle à la fréquence de changement des paramètres variant lentement. De plus, un tel filtre permet l'estimation améliorée des coefficient d'amplitude complexes variant rapidement puisque les composantes estimées du trajet contiennent le signal d'intérêt avec un SINR accru par rapport au signal reçu. On montrera plusieurs méthodes d'annulation d'interference qui sont indépendantes des paramètres variant rapidement tout en évitant l'annulation du signal qui survient dans l'approche d'origine par trajet. Des simulations prouverons les performances de cette approche. Alors que les approches linéaires d'annulation d'interference par trajet produisent de bonnes performances, leurs point faible est la complexité d'implementation. Nous considérons donc des solutions de rechange de complexité inférieures tout en conservant une approche par trajet. En particulier, nous étudions l'application des récepteur avec expansion polynômiale dans le contexte du traitement par trajet. L'expansion polynômiale est une technique d'approximation du récepteur LMMSE. La principale complexité résultant d'une approche LMMSE est dûe à l'inversion d'une matrice de corrélation. Le principe de

l'expansion polynômiale est de rapprocher l'approche LMMSE par une expansion polynômiale dans la matrice de corrélation. Nous montrerons que l'introduction du matrices diagonales pondérées peut sensiblement améliorer la performance des méthodes précédemment proposées même lors d'un déséquilibre de puissance entre usagers ou trajets. De plus, la complexité introduite est très raisonnable due au fait que chaque étage est de complexité double par rapport au RAKE. En outre, la méthode permet d'obtenir une amélioration du SINR par trajet, adoptée à la l'estimation des amplitudes complexes. Cependant, il est difficile d'obtenir une expression analytique de performance pour l'expansion polynômiale en utilisant des techniques standard puisque la performance est toujours une fonction de l'ensemble des séquences d'etalement utilisées. Par conséquent, nous recourons aux méthodes récemment présentées dans la recherche en télécommunications qui aborde le problème en laissant les dimensions du système tendre vers l'infini. L'analyse des grands systèmes permet d'obtenir une expression asymptotique du SINR du récepteur linéaire dûes aux propriétés de certaines classes de matrices aléatoires. Spécifiquement, la distribution des valeurs propres de telles matrices est connue pour converger asymptotiquement vers une distribution déterministe. Il est montre, que les coefficients pondérés introduit dans l'expansion polynômiale sont asymptotiquement indépendant de la puissance de l'utilisateur ou trajet et il n'y a donc aucun avantage à utiliser des coefficients pondérés par trajet dans les grands systèmes pour l'estimation des données. Cependant, pour les besoins d'estimation d'amplitude complexe, une approche par trajet démeure nécessaire.

Abstract

This thesis is concerned with the application of interference cancellation for a DS-CDMA uplink and particularly, pathwise processing. There are essentially two ways of handling the interference cancellation, either before or after the various signal components (multipath, multiple antennas) are recombined. These methods are know as precombining interference cancellation and postcombining interference cancellation, respectively. It will be shown that the received signal can be factored into two components, one of them relying only on slow parameters whereas the other depends on fast parameters also. This observation has motivated pathwise interference cancellation which only requires knowledge of the slow parameters. The obvious advantage of such an approach are the relaxed adaptive requirements since the rate of change in the filter is proportional to the rate of change of the slow parameters only. Furthermore, such a filter allows improved estimation of the fastly varying complex amplitude coefficients since the estimated path components contain the signal of interest with an increased SINR compared to the received signal. We will show several interference cancelling approaches which do not rely on the fastly varying parameter and avoid the signal cancellation which occurs in the original pathwise approach in the case of stationary or nearly stationary mobile stations due to the correlation between the complex amplitude coefficients. Simulations will be used to show the performance of the approaches.

While the pathwise linear interference cancellation approaches produce good performance, their major drawback is a high implementational complexity. We therefore consider lower complexity alternatives while maintaining the pathwise approach. In particular, we investigate the application of polynomial expansion receivers in a pathwise context. Polynomial expansion is an approximation technique to the LMMSE receiver. The main complexity arising from an LMMSE approach is an inverse in a correlation matrix, a fact that is well known. The principle of polynomial expansion is to approximate this inverse

by a low order, weighted polynomial in the correlation matrix to be inverted. We will show that the introduction of carefully chosen diagonal weighting matrices (instead of scalars, as previously proposed) can substantially improve the performance over previously proposed methods under power imbalances between users and/or paths. Furthermore, the complexity introduced is very reasonable due to the fact that every extra stage in the receiver is essentially twice the RAKE receiver. Also, the method allows to obtain SINR enhanced pathwise outputs, suitable for the estimation of the complex amplitudes.

However, it is difficult to get analytical performance expressions for polynomial expansion using standard techniques since the performance is always a function of the correlation properties of the set of spreading codes used. Hence, we resort to methods only recently introduced in the communications community which tackle this issue by letting the system dimensions grow to infinity. Such a large system analysis allows to get quantitative expressions for the asymptotic output SINR of linear receivers based on the properties of certain classes of large random matrices. Specifically, the empirical eigenvalue distributions of such matrices are known to converge to a deterministic distribution in the limit. It is shown, that the weighting coefficients introduced for polynomial expansion are asymptotically independent from the power of the user or even the paths and that there is therefore no benefit in using a weighting coefficient per path in large systems to obtain a data estimate. However, for the purpose of complex amplitude estimation, a pathwise approach remains necessary.

Contents

List of Figures

Chapter 1

Introduction

This chapter will essentially provide background information and in general introduce concepts important to the whole of this work. We will begin by providing some general background information on mobile communication systems and the development of multiuser detection. This is followed by a thesis outline and contributions made. Finally, in the last part of this chapter, a system model and the motivations on which it is based are developed.

1.1 Background

In this section we will give some general background information to mobile communication as it presents itself today. We will begin with an overview of recent mobile communication systems and in particular the move from second generation systems to third generation systems. This is followed by a brief introduction to multiuser detection in CDMA systems by considering the motivations for multiuser detection and the shift in attention of the research community towards suboptimal detector algorithms due to the complexity involved with the optimum receiver.

1.1.1 Mobile Communication Systems - from 2nd to 3rd Generation

In recent years, the number of users of mobile communications and mobile data services has grown at phenomenal rates across the world to such an extent that in many countries, mobile service subscribers now outnumber the fixed line installations. While in some countries, especially in Europe, a certain trend towards a market saturation in terms of mobile equipment can be stated, the current wireless communications technologies such as GSM (Global System for Mobile Communications) are nearing their capacity boundaries. The limited variety of services presently offered, essentially voice and transmission of data at limiting rates, in conjunction with the expected shift from voice to multimedia communications and the steadily growing number of users has led to the development of third generation standards such as UMTS (Universal Mobile Telecommunication Service) in Europe.

Mobile Communication networks and especially cellular networks are capacity limited mainly by interference. In second generation systems, multiple access was essentially achieved by maintaining orthogonality between users through the splitting of the time or frequency band available. In such TDMA (Time Division Multiple Access) and FDMA (Frequency Division Multiple Access) systems, the number of users that can be supported is determined by the number of slots that can be made available within the limits of the bandwidth available. In order to permit an area covering network like GSM, each cell in the network uses a frequency different from its neighbours and cells are grouped into so-called cell clusters of typically 3 to 7 frequencies, the so-called frequency reuse factor. The whole network area is then covered by such clusters and the interference arising is partly due to interference between cells using the same frequency but belonging to different clusters and partly due to co-channel interference between different users of the same cell. Second generation systems were not planned from the outset with a particular handle on interference and interference limitation is basically achieved by careful planning of the cell locations, that is, frequency planning [1–5].

Along with the increasing number of mobile users, the density of users per unit area also increases. Due to the limited number of slots and therefore users that a single basestation can cover, the area which a basestation can cover decreases, which in turn means that more basestations have to be employed. However, by placing the cells increasingly close to each other, the interference among cells increases and effective frequency planning can become very difficult.

When, as in the imminent third generation systems, a wide range of data rates will have to be covered, capacity shortages will be accentuated and flexibility problems will arise. Further, with the expected shift from voice to data transmission, it becomes desirable to operate at a lower probability of transmission errors.

In the third generation mobile system UMTS, the multiple access scheme of choice is DS-CDMA (Direct Sequence Code Division Multiple Access) which no longer provides an orthogonalisation between users in frequency or time but separates users by the signal subspace they occupy through their assigned user waveform. In other words, users transmit at the same time and on the same frequency [1, 6–9] . In CDMA, since no separation in time nor in frequency is required, all cells are transmitting on the same frequency, leading to a unity frequency reuse factor. Clearly, with the notions of cluster and frequency reuse absent, the planning of basestations is facilitated.

The main advantage of CDMA, however, is the bandwidth expansion, which allows a better resolution of the multiple paths and hence a better robustness against severe fading effects. Another advantage is its robustness against narrowband interference.

In DS-CDMA, the symbol sequence is up-sampled to the chip period and modulated by a much faster evolving spreading sequence. The ratio of the symbol period to the chip period is the spreading factor (or processing gain), which is also the factor by which the original bandwidth gets spread. Indeed, DS-CDMA is a special case of Spread Spectrum Multiple Access (SSMA) which was initially introduced by the military to make the transmitted signal look noise-like and hence not easily detectable and identifiable, as well as difficult to jam [10–12]. In fact, this view of the noise-like signal and therefore noise-like interference, is predominant in the case of Random sequence CDMA (RCDMA) in which an aperiodic (random) spreading sequence is used. The US DS-CDMA Mobile System IS-95 (Interim Standard-95) is of this type. In RCDMA, the interfering signals appear as stationary noise with colour depending on their propagation channel. If all the interferers are arbitrarily separated geographically so that their channels become independent, and if the (sufficiently large number of) interfering signals are received with about equal power, then the law of large numbers can be invoked which leads to the result that the correlation sequence of the sum of all the interfering signals corresponds to that of a white noise. In that case, and if the multipath propagation delay spread does not exceed a symbol period, then the optimal receiver (in the maximum-likelihood sequence estimation sense) is the so-called RAKE receiver, which is essentially a matched filter, matched to the cascade of spreading sequence and channel of which the non-zero impulse response coefficients are called ’fingers’, whence the term RAKE. Therefore, the IS-95 system employs strict power control to keep the interference down. This requires fast adaptive power equalisation at the receiver.

1.1.2 Multiuser Detection for DS-CDMA

Up to the 1980s, it was believed that the multiple access interference arising in DS-CDMA systems was accurately modelled by a white Gaussian random process and thus the RAKE is essentially optimal. In the 1980 though, it was realised that this assumption is inaccurate in many situations (for example in near-far situations) but more to the point, it was realised that the performance can be much improved over the RAKE by exploiting the specific and rich structure of the multiuser signal and unravelling the multiple user contributions [13]. This unravelling task is much simplified in the case of deterministic CDMA, in which case a periodic spreading sequence is used with period equal to the symbol period. Another problem with the RAKE receiver is that it only performs optimal MLSE (Maximum Likelihood Sequence Estimation) if the channel delay spread remains smaller than the symbol period. If higher data rates, and therefore symbol rates, are to be used as in UMTS, then this condition will no longer always hold. In fact, in that case the receiver will also have to perform equalisation.

In the wideband CDMA mode of UMTS, the standard proposes a combination of periodic and (pseudo-)random spreading codes. The signal is spread using a mobile-dependent periodic code. This code can be optionally scrambled by a random code. This option will be enabled if simple RAKE receivers will be used. However, this option will be disabled if more sophisticated receivers will be used. In that case, the spreading sequence is periodic and the multiuser signal is cyclostationary with period equal to the symbol period. Due to the spreading however, these cyclostationary signals exhibit significant excess bandwidth with respect to the symbol rate and hence frequency domain diversity. After oversampling with respect to the symbol rate, the stationary, vectorised received signal lives in a spreading sequence dependent subspace. This subspace allows for linear interference cancelling. A further dimensionality increase in signal vector space dimension and hence in diversity can be obtained by considering multi sensor processing.

1.1.3 From the Optimum MUD to suboptimal MUD approaches

As mentioned above, the effective application of the RAKE receiver requires strict and computationally expensive power control. The so-called near-far problem, essentially a power imbalance problem between users so that the signal of users geographically far from the basestations get swamped by much stronger users closer to the basestation, together with the computational complexity of precise power control, prompted the search for near-far resistant multiuser detectors [11, 14, 15]. About 1983, the optimum MLSE MUD was discovered [16–18] and presented for asynchronous multiple access Gaussian channels. The MLSE solution can be implemented as a Viterbi algorithm.

Unfortunately, the Viterbi algorithm for multiuser MLSE as applied to MUD suffers from a complexity which is exponential in the number of users. This prohibitive computational cost has therefore prompted much research into suboptimal detector methods to try and strike a balance between performance increase and complexity.

In multiuser detection there are essentially two categories of approaches: Linear and non-linear. The linear approaches, e.g. [19, 20], consist of replacing the RAKE receiver by another linear receiver which is derived using an interference zero-forcing constraint or a minimum mean square error criterion, see for example [21–23]. Zero-forcing approaches are often hybrids with MMSE techniques (ZF-MMSE) since the zero-forcing constraints typically do not result in a unique solution and hence MMSE techniques are applied on the remaining degrees of freedom to reduce mean square error (MSE). The non-linear approaches [24–26] are iterative, subtractive processes. By ordering the users according to their relative powers, a type of causality is introduced which can be mixed with the temporal aspect in the case of multipath propagation. There are three basic variants among non-linear interference cancelling schemes, namely, Serial Interference Cancellation (SIC) where only the causal interference can be cancelled, Parallel Interference Cancellation (PIC) which allows cancellation of all interference and, finally, Decision Feedback Interference cancellation (DF) where the non-causal interference is cancelled in a linear fashion whereas the causal interference is cancelled by subtraction. Often, SIC and PIC can be found combined in multistage Interference cancellers. It appears, that PIC is the most powerful of these approaches, in particular when used in conjunction with soft decisions. However, due to its iterative nature, the approach requires a reasonably good initialisation which has to be provided by another technique, typically linear. Also, because the PIC is a coherent detection method, precise knowledge of parameters is paramount. In this study, we hence present linear approaches to MUD detection with a special focus on parameters which could eventually be used to initialise data for one of several stages of a PIC or, indeed, be developed into a PIC-like structure. In particular, we focus on pathwise processing which is a particularly suitable approach for low complexity linear multiuser detection.

1.2 Thesis Outline

The remainder of this document is organised as follows: In the rest of this chapter, we will give a brief introduction to the mobile radio environment encountered in a CDMA system to motivate the resulting channel model which is used throughout the document. With the channel model defined, a general DS-CDMA system model will be introduced, followed by a short introduction to the conventional RAKE receiver. We then start in earnest in chapter 2 and introduce the ideas and motivations behind pathwise interference cancellation. We will present approaches which will avoid the signal cancellation trap of the original approach introduced by Latva-aho which occurs when the multiple paths of a user are strongly correlated. To finish the chapter off, we will show simulation results confirming the proposed approach. While the approaches in chapter 2 are performing well, their principle disadvantage is the complexity of a practical implementation and we therefore continue in chapter 3 by focusing on low complexity implementations of pathwise interference cancelling filters. Specifically, we will consider the application of polynomial expansion. Initially, we will introduce the principles of polynomial expansion and explain some previously proposed approaches that either work on the received signal directly, or on the RAKE outputs. We then carry on to propose the application of polynomial expansion receivers to the pathwise RAKE outputs and the implementation thereof, using diagonal weighting matrices with a scalar per signal component in contrast to previous approaches, which employ simply a scalar weighting coefficient. While the approaches in chapter 2 were focused on the possibility of obtaining filters independent from the fastly varying channel amplitudes, the focus in chapter 3 shifts towards the estimation of the channel amplitudes and the ability to obtain pathwise, SINR enhanced signals to be used for the estimation of the complex amplitudes. Using numerical simulation results, we then show that significant performance gains can be attained over the scalar approaches under power imbalances between users and multipath components. The nature of the polynomial expansion receivers introduced, makes it difficult to gain much analytical insight into their characteristics. In chapter 4, we are therefore introducing results from large system theory which allow to characterise polynomial expansion performance asymptotically. This is done by letting the system dimensions grow to infinity and making use of the fact that the empirical eigenvalue distributions of certain random matrices asymptotically converge to a deterministic limit. It is found that the introduction of a weighting coefficient per path is asymptotically not necessary, even under power imbalances between users and paths. The document is finished with a section of conclusions and remarks.

1.3 Preliminaries

In the next few pages, we will outline some concepts necessary to the work that follows in the next chapters. Notably, a short discussion of mobile channels and their effects is included to motivate the choice of channel model that is used throughout this work. With the channel model defined, we then establish a baseband signal model for a DS-CDMA system which provides us with the notation that is used in subsequent chapters.

1.3.1 Mobile Radio Channels

1.3.1.1 Propagation Environment

The type of propagation environment that is encountered in the transmission of information is clearly very important. In the context of mobile radio communications for the uplink, we are interested in the characterisation of the channel from the various mobile users to the basestation of interest.

The usual starting point to characterise any communication system is the additive white Gaussian noise (AWGN) channel with statistically independent Gaussian noise samples corrupting the data samples. The primary source of degradation in this case, is thermal noise generated in the receiver. In a practical system, it is always necessary to operate under certain bandwidth constraints which require the introduction of band-limiting filters. At the transmitter end, the band-limiting filter typically serves to constrain the signal to some bandwidth dictated by regulatory constraints whereas at the receiver end, the filter is typically matched to the signal bandwidth. Due to these band-limiting operations and the filter induced distortions, the channel introduces intersymbol interference (ISI). To reduce these effects and to allow reliable reception, it may be necessary to employ equalisation and/or special signal design techniques.

For a radio channel, in the absence of further specification on the propagation characteristics, one normally assumes a *free space* propagation model. In this idealised model, the region between the transmitter and the receiver is assumed to be free of obstacles that might absorb or reflect the transmitted signal. In this region, it is hence also assumed that the atmosphere is behaving like a perfectly uniform and non-absorbing medium and the attenuation of the radio frequency signal essentially follows the inverse-square law. The received power in terms of the power of the transmitted signal is therefore attenuated by a factor which is known as *path loss* or *free space loss* [7, 8]. However, for propagation encountered in mobile communications and most other practical radio applications, the free space propagation model is inadequate to describe a channel where propagation takes place close to the ground, in a non-ideal atmosphere. Furthermore, the transmitted signal will be reflected off obstacles and arrive over multiple reflective paths at the receiver. This effect, called *multipath propagation*, can give rise to changes in the signal's amplitude, phase, delay and angle of arrival. This is known as *multipath fading* where fading is the term employed to describe a signal's random fluctuations due to propagation over multiple paths.

1.3.1.2 Multipath Fading

To qualify multipath fading further, we have to distinguish between two types of fading that occur in mobile communications, *large scale fading* and *small scale fading*, respectively.

Large scale fading is the term employed to speak of fading due to motion over large areas and is affected by landmark sized objects such as hills, forests, built-up areas and the like. Sometimes, the term *shadowing* is also used which can be understood by considering the receiver as being in the 'shadow' of a prominent land feature. In essence, large scale fading estimates an average path loss as a function of the distance between transmitter and receiver. In mobile communications, the mean loss as a function of distance is proportional to the n-th power of the distance relative to some reference distance. The reference distance and n are factors that depend on the transmission frequency, antenna height, the type of channel (indoor, outdoor) etc. [1, 4, 27]. These results are based on comprehensive path loss measurements and their transformation in parametric formulas [28–31].

The significant effects that small changes (as small as half a wavelength) in spatial separation between the transmitter and the receiver can have are known as small scale fading. There are two effects of small scale fading, namely time-spreading (or signal dispersion) and time-variant behaviour of the channel. In a mobile setting, the channel will be time-variant due the the motion of the mobile user or also of motion in the propagation environment, for example nearby vehicles. Hence, the rate at which the propagation characteristics change characterises the rapidity of the fading. If there is a dominant propagation path, for example line-of-sight, the small scale fading envelope statistics are described by a Rician probability density function, termed *Rician fading*. In the absence of such a prominent propagation path, the Rayleigh probability density function approximates the small scale fading envelope, whence the name *Rayleigh fading* [1,7,8]. Typically, Rayleigh fading models are used more often as it is the pdf associated with a worst case of fading per mean received signal power due to the lack of a prominent (or specular) component in the signal. The composite fading experienced in the mobile system is a combination of small scale fading superimposed on large scale fading.

In 1963, Bello [32] introduced the notion of wide-sense stationary uncorrelated scattering (WSSUS) models which treat the signal variations arriving with different delays as uncorrelated. The model consists essentially of four functions which allow the characterisation of the channel. The *multipath-intensity profile*, $S(\tau)$ where τ is time delay, describes the average received power as a function of time delay. For wireless channels, the received signal normally consists of a discrete number of multipath components, also referred to as *fingers*. The delay difference between the first and the last path received, T_m, is called the *delay spread*. The relation of the delay spread to the symbol time,T_s, allows to define two categories of degradation: *frequency-selective fading* $(T_m > T_s)$ and *flat fading* $(T_m < T_s)$. In other words, in frequency-selective fading, the multipath components of a symbol extend beyond the duration of the symbol and therefore cause the same kind of ISI as a band-limiting filter. Equivalently, and hence the name, it means that not all spectral components of the signal are affected equally by the channel. Often though, ISI arising this way can be combated effectively since many paths can be resolved at the receiver and use of multipath diversity can be made. In the case of flat fading, all the paths are received during a symbol period and can therefore not be resolved in general. Indeed, a major benefit of DS-CDMA systems is the fact that the bandwidth expansion introduced with the spreading and the corresponding oversampling at the receiver (at chip rate or higher) with respect to the symbol period allows much better path resolution. That is to say, the path resolvability is determined by the sampling rate and not the symbol rate, in a DS-CDMA system.

An analogous description to signal dispersion can also be given in the frequency domain through the *spaced-frequency correlation* function, $|R(\Delta f)|$. It is simply the Fourier transform of $S(\tau)$. $R(\Delta f)$ provides a description of how correlated two signals, spaced Δf in frequency, are at the receiver. From the spaced-frequency correlation function, we obtain the *coherence bandwidth*, f_0, which gives the range of Δf for which two signals have a roughly equal gain and phase, i.e. a strong potential for amplitude correlation. Note that $f_0 \approx \frac{1}{T_m}$.

So far, the description in the last paragraphs has only described the behaviour of the signal from a signal-dispersion point of view but does not allow us to say anything about the time-varying nature of the channel due to movement of the mobile or movement of objects in the channel, i.e. about the rapidity of the fading. This is where the last two of the functions due to Bello come in. The function $R(\Delta t)$, called *spaced-time correlation* function, measures the correlation of two sinusoids sent over the channel, spaced Δt in time. Similarly to the coherence bandwidth, we get a *coherence time*, T_0, which tells us for how long the channel remains approximately stationary. In other words, it tells us whether the channel is *slowly fading* $(T_0 > T_s)$ or *fastly fading* $(T_0 < T_s)$. Assuming a mobile travelling at a constant velocity, it is clear that the coherence time can be measured both in time and distance.

Equivalently, the time-variation of the channel can be described, using the *Doppler power spectral density*, $S(v)$, where v is the Doppler frequency-shift. The Doppler power spectral density is just the Fourier transform of the spaced-time correlation function, $R(\Delta t)$. Knowledge of $S(v)$ provides us with the *Doppler spread*, f_d, which is the width of the Doppler power spectrum. The Doppler spread give us information on the fading rate of the channel. More precisely, it is a measure of the spectral spreading a signal undergoes when it passes through the channel as a function of the time variation of the channel. The Doppler spread is hence a function of the wavelength and relative velocity between transmitter and receiver. This point is maybe more easily understood thinking of the coherence time rather than the Doppler power spectral density.

1.3.1.3 Diversity in multipath fading channels

As mentioned earlier, an advantage of a wideband DS-CDMA system is the fact that it provides diversity at the receiver. Signals with a bandwidth, W, much greater than the coherence bandwidth, will be able to resolve paths up to a time resolution of about $1/W$. Therefore, there will be approximately $T_m W$ resolvable signal components. Using the approximate relation between the delay spread and the coherence bandwidth, i.e. $f_0 \approx \frac{1}{T_m}$, we can see that the the number of resolvable paths can be written approximately as W/f_0 and can therefore be viewed as a means of obtaining frequency diversity. Frequency diversity could of course also be provided by transmitting a signal over a number of different carriers, e.g. for a narrowband signal. Other types of diversity could be time diversity, space diversity through multiple antennas or also angle-of-arrival diversity and polarisation diversity.

1.3.1.4 Channel model

In DS-CDMA systems such as IS-95 or the CDMA standard as defined for UMTS, the signalling rate is sufficiently high to ensure that the symbol duration remains well below the coherence time and we can therefore consider the fading process slow. Hence, for our purpose, the channel can be considered constant over at least one symbol period. We will therefore consider a slowly fading, frequency-selective channel. Returning to the channel model, it is known that the wideband, frequency-selective CDMA channel can be modelled as a tapped delay line (e.g. [1, 7, 33]). The channel is modelled by M discrete multipath components having random, complex gains and different delays, so that the channel transfer function for users $k \in [1 \ldots K]$ at the basestation receiver is

$$\mathbf{h}_k(t) = \sum_{m=1}^{M} A_{k,m} \mathbf{h}_{k,m} \delta(t - \tau_{k,m}) \tag{1.3.1}$$

where $\mathbf{h}_k$ and $\mathbf{h}_{k,m} = \mathbf{h}(\theta_{k,m})$ are column vectors of dimension Q, the number of sensors employed at the basestation receiver. $\mathbf{h}_{k,m}$ defines the response of the antenna array and is a function of the Direction of Arrival (DoA), $\theta_{k,m}$, of the signal. For typical wireless channels, the different paths not only arrive at different delays, but also from different angles. In classical wireless channels, it is often assumed that the antennas are omni-directional and that the DoA of multipath signals is uniformly distributed at the receiver, in which case the multipath intensity profile is independent from the DoA. In the case of antennas with directivity and especially for applications in space-time processing it is generally necessary to establish a more exact relationship between the channel and the DoA. We will not pursue this any further here and refer the interested reader to [34]. For identifiability reasons, we chose the antenna response vector to have unity power, $\mathbf{h}_{k,m}^H \mathbf{h}_{k,m} = 1$. Further, the specular channel is characterised by $A_{k,m}$ and $\tau_{k,i}$, the complex amplitude and the path delays, respectively. These channel parameters can be divided into two classes: fast and slowly varying parameters. The slowly varying parameters are the delays, $\tau_{k,m}$, the DoA, $\theta_{k,m}$, and the short-term path power, $\mathrm{E}|A_{k,m}|^2$. Hence, the fast varying parameters are the complex phases and amplitudes, $A_{k,m}$. The direction of arrival, $\theta_{k,m}$, can be considered constant over an interval of several tens of wavelengths [35]. Since scatterers are usually assumed to be relatively far from the BS receiver with respect to the beamwidth(spatial distance over which a given path may be observed), the DoA does not appreciably change over this interval. This allows the assumption of plane wave transmission [36]. Along the same lines, we can argue that the delays as well as the path powers attributed to a given path will change slowly, being dependent on large scale effects. For various statistical and other models to model the parameters of the channel please refer to [1, 7, 27, 30, 33–35, 37–39].

1.3.2 Baseband system and signal model

1.3.2.1 Asynchronous received signal model

In a DS-CDMA system, the transmitted data bits from a particular user are multiplied by a spreading code which is of much larger bandwidth than the data signal. The chip-rate signal is then passed through a pulse-shaping filter to render it continuous-time before is is transmitted through the mobile channel. This is shown in Figure 1.1. In what follows, we are assuming the use of symbol-periodic spreading codes.

Denoting a given user by index $k \in \{1, \ldots, K\}$, the transmitted data bit $a_k[n]$ at time instant n with symbol period T is first upsampled to chip-rate (period $T_c = T/L$), with a slight misuse of the definition of upsampling in the sense that the symbol is repeated L times during the symbol period T, where L is the *spreading factor* or *processing gain*. The upsampled data signal is then multiplied with a periodic spreading code (periodic w.r.t. the symbol period), $s_k[l]$, and passed through a chip-pulse-shape filter to render the signal continuous in time.

The signal is then transmitted through the mobile channel, as defined in section 1.3.1.4. At the receiver, we receive the sum of all K users in the system through a Q element antenna array. The received signals are then low-pass filtered (anti-aliasing) and sampled at rate $1/T_s = LJ/T$, where J is the oversampling factor with respect to the chip rate. The continuous-time baseband signal for user k at the output of the transmitter in figure 1.1 can be written as

$$y'_k(t) = \sum_{n=-\infty}^{\infty} a_k[n]\psi_k(t - nT)$$

where $\psi_k(t)$ is sometimes called the signature waveform and defined by the convolution of

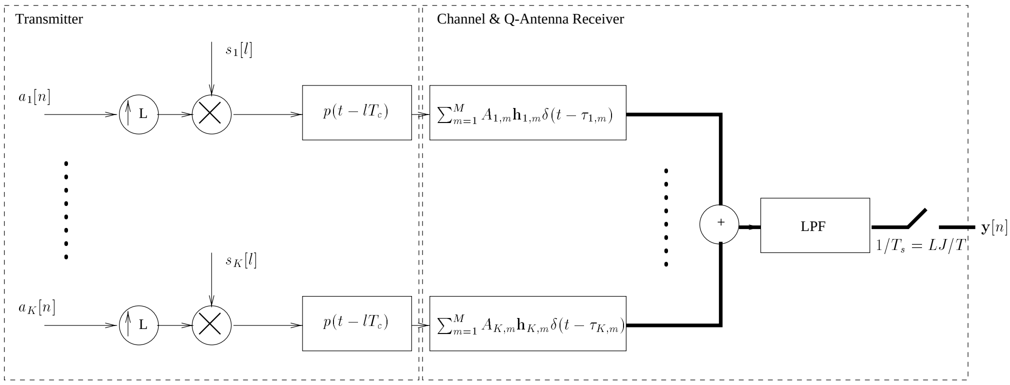

Figure 1.1: Received signal model from the transmitted data to the bandlimited and sampled signal at the receiver

the pulse-shape and the spreading code.

$$\psi_k(t) = \sum_{l=0}^{L-1} s_k[l]p(t - lT_c) \tag{1.3.2}$$

$p(t)$ is the pulse-shaping filter and assumed to be a perfect, normalised sinc and hence has strictly limited bandwidth. The received continuous-time signal before sampling can now be written as the convolution of $y'_k(t)$ with $\mathbf{h}_k(t)$ and summing over all K users gives the received signal:

$$\mathbf{y}(t) = \sum_{k=1}^{K}\left\{\sum_{n=-\infty}^{\infty}\sum_{m=1}^{M}(A_{k,m}a_k[n])\sum_{l=0}^{L-1} s_k[l]\mathbf{h}_{k,m}p(t-\tau_{k,m}-lT_c-nT)+\mathbf{n}(t)\right\} \tag{1.3.3}$$

$\mathbf{y}(t)$ and the Additive White Gaussian Noise (AWGN), $\mathbf{n}(t)$, are vector signals due to the use of multiple sensors and are of dimensions $Q \times 1$. $a_k[n]$, $p(t)$ are the transmitted symbols for user k and the pulse-shaping filter, respectively. At the receiver front-end, the received signal given in equation (1.3.3) is lowpass-filtered and sampled at $1/T_s$. After sampling, we obtain the discrete-time vector signal model

$$\mathbf{y}[n] = \sum_{i=-\infty}^{\infty} \mathbf{P}[n-i]\mathbf{SHAa}[i] + \mathbf{v}[n] \tag{1.3.4}$$

where $\mathbf{y}[n] = [\mathbf{y}[n+0\cdot T_c/J] \ldots \mathbf{y}[n+(LJ-1)\cdot T_c/J]^T$, i.e. we stacked all samples of the received signal for the duration of a symbol period T into $\mathbf{y}[n]$ $(LJQ \times 1)$. $\mathbf{v}[n]$ is the sampled and low-pass filtered contribution of the noise, $\mathbf{n}(t)$. $\mathbf{a}[n] = [a_1(n)a_2(n)\ldots a_K(n)]^T$ contains the data symbols of all K users for a given time instant n, ^{T} indicating the matrix transpose, $\mathbf{A} = diag\{\mathbf{A}_1, \ldots, \mathbf{A}_K\}$ is the block diagonal matrix containing the complex amplitude coefficients for each user such that $\mathbf{A}_k = [A_{k,1}\ldots A_{k,M}]^T$, $\mathbf{H} = diag\{\mathbf{H}_1, \ldots, \mathbf{H}_K\}$ contains the antenna array responses where $\mathbf{H}_k = diag\{\mathbf{h}_{k,1}, \ldots, \mathbf{h}_{k,M}\}$ where both $\mathbf{H}_k$ and $\mathbf{H}$ are block diagonal matrices and $\mathbf{h}_{k,m} = [h_{k,m,1}\ldots h_{k,m,Q}]^T$ is a column vector containing the antenna array response of every antenna. $\mathbf{S} = diag\{\mathbf{S}_1, \ldots, \mathbf{S}_K\}$ where $\mathbf{S}_k = [\mathbf{I}_M \otimes (\mathbf{s}_k \otimes \mathbf{I}_Q)]$; $\mathbf{s}_k = [s_k[0]\ldots s_k[L-1]]^T$ represents the spreading code vector, $\mathbf{I}_M$ and $\mathbf{I}_Q$ denote identity matrices of dimensions $M \times M$ and $Q \times Q$, respectively. $\otimes$ signifies the Kronecker product. Finally, we have the contribution of the pulse-shaping filter and the delays in $\mathbf{P}[n] = [\mathbf{p}_{n,1}\ldots\mathbf{p}_{n,K}]$; $\mathbf{p}_{n,k} = [\mathbf{p}_{n,k,1}\ldots\mathbf{p}_{n,k,M}]$ and

$$\mathbf{p}_{n,k,m} = \begin{bmatrix} \mathbf{p}_{n,k,m,0,0} & \cdots & \mathbf{p}_{n,k,m,0,L-1} \\ \vdots & \ddots & \vdots \\ \mathbf{p}_{n,k,m,LJ-1,0} & \cdots & \mathbf{p}_{n,k,m,LJ-1,L-1} \end{bmatrix}$$

where $\mathbf{p}_{n,k,m,r,l} = [p\,(nT + (r/J - l)T_c - \tau_{k,m}) \otimes \mathbf{I}_Q]$. The matrices for the model introduced above are therefore of the following dimensions: $\mathbf{P}[n](JLQ \times KLMQ)$, $\mathbf{S}(KMLQ \times KMQ)$, $\mathbf{H}(KMQ \times KM)$, $\mathbf{A}(KM \times K)$, $\mathbf{y}[n](JLQ \times 1)$.

1.3.2.2 Conventional DS-CDMA Receiver/RAKE receiver

The *conventional* or *single-user* receiver for DS-CDMA is the matched filter. It derives from analysing communication in an AWGN channel where the users are synchronous (i.e. no multipath and $\tau_k = 0$) and is a correlation demodulator. We consider the case of a single receiver antenna and sampling at the chip rate $(Q = 1,\ J = 1)$. We can write equation (1.3.4)

$$\begin{aligned} \mathbf{y}[n] &= \sum_{i=-\infty}^{\infty} \mathbf{E}[n-i]\mathbf{a}[n] + \mathbf{v}[n] \\ \mathbf{E}[n] &= \mathbf{P}[n]\mathbf{SHA} \end{aligned}$$

In this case, the matched filter is simply given by $\mathbf{E}^H[-n]$. Note that since

$$\begin{aligned}\mathbf{E}^H[n] &= \mathbf{A}^H\mathbf{H}^H\mathbf{S}^H\mathbf{P}^H[n] \\ &= \begin{bmatrix} \mathbf{A}_1^H\mathbf{H}_1^H\mathbf{S}_1^H\mathbf{p}_{n,1}^H \\ \vdots \\ \mathbf{A}_K^H\mathbf{H}_K^H\mathbf{S}_K^H\mathbf{p}_{n,K}^H \end{bmatrix} \end{aligned} \tag{1.3.5}$$

and also

$$\mathbf{A}_k^H\mathbf{H}_k^H\mathbf{S}_k^H\mathbf{p}_{n,k}^H = [A_{k,1}^* \dots A_{k,M}^*] \begin{bmatrix} \mathbf{h}_{k,1}^H(\mathbf{s}_k^H \otimes \mathbf{I}_Q)\mathbf{p}_{n,k,1}^H \\ \vdots \\ \mathbf{h}_{k,M}^H(\mathbf{s}_k^H \otimes \mathbf{I}_Q)\mathbf{p}_{n,k,M}^H \end{bmatrix} \tag{1.3.6}$$

the matched filter operation is in fact equivalent to a bank of filters matched to each user (from equation (1.3.5)) or also to every path of every user (from equation (1.3.6)). Indeed, in the case of multiple receive antennas, the matched filter could also be written as a filter bank operating on every path of every user at every antenna. Further note that the matched filtering consists of pulse-shape and spreading matched filtering, followed by antenna recombination which is followed by amplitude recombination. The fact that the operation can easily be viewed as matched-filtering of each of the 'fingers' and then collecting all the energy through recombining, the filter's action is vaguely analogous to an ordinary garden rake, hence also the name of RAKE receiver. Returning to 'joint' matched filtering (with $Q = 1$, $J = 1$), we can now write

$$\begin{aligned}\mathbf{E}^H[-n] * \mathbf{y}[n] &= \mathbf{A}^H\mathbf{H}^H\mathbf{S}^H \sum_{m=-\infty}^{\infty} \underbrace{\sum_{l=-\infty}^{\infty} \mathbf{P}^H[l]\mathbf{P}[l+(n-m)]}_{\Phi[n-m]} \mathbf{SHAa}[m] + \mathbf{E}^H[-n] * \mathbf{v}[n] \\ &= \mathbf{A}^H\mathbf{H}^H\mathbf{S}^H \sum_{m=-\infty}^{\infty} \Phi[n-m]\mathbf{SHAa}[m] + \mathbf{E}^H[-n] * \mathbf{v}[n] \end{aligned} \tag{1.3.7}$$

where $*$ denotes the convolution and we have substituted $l = -i$. $\Phi[n-m]$ can be seen to be the autocorrelation for the pulse-shaping matrix at shift $n-m$, this is were the name of correlation receiver comes from. From the expression for $\Phi[.]$, it can be seen that the Nyquist condition for zero ISI is

$$\Phi[n-m] = \begin{cases} \mathbf{1}^H\mathbf{1} & n-m=0 \\ \mathbf{0} & \text{otherwise} \end{cases} \tag{1.3.8}$$

where in the case of a single receiver antenna $\mathbf{1} = [\mathbf{I}_{\mathbf{L}\times\mathbf{L}} \ldots \mathbf{I}_{\mathbf{L}\times\mathbf{L}}]$, i.e. a block row vector of identity matrices. This condition is satisfied if $p(t)$ is a sinc Nyquist pulse and the users are at least chip-synchronous, sampled at chip-rate where the sampling is synchronous to the users. Assuming the Nyquist condition to be met, we obtain

$$\mathbf{E}^H[-n] * \mathbf{y}[n] \quad = \quad \mathbf{A}^H\mathbf{H}^H\mathbf{S}^H\mathbf{1}^H\mathbf{1}\mathbf{S}\mathbf{H}\mathbf{A}\mathbf{a}[n] + \mathbf{E}^H[-n] * \mathbf{v}[n] \tag{1.3.9}$$

Note that $\mathbf{1}\mathbf{S} = [\mathbf{s}_1 \ldots \mathbf{s}_K]$ (no multipath and one receiver antenna) and therefore, $\mathbf{S}^H\mathbf{1}^H\mathbf{1}\mathbf{S}$ is simply the spreading code correlation matrix. In the case where the users are synchronous and orthogonal spreading codes, $\mathbf{s}_k$, are used, we obtain $\mathbf{S}^H\mathbf{1}^H\mathbf{1}\mathbf{S} = \mathbf{I}$ and

$$\begin{aligned}\mathbf{E}^H[-n] * \mathbf{y}[n] &= \mathbf{A}^H\mathbf{H}^H\mathbf{H}\mathbf{A}a[n] + \mathbf{E}^H[-n] * \mathbf{v}[n] \\ &= \begin{bmatrix} |A_1|^2|h_1|^2 a_1[n] \\ \vdots \\ |A_K|^2|h_K|^2 a_K[n] \end{bmatrix} + \mathbf{E}^H[-n] * \mathbf{v}[n]\end{aligned} \tag{1.3.10}$$

Under the assumption of synchronous users with orthogonal codes in AWGN, this result is the classical matched filter which maximises the output SINR (e.g. [7]). Therefore, the conventional receiver manages under these ideal conditions to cancel any interference between users due to the orthogonality of the spreading codes. However, any deviation from such an idealised scenario such as non-ideal Nyquist pulse-shapes, timing offsets at the receiver, asynchronism between users or multipath propagation will destroy the orthogonality of the users and therefore interference can no longer be nulled out and the receiver will suffer from a non-reducible error floor even under zero noise conditions. In other words, the receiver is interference limited.

Chapter 2

Pathwise Interference Cancellation

2.1 Introduction

In linear multiuser detection approaches, there are two different ways of handling multipath channels. The Interference Cancellation (IC) can either take place prior or after the various multipath components are recombined. These two methods are known as *precombining interference cancellation* and the more common *postcombining interference cancellation*, respectively, as defined in [40–44]. The received signal can be factored into two components, one of them relying only on slow parameters as defined in section 1.3.1.4, the other component relying on fast parameters, namely, the product of the data symbols with the complex path amplitudes, $A_{k,m}a_k[n]$. This observation motivates *pathwise interference cancellation* (PWIC) which only requires the knowledge of the slowly varying parameters as opposed to the more common *postcombining* approach which requires complete knowledge of the channel. Hence, in a pathwise scenario, the interference cancellation typically takes place between individual multipath components before they are spatio-temporally recombined. The obvious advantage of an interference cancelling filter that relies only on slow parameters, $\tau_{k,m}$ and $\mathbf{h}_{k,m}$ as a function of the DoA, $\theta_{k,m}$, is that the adaptation requirements of the filter will be based on the rate of change of the slow parameters also, which are easier to estimate as well as to relax the update rate of the adaptive interference cancelling filter, thereby reducing the complexity of the filter. Furthermore, a pathwise filtering approach allows improved channel parameter estimation since the estimated path components contain the signal of interest with an increased SINR compared to the received signal.

2.1.1 Extension to the signal model

From equation (1.3.4) we know that the received discrete time signal at the receiver is given by

$$\mathbf{y}[n] = \sum_{i=-\infty}^{\infty} \mathbf{P}[n-i]\mathbf{SHAa}[i] + \mathbf{v}[n] \tag{2.1.1}$$

Due to the delay spread of the multipath channel, $\mathbf{h}_k(t)$, the transmitted symbols are spread out in time over the duration of possibly several symbol periods. Assuming that the maximum delay spread, τ_{max}, experienced in the channel, $\mathbf{h}_k(t)$, is known and given the asynchronism between transmitter and receiver, a processing window of length $b = \lceil(\tau_{max} + 2uT)/T\rceil + 1$ symbol periods for the receiving filter will guarantee to capture the entire contribution of a certain data symbol, $a_k[n]$. It is therefore often advantageous to use samples from the received signal over the duration of several symbol periods rather than just one, thereby also increasing the available data for interference cancellation. Hence, in what follows, we consider a *multi-shot* detector. For notational ease, let us rewrite equation (2.1.1) as follows:

$$\mathbf{y}[n] = \sum_{i=-\infty}^{\infty} \tilde{\mathbf{P}}[i]\tilde{\mathbf{S}}\tilde{\mathbf{H}}\tilde{\mathbf{A}}\mathbf{a}[n-i] + \mathbf{v}[n] \tag{2.1.2}$$

where simply we let $\mathbf{P}[n] \rightarrow \tilde{\mathbf{P}}[n]$, $\mathbf{S} \rightarrow \tilde{\mathbf{S}}$ etc. In order to consider the multi-shot detector, let us stack N vectors $\mathbf{y}[n]$ into a vector $\mathbf{Y}[n]$ which represents the received signal samples over a duration of NT, such that

$$\mathbf{Y}[n] = \begin{bmatrix} \mathbf{y}[n] \\ \vdots \\ \mathbf{y}[n-N+1] \end{bmatrix}$$

$$\mathbf{Y}[n] = \mathbf{PSHAa}_n + \mathbf{V}[n] \tag{2.1.3}$$

where $\mathbf{a}_n = \left[\mathbf{a}[n]^T \ldots \mathbf{a}[n-N-b+2]^T\right]^T$, $\mathbf{A} = \mathbf{I}_{N+b-1} \otimes \tilde{\mathbf{A}}, \mathbf{H} = \mathbf{I}_{N+b-1} \otimes \tilde{\mathbf{H}}, \mathbf{S} = \mathbf{I}_{N+b-1} \otimes \tilde{\mathbf{S}}$ and $\tilde{\mathbf{P}}$ is a banded block Toeplitz matrix of dimensions $NLPQ \times KMQL(N+$

$b-1)$, as shown in (2.1.4). $\mathbf{V}[n]$ are the stacked noise samples.

$$\mathbf{P} = \begin{bmatrix} \tilde{\mathbf{P}}[-u] & \mathbf{0} & \mathbf{0} \\ \tilde{\mathbf{P}}[-u+1] & \ddots & \mathbf{0} \\ \vdots & \ddots & \tilde{\mathbf{P}}[-u] \\ \tilde{\mathbf{P}}[u-1] & \ddots & \tilde{\mathbf{P}}[-u+1] \\ \tilde{\mathbf{P}}[u] & \ddots & \ddots \\ \mathbf{0} & \ddots & \tilde{\mathbf{P}}[u-1] \\ \mathbf{0} & \mathbf{0} & \tilde{\mathbf{P}}[u] \end{bmatrix} \tag{2.1.4}$$

In addition, to allow the structure of the received signal to be more lucid, we can rewrite equation (2.1.3) in terms of user k's desired symbol's contribution and interference terms, in particular, ISI and MAI. This is given in equation (2.1.5),

$$\begin{aligned} \mathbf{Y}[n] &= \underbrace{\mathbf{PSHA}}_{\mathbf{E}}\mathbf{a}_n + \mathbf{V}[n] \\ &= \mathbf{E}\mathbf{a}_n + \mathbf{V}[n] \\ &= [\mathbf{E}_{1,n} \cdots \mathbf{E}_{K,n}\mathbf{E}_{1,n-1} \cdots \mathbf{E}_{K,n-N-b+2}]\,\mathbf{a}_n + \mathbf{V}[n] \\ &= \mathbf{E}_k a_k[n-d] + \overline{\mathbf{E}}_k\overline{\mathbf{a}}_{k,n} + \sum_{i=1;i\neq k}^{K} \overline{\overline{\mathbf{E}}}_i\mathbf{a}_{i,n} + \mathbf{V}[n] \\ &= \underline{\underline{\mathbf{E}}}_k\mathbf{H}_k\mathbf{A}_k a_k[n-d] + \underbrace{\underbrace{\overline{\mathbf{E}}_k\overline{\mathbf{a}}_{k,n}}_{ISI} + \underbrace{\sum_{i=1;i\neq k}^{K} \overline{\overline{\mathbf{E}}}_i\mathbf{a}_{i,n}}_{MAI} + \mathbf{V}[n]}_{\nu[n]} \end{aligned} \tag{2.1.5}$$

where

$$
\begin{aligned}
\overline{\mathbf{a}}_{k,n} &= [a_k[n]\cdots a_k[r]\cdots a_k[n-N-b+2]]\,,\, r\neq n-d \\
\mathbf{a}_{i,n} &= [a_i[n]\cdots a_i[n-N-b+2]] \\
\mathbf{E}_{k,n-d} &\triangleq \mathbf{E}_k \text{for user of interest at delay of interest only} \\
\overline{\overline{\mathbf{E}}}_i &= [\mathbf{E}_{i,n}\cdots \mathbf{E}_{i,n-N-b+2}] \\
\overline{\mathbf{E}}_k &= [\mathbf{E}_{k,n}\cdots \mathbf{E}_{k,r}\cdots \mathbf{E}_{k,n-N-b+2}]\,,\, r\neq n-d \\
\underline{\underline{\mathbf{E}}}_k \mathbf{H}_k \mathbf{A}_k &= \sum_{m=1}^{M} \underline{\mathbf{E}}_{k,m}\mathbf{h}_{k,m}A_{k,m} = \sum_{m=1}^{M} \mathbf{E}_{k,m}A_{k,m} = \underline{\mathbf{E}}_k \mathbf{A}_k = \mathbf{E}_k \\
\underline{\mathbf{E}}_{k,m} &= \mathbf{p}'_{k,m}\mathbf{s}'_k;\ \mathbf{p}'_{k,m} = [\mathbf{0}_d\ \mathbf{p}_{-u,k,m}\cdots \mathbf{p}_{u,k,m}\ \mathbf{0}_{N-d-2u-1}]^T \\
\mathbf{s}'_k &= \mathbf{s}_k \otimes \mathbf{I}_Q;\ \mathbf{0}_z = \mathbf{0}_{(zJLQ\times LQ)}
\end{aligned}
\tag{2.1.6}
$$

In this notation, the individual columns of the matrix product $\mathbf{PSHA}$ are denoted by $\mathbf{E}_{k,r}$ and hence represent the contribution of a data symbol $a_k[r]$ in the received signal vector, $\mathbf{Y}[n]$. Therefore, the ISI term consists of the columns and data bits in $\mathbf{PSHA}$ corresponding to the user of interest's data symbols in the past and in the future w.r.t. the time instant $n-d$ which defines the data symbol of interest at a given moment. Similarly, the MAI term is given by the sum of the contributions of all users other than the one of interest in $\mathbf{Y}[n]$.

From equation (2.1.3), it can now clearly be seen that the signal can be divided into a fastly varying component and a slowly varying component.Explicitly, the product $\mathbf{PSH}$ containing the pulse-shaping as a function of the delays, $\tau_{k,m}$, the spreading codes matrix , $\mathbf{S}$, and the antenna array response matrix , $\mathbf{H}$, are dependent only on slow channel parameters, whereas the amplitude data product matrix, $\mathbf{A}\mathbf{a}_n$, is fastly varying due to its dependence on the complex amplitudes. This observation has led to the idea of *precombining interference cancellation*.

2.2 Precombining LMMSE PWIC

The original *precombining interference cancellation* approach was proposed by Latva-aho [40], the motivation being an adaptive filter implementation of an interference cancelling scheme that relies only on slowly varying parameters of the channel as well as the estimation of the channel coefficients. Namely, the fast varying parameters, $A_{k,m}$, can be estimated using scarce training data and are not required for the IC-filter design. The slow parameters can be estimated over a longer duration. This allows to find filters for each path m of a user k by employing filters $\mathbf{F}_{k,m}$ to each path and to cancel both Inter user Interference (IUI) as well as Inter symbol Interference (ISI), caused by the multipath propagation channels. The filter coefficients can typically be derived using a Linearly Constrained Minimum Variance (LCMV) or Minimum Output Energy (MOE) approach. Using carefully chosen constraints ,which guarantee the contribution of the target path to be present in the filter output, such an approach is in principle equivalent to maximising the Signal to Interference plus Noise ratio (SINR) at the filter output. Since in a RAKE receiver the treatment of the received signal is naturally pathwise in the sense that there exists a 'finger' or pulse-shaped matched filter in cascade with a correlator matched to the spreading code of the user of interest, the precombining approach lends itself as an extension to the classical receiver in DS-CDMA, the RAKE receiver. It is hence possible to envisage two ways of proceeding with the pathwise interference cancellation, namely by using the correlator outputs of the RAKE(i) as suggested above, or to use the received signal directly(ii). It may be noted here, that it is in fact not important that the interference cancellation be necessarily before spatio-temporal recombining of the multipath components but that there is a pathwise treatment. Approach (i) is inherently attractive since the entry vector size to the filter in this case is proportional to KM whereas in approach (ii), the entry vector is proportional to LKM. This is particularly true in the case where the number of users, K, is small compared to the processing gain, L, and hence promises reduced complexity. However, approach (i) is more difficult to formulate in a discrete-time processing context, as well as to present the inconvenience of signal structural change with a varying no. of users and/or number of paths. Approach (i) is a true multi-user approach and is used by Latva-aho [42] to present the filter theory, but approach (ii) is used in the context of adaptive filtering, since it allows to follow a single-user approach, in the sense that only the information relative to the user of interest, k, is required. Approach (ii) can hence be formulated such that the IC-filter, $\mathbf{F}_{k,m}$ for path m of user k, works directly on the received signal given in (2.1.3), such that the filter output can be written as $\mathbf{F}_{k,m}\mathbf{Y}[n]$. Figure 2.1 clearly shows the matched-filter structure of the path-wise approach. Indeed, it can be seen that the 2D RAKE receiver is but a special case of the proposed filter structure where the filters $\mathbf{F}_{k,m} = \mathbf{E}_{k,m}^H$ are matched to $\mathbf{E}_{k,m}$. From

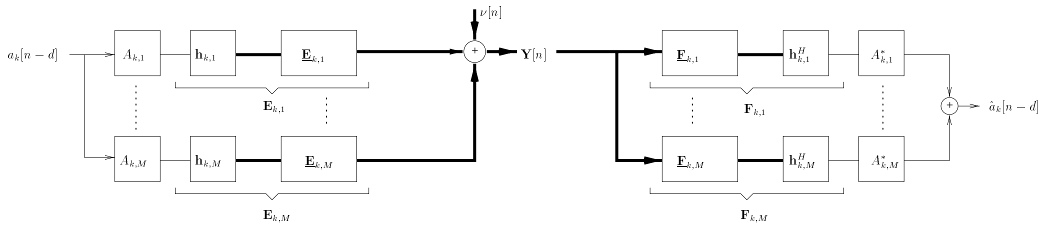

Figure 2.1: Receiver showing the matched-filter structure of the proposed approach

figure 2.1 we see that the data symbol estimate is described by

$$\hat{a}_k[n-d] = \underbrace{\hat{\mathbf{A}}^H_k[n]\,\underbrace{\hat{\mathbf{H}}^H_k\hat{\underline{\underline{\mathbf{F}}}}_k}_{\hat{\underline{\mathbf{F}}}_k}}_{\hat{\mathbf{F}}_k}\mathbf{Y}[n] \tag{2.2.1}$$

where

$$\underline{\underline{\mathbf{F}}}_k = \left[\underline{\mathbf{F}}_{k,1}\cdots\underline{\mathbf{F}}_{k,M}\right]\,;\ \underline{\mathbf{F}}_k = \left[\mathbf{F}_{k,1}\cdots\mathbf{F}_{k,M}\right]; \tag{2.2.2}$$

are the stacked contributions of the path-wise filters to give a filter per user. We can see here that the path-wise processing can be further broken down from purely path-wise processing (estimating $\underline{\mathbf{F}}_k$) to path-wise and antenna-wise processing (estimating $\underline{\underline{\mathbf{F}}}_k$).

The LCMV optimisation criterion to solve for a purely path-wise filter $\mathbf{F}_{k,m}$ is hence given by

$$\mathbf{F}^o_{k,m} = \arg\min_{\mathbf{F}_{k,m}\mathbf{E}_{k,m}=1}\mathbf{F}_{k,m}\mathbf{R}_{YY}\mathbf{F}^H_{k,m} \tag{2.2.3}$$

where $\mathbf{E}_{k,m}$ is the constraint vector, chosen such that it represents the contribution of the path of interest, $A_{k,m}a_k[n-d]$, in $\mathbf{Y}[n]$, i.e the column in $\mathbf{PSH}$ corresponding to $A_{k,m}a_k[n-d]$ in $\mathbf{Aa}_n$. d denotes some delay with respect to the input signal time index n, typically chosen such that the symbols contribution corresponds roughly to the middle portion of the received vector $\mathbf{Y}_n$. This leads to the solution of

$$\mathbf{F}^o_{k,m} = (\mathbf{E}^H_{k,m}\mathbf{R}^{-1}_{YY}\mathbf{E}_{k,m})^{-1}\mathbf{E}^H_{k,m}\mathbf{R}^{-1}_{YY} \tag{2.2.4}$$

Hence, it can be seen that the $\mathbf{E}_{k,m}$ and therefore $\mathbf{F}_{k,m}$ only depends on the slowly varying parameters as defined earlier in section 1.3.1.4.

2.3 User-wise Distortionless Pathwise Interference Cancellation

In the approach described in section 2.2 it is supposed that the estimation time for R_{YY} is such that the complex amplitudes $A_{k,m}$ of the paths vary strongly over the estimation time of R_{YY} so that the coefficients $A_{k,m}$ can be considered mutually independent and hence decorrelated between different paths for a given user k. If this decorrelation is perfect, the approach of section 2.2 is optimal in the sense that it corresponds to a maximisation of the SINR of each path. However, if it cannot be assumed that the mobile terminal moves sufficiently, the performance of the approach given in [42] will be limited severely as the signal $A_{k,m}a_k[n-d]$ for the path m of the user k can be strongly correlated with the other paths $i \neq m$ since they belong to the same data symbol(see also appendix 2.A). In the following, we present alternative approaches which avoid the problem of signal cancellation due to amplitude correlations.

2.3.1 User-wise Distortionless PWIC (1)

It is now possible to resolve the problem of signal cancellation by requiring that the filter $\mathbf{F}_{k,m}$ for path m blocks the contribution of the other paths $i \neq m$ according to the following LCMV criteria:

$$\mathbf{F}_{k,m} = \arg \min_{\mathbf{F}_{k,m}\mathbf{E}_{k,j}=\delta_{m,j}} \mathbf{F}_{k,m}\mathbf{R}_{YY}\mathbf{F}_{k,m}^H \tag{2.3.1}$$

where the number of vector constraints has become equal to the number of paths, M, of user k. Stacking the filters $\mathbf{F}_{k,m} : m \in \{1 \dots M\}$ into a matrix $\underline{\mathbf{F}}_k = [\mathbf{F}_{k,1}^H \dots \mathbf{F}_{k,M}^H]^H$ and $\mathbf{E}_{k,m} : m \in \{1 \dots M\}$ into $\underline{\mathbf{E}}_k = [\mathbf{E}_{k,1} \dots \mathbf{E}_{k,M}]$, the LCMV criteria can be rewritten as

$$\underline{\mathbf{F}}_k = \arg \min_{\underline{\mathbf{F}}_k\underline{\mathbf{E}}_k=\mathbf{I}_M} \underline{\mathbf{F}}_k\mathbf{R}_{YY}\underline{\mathbf{F}}_k^H \tag{2.3.2}$$

with solution

$$\underline{\mathbf{F}}_k^o = (\underline{\mathbf{E}}_k^H\mathbf{R}_{YY}^{-1}\underline{\mathbf{E}}_k)^{-1}\underline{\mathbf{E}}_k^H\mathbf{R}_{YY}^{-1} \tag{2.3.3}$$

In this approach, the filter will let pass all the paths, m of user k without distortion and allows for zero-forcing. The estimate of the signal will be obtained by maximum ratio combining, $\hat{a}_k[n-d] = \sum_{m=1}^{M} A_{k,m}^*\mathbf{F}_{k,m}\mathbf{Y}[n]$. This PWIC approach is also suitable to the estimation of the complex amplitude coefficients, $A_{k,m}$, since they are contained in the filter outputs at improved SINR as compared to the unprocessed signal $\mathbf{Y}[n]$. The complex coefficient estimation hence can be achieved through the use of a training sequence according to the following Least-Square (LS) criterion

$$\hat{A}_{k,m} = \arg\min_{A_{k,m}} \sum_n \|A_{k,m} a_k[n-d] - \mathbf{F}^o_{k,m}\mathbf{Y}[n]\|^2 \tag{2.3.4}$$

The disadvantage of this method lies therein that it does require the knowledge of the antenna response vector $\mathbf{h}_{k,m}$ but does not permit the estimation thereof since the spatial recombination is implicit in the interference cancelling filter. Hence, the estimation of $\mathbf{h}_{k,m}$ would have to be obtained independently from a different source. In the next section, we show an alternative which allows spatial recombination after interference cancellation.

2.3.2 User-wise Distortionless PWIC (2)

In order to allow also the estimation of the channel response vectors, $\mathbf{h}_{k,m}$, the approach in section (2.3.1) can be extended directly, so as to achieve explicit spatial recombination after IC-filtering. This requires the filter to become a matrix filter, $\underline{\mathbf{F}}_{k,m}$, instead of a vector filter unlike (2.3.1), further increasing the degrees of freedom available. Let us define

$$\mathbf{E}_{k,m} = \underline{\mathbf{E}}_{k,m}\mathbf{h}_{k,m} \tag{2.3.5}$$

where $\underline{\mathbf{E}}_{k,m}$ is a matrix, containing the contribution of $\mathbf{h}_{k,m}A_{k,m}a_k(z)$ in $\mathbf{PS}$ of equation (2.1.3), the spreading and the pulse-shaping matrix, as detailed in section 2.1.1. We can then write the LCMV criteria as

$$\underline{\mathbf{F}}_{k,m} = \arg\min_{\underline{\mathbf{F}}_{k,m}\underline{\mathbf{E}}_{k,j}=\mathbf{I}_Q\delta_{m,j}} \underline{\mathbf{F}}_{k,m}\mathbf{R}_{YY}\underline{\mathbf{F}}^H_{k,m} \tag{2.3.6}$$

if we now stack the filters $\underline{\mathbf{F}}_{k,m}$ and the constraint matrices $\underline{\mathbf{E}}_{k,m}$ as in section 2.3.1, we obtain $\underline{\underline{\mathbf{F}}}_k$ and $\underline{\underline{\mathbf{E}}}_k$ and the LCMV criterion can be written as

$$\underline{\underline{\mathbf{F}}}_k = \arg\min_{\underline{\underline{\mathbf{F}}}_k\underline{\underline{\mathbf{E}}}_k=\mathbf{I}_{QM}} \underline{\underline{\mathbf{F}}}_k\mathbf{R}_{YY}\underline{\underline{\mathbf{F}}}^H_k \tag{2.3.7}$$

leading to

$$\underline{\underline{\mathbf{F}}}_k = (\underline{\underline{\mathbf{E}}}^H_k\mathbf{R}^{-1}_{YY}\underline{\underline{\mathbf{E}}}_k)^{-1}\underline{\underline{\mathbf{E}}}^H_k\mathbf{R}^{-1}_{YY} \tag{2.3.8}$$

The symbol estimate is therefore given by $\hat{a}_k[n-d] = \sum_m^M A_{k,m}^* \mathbf{h}_{k,m}^H \underline{\mathbf{F}}_{k,m} \mathbf{Y}[n]$. This method clearly allows for the estimation of a path's channels response, requiring only the knowledge of the delays, $\tau_{k,m}$, and the spreading code, $\mathbf{s}_k$, for the user of interest, k, to adapt the interference cancelling filter $\underline{\underline{\mathbf{F}}}_k$. The antenna array response, $\mathbf{h}_{k,m}$, can be estimated over the duration of several bursts where as the complex channel coefficients, $A_{k,m}$, can be obtained by estimation over a much shorter time interval. The estimates can be found by

$$\min_{A_{k,m},\mathbf{h}_{k,m}:\mathbf{h}_{k,m}^H\mathbf{h}_{k,m}=1} \sum_n ||\mathbf{h}_{k,m} A_{k,m} a_k[n-d] - \underline{\mathbf{F}}_k^o \mathbf{Y}[n]||^2 \tag{2.3.9}$$

with solutions given in (2.3.10), using Training Sequences (TS).

$$\begin{aligned} \hat{\mathbf{h}}_{k,m} &= \mathbf{V}_{max}(\underline{\mathbf{F}}_{k,m}^o \mathbf{R}_{YY} \underline{\mathbf{F}}_{k,m}^{o\,H}) \approx \mathbf{h}_{k,m} e^{j\phi} \\ \hat{A}_{k,m} &= \frac{\sum_{n\in TS} a_k^*[n-d]\mathbf{h}_{k,m}^H \underline{\mathbf{F}}_{k,m}^o \mathbf{Y}[n]}{\sum_{n\in TS} |a_k[n-d]|^2} \approx A_{k,m} e^{-j\phi} \end{aligned} \tag{2.3.10}$$

In the case where a pilot in quadrature is used rather than a TS, we can find the complex amplitudes through

$$\hat{A}_{k,m} = \frac{-j\sum_n \left\{ Im\left\{a_k[n-d]\right\} \hat{\mathbf{h}}_{k,m} \underline{\mathbf{F}}_{k,m}^o \mathbf{Y}[n] \right\}}{\sum_n \left(Im\left\{a_k[n-d]\right\}\right)^2} \approx A_{k,m} e^{-j\phi} \tag{2.3.11}$$

Due to the extra degrees of freedom compared to the approach of section 2.3.1 this approach allows even more powerful interference cancellation. On the other hand, with the extension of the degrees of freedom, this also means that the complexity is higher.

2.3.3 User-wise Distortionless PWIC(3)

From the filter expression for UDPWIC(2), equation (2.3.8) it can be seen that the solution is identical to (2.3.3) in the case where we use $\mathbf{H}^H$ for the spatial recombination in (2.3.8). That is to say that

$$\underline{\mathbf{F}}_k = \mathbf{H}_k^H \underline{\underline{\mathbf{F}}}_k$$

Using $\mathbf{q}$ as a generic spatio-temporal recombination vector, we can express the SINR at the symbol estimator output from

$$\hat{a}_k[n-d] = \mathbf{q}^H \underline{\underline{\mathbf{F}}}_k \mathbf{Y}[n] \tag{2.3.12}$$

and

$$\mathbf{Y}[n] = \underline{\underline{\mathbf{E}}}_k \mathbf{H}_k \mathbf{A}_k a_k[n-d] + \nu[n]$$

where $\underline{\underline{\mathbf{E}}}_k \mathbf{H}_k \mathbf{A}_k$ is the signal term and $\nu[n]$ represents the noise and interference term as

$$SINR = \frac{\sigma_a^2 \mathbf{q}^H \mathbf{H}_k \mathbf{A}_k \mathbf{A}_k^H \mathbf{H}_k^H \mathbf{q}}{\mathbf{q}^H (\underline{\underline{\mathbf{F}}}_k \mathbf{R}_{YY} \underline{\underline{\mathbf{F}}}_k^H - \sigma_a^2 \mathbf{H}_k \mathbf{A}_k \mathbf{A}_k^H \mathbf{H}_k^H) \mathbf{q}}$$

In order to maximise the above SINR w.r.t. $\mathbf{q}$, the problem can be reformulated into a generalised eigenvalue problem of the following form:

$$\mathbf{q}_{max} = \arg\max_{\mathbf{q}} \frac{\mathbf{q}^H \mathbf{H}_k \mathbf{A}_k \mathbf{A}_k^H \mathbf{H}_k^H \mathbf{q}}{\mathbf{q}^H \underline{\underline{\mathbf{F}}}_k \mathbf{R}_{YY} \underline{\underline{\mathbf{F}}}_k^H \mathbf{q}}$$

with solution

$$\mathbf{q}_{max} = \mathbf{A}_k^H \mathbf{H}_k^H (\underline{\underline{\mathbf{F}}}_k \mathbf{R}_{YY} \underline{\underline{\mathbf{F}}}_k^H)^{-1}$$

Upon backsubstitution into equation (2.3.12) we find

$$\hat{a}_k[n-d] = \mathbf{A}_k^H \mathbf{H}_k^H \mathcal{F}_k \mathbf{Y}[n]$$

where

$$\mathcal{F}_k = \underline{\underline{\mathbf{E}}}_k^H \mathbf{R}_{YY}^{-1} = \mathbf{R}_{aY} \mathbf{R}_{YY}^{-1} \tag{2.3.13}$$

is a matrix filter, equivalent to an unconstrained LMMSE/max. SINR receiver. This shows that pathwise processing does not necessarily imply sub-optimality w.r.t an LMMSE receiver. Note, however, that the filter only simplifies in the case where the estimation interval of $\mathbf{R}_{YY}$ used in the construction of $\underline{\underline{\mathbf{F}}}_k$ is equal to the estimation interval of $\mathbf{A}_k$ and hence q. In the case where the filter is constructed with an $\mathbf{R}_{YY}$ that is averaged over several realisations of $\mathbf{A}_k$, the $\mathbf{R}_{YY}$ used in q, will have to be computed separately and we will use equation (2.3.12). This filter is substantially less complex to compute than the filter in (2.3.8) while also maximising the output SINR. It is worth noting that this is neither the case for UDPWIC(2) nor UDPWIC(1) unless the interference plus noise covariance matrix is identity. Furthermore, this approach allows the filter to be constructed with a minimum of a priori knowledge, in particular the path delays and the spreading code of user k, while still allowing the estimation of the channel coefficients.

2.3.4 Structural Filter Constraints

So far, the filters shown in the preceding sections had no structural constraints imposed on them, other than being FIR. It is however possible, to define an a priori structural constraint on the filter $\mathbf{F}_{k,m}$ with the aim of further reducing the complexity and/or improve the performances. Possible constraints are to define the filter $\mathbf{F}_{k,m}$ to be the cascade of a free, shorter filter and a pulse-shaped matched filter, $p^*(-t)$ or even a cascade of the pulse-shaped matched filter as well as the spreading code correlator and a free filter part. We will, however, not pursue this any further at this point but introduce a lower complexity method in the next chapter.

2.4 Numerical Simulation Results

We consider a scenario with $L = 8$, $K = 2$, $M = 2$ and SIR=-10dB. Three cases are shown, in which R_{YY} is averaged over 1 (figure 2.2), 2 (figure 2.3) and 10 (figure 2.4) slots, respectively. By this, we simulate a situation with varying vehicle speed since the correlation between the complex amplitudes is a function of vehicle speed. The fast parameters are drawn randomly in each slot, while the slow parameters are constant. The simulations show that the original approach by Matti Latva-Aho (PLMMSE curves) suffers from signal cancellation when the fast parameters do not vary fast enough, whereas the new approaches are fairly insensitive to the speed of variation of the fast parameters.

2.5 Conclusions

We have established the concept of user-wise distortionless pathwise interference cancellation and introduced novel interference cancelling filters on a pathwise basis which do not rely on the fastly varying complex amplitude coefficients. This is achieved using the fact that the signal can be split into parts which depend on slowly varying channel parameters and fastly varying parameters, respectively. Furthermore, we have shown how to alleviate the problem of signal cancellation in the original pathwise approach [40–42, 45] by introducing the extra constraint to null out other paths of the user of interest belonging to the data to be received. The obvious advantage of such an approach is its independence from the fastly varying complex amplitude coefficients. This allows to relax the update rate

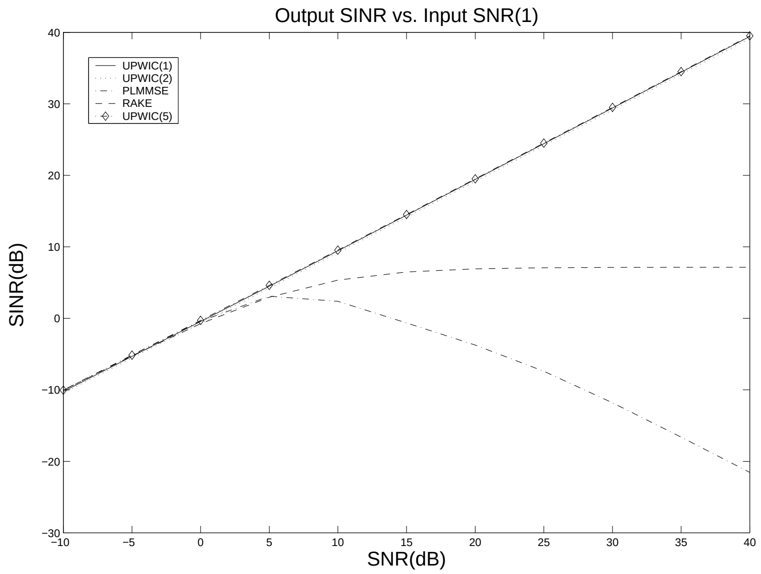

Figure 2.2: UDPWIC compared to RAKE and PLMMSE when averaged over 1 slot

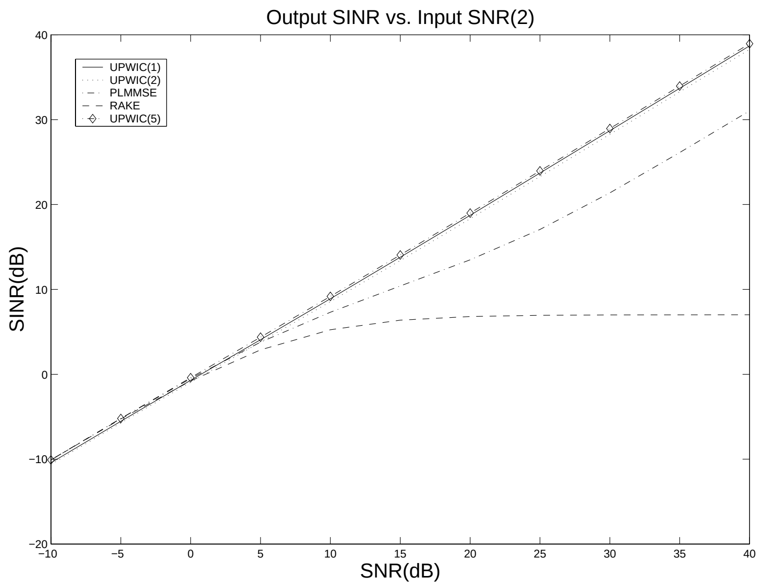

Figure 2.3: UDPWIC compared to RAKE and PLMMSE when averaged over 2 slots

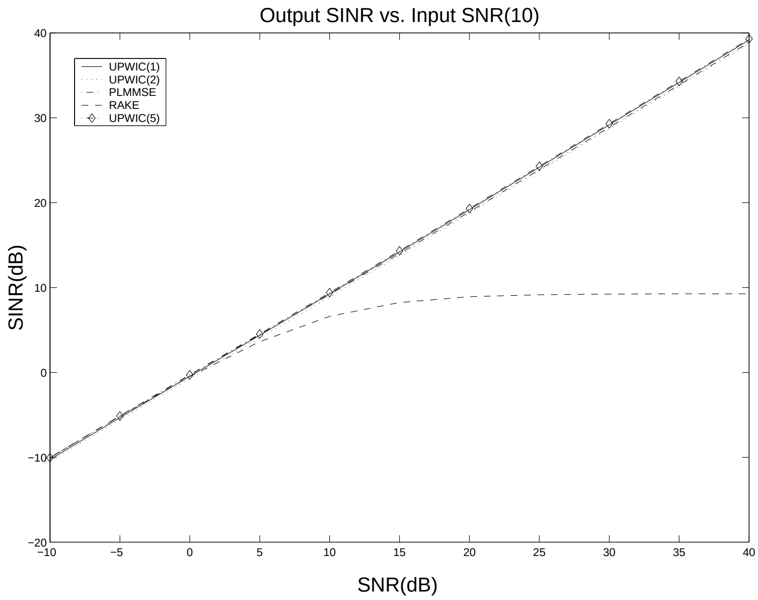

Figure 2.4: UDPWIC compared to RAKE and PLMMSE when averaged over 10 slots

of the IC filter. Pathwise Interference Cancellation (PWIC) is an approach that allows to separate the parameters into fastly varying and slowly varying parameters, thereby allowing the scarce training data to be used in the estimation of the fastly varying parameters while the whole of the received signal can be used to estimate the slowly varying parameters over a much larger time interval. Since the interference cancellation takes place between individual multipath components before spatial-temporal recombination, the signal thus obtained contains the desired parameters at an improved SINR compared to the received signal and hence allows improved channel estimation. These results have been published in [46].

However, the optimal FIR approaches of the previous pages are still computationally very costly and therefore difficult to implement in practice. In the next chapter, we will introduce an alternative sub-optimal pathwise method that allows considerable gains compared to the RAKE receiver while being substantially less costly to implement than the above approaches.

2.A Appendix: Signal cancellation in the case of correlated amplitudes

Consider the simple case of one user with two paths and a single transmitted data symbol, a. The received signal can be written as

$$\begin{aligned}\mathbf{y} &= \mathbf{s}_1 A_1 a + \mathbf{s}_2 A_2 a + \mathbf{n} \\ &= [\mathbf{s}_1\ \mathbf{s}_2]\begin{bmatrix} A_1 \\ A_2 \end{bmatrix} a + \mathbf{n} = \mathbf{S}\mathbf{A}a + \mathbf{n}\end{aligned}$$

where $\mathbf{s}_1$ is the $L \times 1$ spreading code of user one which we assume to be (without loss of generality) at zero delay. $\mathbf{s}_2$ is a delayed copy of $\mathbf{s}_1$, which for the sake of simplicity, we just model as a different spreading code, synchronous with $\mathbf{s}_1$. $\mathbf{n}$ denotes the noise vector. The filter in the original pathwise LMMSE approach of equation (2.2.3) to estimate the first path amplitude data product $A_1 a$ is given by

$$\mathbf{F}_1^o = \arg\min_{\mathbf{F}_1\mathbf{s}_1 = 1} \mathbf{F}_1 \mathbf{R}_{yy} \mathbf{F}_1^H$$

Recall that the constraint was imposed to ensure the contribution of the first path in the filter output. The minimum output variance achieved is given by

$$\mathbf{F}_1^o \mathbf{R}_{yy} \mathbf{F}_1^o = \left(\mathbf{s}_1^H \mathbf{R}_{yy}^{-1} \mathbf{s}_1\right)^{-1} \tag{2.A.1}$$

The received signal covariance matrix is

$$\begin{aligned}\mathbf{R}_{yy} &= \sigma_a^2 \mathbf{S}\mathbf{R}_{AA}\mathbf{S}^H + \sigma_n^2 \mathbf{I} \\ &= \sigma_a^2 \underbrace{\mathbf{S}\mathbf{D}}_{=\mathbf{B}} \Lambda \mathbf{D}^H \mathbf{S}^H + \sigma_n^2 \mathbf{I} \\ &= \sigma_a^2 \mathbf{B}\Lambda\mathbf{B}^H + \sigma_n^2 \mathbf{I}\end{aligned}$$

where we defined the amplitude correlation matrix, $\mathbf{R}_{AA}$,

$$E\begin{bmatrix} A_1 \\ A_2 \end{bmatrix}[A_1^* A_2^*] = \begin{bmatrix} \sigma_1^2 & \rho\sigma_1\sigma_2 \\ \rho^*\sigma_1\sigma_2 & \sigma_2^2 \end{bmatrix} = \underbrace{\begin{bmatrix} \sigma_1^2 & 0 \\ 0 & \sigma_2^2 \end{bmatrix}}_{=\mathbf{D}} \underbrace{\begin{bmatrix} 1 & \rho \\ \rho^* & 1 \end{bmatrix}}_{=\Lambda} \begin{bmatrix} \sigma_1^2 & 0 \\ 0 & \sigma_2^2 \end{bmatrix}$$

where ρ denotes the correlation coefficient between the amplitudes. Using the matrix inversion lemma on $\mathbf{R}_{yy}$, we can write:

$$\begin{aligned} \mathbf{s}_1^H \mathbf{R}_{yy}^{-1} \mathbf{s}_1 &= \frac{1}{\sigma_n^2} \left[1 - \mathbf{s}_1^H \mathbf{B} \left[\mathbf{B}^H \mathbf{B} + \Lambda^{-1} \frac{\sigma_n^2}{\sigma_a^2} \right]^{-1} \mathbf{B}^H \mathbf{s}_1 \right] \\ &= \frac{1}{\sigma_n^2} \left[1 - [1\ \alpha] \left[\mathbf{S}^H \mathbf{S} + \mathbf{D}^{-1} \Lambda^{-1} \mathbf{D}^{-1} \frac{\sigma_n^2}{\sigma_a^2} \right]^{-1} \left[\begin{array}{c} 1 \\ \alpha^* \end{array} \right] \right] \end{aligned} \tag{2.A.2}$$

where we have used $\mathbf{s}_1^H \mathbf{B} = \mathbf{s}_1^H \mathbf{S} \mathbf{D} = [1\ \alpha] \mathbf{D}$ and taken $\mathbf{D}$ inside the inverse. α can therefore be seen to be the correlation between the codes, i.e. $\mathbf{s}_1^H \mathbf{s}_2 = \alpha,\ \mathbf{s}_1^H \mathbf{s}_1 = 1$, and the codes are normalised, as usual. Consider now the inverse term, i.e.

$$\begin{aligned} \left[\mathbf{S}^H \mathbf{S} + \mathbf{D}^{-1} \Lambda^{-1} \mathbf{D}^{-1} \frac{\sigma_n^2}{\sigma_a^2} \right]^{-1} &= \left(\mathbf{S}^H \mathbf{S} \right)^{-1} \left[\mathbf{I} + \mathbf{D}^{-1} \Lambda^{-1} \mathbf{D}^{-1} \frac{\sigma_n^2}{\sigma_a^2} \left(\mathbf{S}^H \mathbf{S} \right)^{-1} \right]^{-1} \\ &\approx \left(\mathbf{S}^H \mathbf{S} \right)^{-1} \left[\mathbf{I} - \mathbf{D}^{-1} \Lambda^{-1} \mathbf{D}^{-1} \frac{\sigma_n^2}{\sigma_a^2} \left(\mathbf{S}^H \mathbf{S} \right)^{-1} \right] \end{aligned} \tag{2.A.3}$$

where we have used a first order approximation for the inverse term, i.e. we approximate the higher order terms in the noise power, σ_n^2, with zero under the assumption that the SNR is high. This is reasonable since the signal cancellation occurs at high SNR. Further note that we can write

$$\left(\mathbf{S}^H \mathbf{S} \right)^{-1} = \frac{1}{1 - |\alpha|^2} \left[\begin{array}{cc} 1 & -\alpha \\ -\alpha^* & 1 \end{array} \right] \tag{2.A.4}$$

and therefore

$$[1\ \alpha] \left(\mathbf{S}^H \mathbf{S} \right)^{-1} = [1\ 0] \tag{2.A.5}$$

Resubstituting equation (2.A.3) into (2.A.2), we can now write

$$\left(\mathbf{s}_1^H \mathbf{R}_{yy}^{-1} \mathbf{s}_1 \right)^{-1} \approx \frac{1}{\sigma_n^2} \left\{ 1 - \left[1 - \frac{\sigma_n^2}{\sigma_a^2} [1\ 0] \mathbf{D}^{-1} \Lambda^{-1} \mathbf{D}^{-1} \left[\begin{array}{c} 1 \\ 0 \end{array} \right] \right] \right\} \tag{2.A.6}$$

$$= \frac{1}{\sigma_a^2 \sigma_1^2 \left(1 - |\rho|^2 \right)} \tag{2.A.7}$$

Therefore, with a high input SNR, we can see that the SINR at the filter output is approximately given by

$$SINR = \sigma_a^2 \sigma_1^2 \left(1 - |\rho|^2 \right) \tag{2.A.8}$$

Hence, in the case where the amplitudes are perfectly correlated, $|\rho| = 1$, and the noise power is low, we see that the signal of interest is cancelled. This can occur when the mobile is stationary and therefore the amplitudes will be strongly correlated. Whence, we introduce further constraints on the filter, in particular that $\mathbf{F}_m \mathbf{s}_j = \delta_{m,j}$ which is equivalent to zero-forcing the other paths of the same user that might be correlated to the path of interest.

Chapter 3

Polynomial Expansion Interference Cancellation

3.1 Introduction

The last chapter has clearly shown the benefits of using pathwise processing that allows the separation between fastly and slowly varying parameters. Despite the good performances of the approach presented in the last chapter, the approach is hampered by its high complexity due to the use of the received signal directly, hence dimensions involved are large. Not least the estimation of $\mathbf{R}_{YY}$, the received signal correlation matrix, would require a lot of data. In this chapter, we will introduce an alternative, low-complexity pathwise approach, based on Polynomial Expansion (PE).

Polynomial expansion is an approximation technique for LMMSE receivers and is particularly well suited for CDMA due to the presence of a large number of small correlations. The fundamental principle of PE is to avoid the relatively costly correlation matrix inverse required by an LMMSE/Decorrelator receiver by considering the correlation matrix to be a small perturbation of an identity matrix and approximating the inverse of the correlation matrix by a polynomial expansion in the perturbation matrix or, equivalently, in the correlation matrix itself. However, for PE to work, adapted weighting factors have to be introduced. By appropriately choosing the weighting coefficients, every additional term in the PE can be guaranteed to improve performance and hence divergence concerns are largely eliminated.

PE has, in various forms, received a fair amount of attention recently in the literature [47–50] etc. Some works on PE have analysed the choice of scalar weighting factors on the basis of asymptotic system analysis, leading to weight values that can be determined a priori. In this chapter, we propose to introduce diagonal weighting matrices, which corresponds to one weighting factor per signal component. We shall see that such multiple coefficients not only improve performance substantially in the presence of power imbalances between users and paths, but also further improvement due to the fast adaptation of these weights is possible since the instantaneous channel states will reflect the power imbalances very strongly.

Moshavi, who first introduced PE [51], applied polynomial expansion to the joint set of RAKE outputs for the various users. In this way, the polynomial expansion receiver involves only (de)spreading and channel (matched) filtering operations and hence is mostly parameterised in terms of the channel parameters (as opposed to the general coefficients of a general linear receiver). Honig and coworkers apply the PE principle to the received signal directly and were able to show [52] that PE is equivalent to the *Multistage Wiener Filter* [53] in this case. We propose to introduce polynomial expansion at the level of the pathwise RAKE outputs. As compared to Moshavi's approach, the PE is situated before maximum ratio combining of the path contributions and leads to pathwise interference cancellation which will allow to estimate the path parameters (amplitudes, or even angles in the spatio-temporal case) with improved SINR and hence with reduced estimation error. The diagonal weighting factors we introduce hence provide a weighting per path (or even possibly per antenna element per path in the spatio-temporal case). Maximum ratio combining after pathwise PE then corresponds to a version of the *Generalised RAKE*, the G-RAKE (the path amplitudes multiplied by arbitrary weighting factors become arbitrary recombination coefficients).

3.2 Principle of Polynomial Expansion

To illustrate the principle of pathwise polynomial expansion, it is beneficial to briefly consider a simplified, synchronous signal model with a single path per user, a single receiver antenna and chip-rate sampling (i.e. $J = 1,\ M = 1,\ Q = 1$). We can write the discrete-time received signal, $\mathbf{y}[n]$, for K users as:

$$\mathbf{y}[n] = \mathbf{S}_e \mathbf{A}\mathbf{a}[n] + \mathbf{v}[n] \tag{3.2.1}$$

where we have used the following definitions:

$$\begin{aligned} \mathbf{S}_e &= [\mathbf{s}_1 \dots \mathbf{s}_K] \ (L \times K) \\ \mathbf{A} &= diag\{A_1, \dots, A_K\} \ (K \times K) \\ \mathbf{a}[n] &= [a_1[n] \dots a_K[n]]^T \ (K \times 1) \end{aligned} \tag{3.2.2}$$

where $\mathbf{s}_k$ is the spreading code of user k and A_k the corresponding complex amplitude coefficient. $\mathbf{v}[n]$ is considered white Gaussian noise, as usual. In this model, the spreading matched filter is given by $\mathbf{S}_e^H$ and we can write

$$\begin{aligned} \mathbf{x}[n] &= \mathbf{S}_e^H \mathbf{S}_e \mathbf{A}\mathbf{a}[n] + \mathbf{S}_e^H \mathbf{v}[n] \\ &= \mathbf{R}\mathbf{A}\mathbf{a}[n] + \mathbf{S}_e^H \mathbf{v}[n] \\ \mathbf{R} &= \mathbf{S}_e^H \mathbf{S}_e \ (K \times K) \end{aligned} \tag{3.2.3}$$

it is clear that the matrix $\mathbf{R}$ is simply the spreading code cross-correlation matrix. Using normalised spreading codes, i.e. $\mathbf{s}_k^H \mathbf{s}_k = 1$, we see that $\mathbf{R}$ has unit elements on the diagonal. Therefore, let us write

$$\mathbf{R} = \mathbf{I} + \overline{\mathbf{R}} \tag{3.2.4}$$

where $\overline{\mathbf{R}}$ contains the off-diagonal elements of $\mathbf{R}$, $[\overline{\mathbf{R}}]_{ij} \leq 1 \forall \{i,j\}$. The off-diagonal elements are small and inversely proportional to the spreading gain. We can therefore view $\mathbf{R}$ as a perturbed identity matrix. From equation (3.2.3) we can see that the Linear Minimum Mean Square Error (LMMSE) receiver and the decorrelator/zero-forcing receiver to estimate $\mathbf{a}[n]$ from $\mathbf{x}[n]$ are given by (for reference see e.g. [21, 54, 55])

$$\begin{aligned} \hat{\mathbf{a}}_{dec}[n] &= \mathbf{F}_{dec}\mathbf{x}[n] = \mathbf{A}^{-1}\mathbf{R}^{-1}\mathbf{x}[n] \\ \hat{\mathbf{a}}_{LMMSE}[n] &= \mathbf{F}_{LMMSE}\mathbf{x}[n] = \mathbf{A}^H \left(\sigma_a^2 \mathbf{R}\mathbf{A}\mathbf{A}^H + \sigma_v^2 \mathbf{I}\right)^{-1} \mathbf{x}[n] \end{aligned}$$

where we assume uncorrelated data symbols and white noise, i.e. $E\{\mathbf{a}[n]\mathbf{a}^H[n] = \sigma_a^2 \mathbf{I}\}$ and $E\{\mathbf{v}[n]\mathbf{v}^H[n] = \sigma_v^2 \mathbf{I}\}$. Equally, for the estimation of the amplitude data product, we have

$$\begin{aligned} \widehat{\mathbf{A}\mathbf{a}}_{dec}[n] &= \mathbf{F}_{dec}\mathbf{x}[n] = \mathbf{R}^{-1}\mathbf{x}[n] \\ \widehat{\mathbf{A}\mathbf{a}}_{LMMSE}[n] &= \mathbf{F}_{LMMSE}\mathbf{x}[n] = \left(\sigma_a^2 \mathbf{R} + \sigma_v^2 (\mathbf{A}^H\mathbf{A})^{-1}\right)^{-1} \mathbf{x}[n] \end{aligned} \tag{3.2.5}$$

Since $\mathbf{A}$ and $\mathbf{A}\mathbf{A}^H = \mathbf{A}^H\mathbf{A}$ are diagonal matrices, the main complexity in either the decorrelator or the LMMSE receiver is the matrix inverse involving the $K \times K$ matrix $\mathbf{R}$. The fundamental idea in polynomial expansion is now to avoid the costly inverse by approximating the inverse as a polynomial. For simplicity, let us look at the amplitude-data decorrelator from (3.2.5). We can write for a general, invertible matrix $\mathbf{R}$ [56]:

$$\mathbf{R}^{-1} = \left(\mathbf{I} + \overline{\mathbf{R}}\right)^{-1} = \sum_{b=0}^{\infty} \left(-\overline{\mathbf{R}}\right)^b \tag{3.2.6}$$

provided there is a matrix norm $|||\overline{\mathbf{R}}||| < 1$ to guarantee convergence. Assuming for the time being that the convergence condition is satisfied, we can therefore approximate $\mathbf{R}^{-1}$ by truncating the infinite series expansion to $B+1$ terms, i.e.

$$\mathbf{R}^{-1} \approx \tilde{\mathbf{R}}^{-1} = \sum_{b=0}^{B} (-\overline{\mathbf{R}})^b \tag{3.2.7}$$

Note that we could equivalently form the expansion in $\mathbf{R}$ instead of $\overline{\mathbf{R}}$ since there is a one-to-one relationship between the two (this will be shown later in section 3.4.1). Typically, in approximating the decorrelator in this fashion, we would be interested only in a polynomial of very low order, such as $B = 1$, to keep complexity at a reasonable level. In the noiseless case (where the decorrelator is equivalent to the LMMSE), a first-order expansion $(B = 1)$ in (3.2.7) leads to an amplitude-data product estimate from (3.2.5) given by

$$\begin{aligned} \widehat{\mathbf{Aa}}[n] &= \tilde{\mathbf{R}}^{-1}\mathbf{x}[n] = \left(\mathbf{I} - \overline{\mathbf{R}}\right)\mathbf{x}[n] \\ &= (2\mathbf{I} - \mathbf{S}_e^H\mathbf{S}_e)\mathbf{S}_e^H\mathbf{S}_e\mathbf{A}\mathbf{a}[n] \\ &= (2\mathbf{I} - \mathbf{R})\mathbf{R}\mathbf{A}\mathbf{a}[n] \end{aligned} \tag{3.2.8}$$

Note that the complexity introduced by PE is essentially twice the complexity of the RAKE for every stage. In particular, every stage introduces an additional spreading followed by a despreading operation ($\mathbf{S}_e^H\mathbf{S}_e$). From (3.2.8) we can write the expression for the signal-to-interference ratio (SIR) for user one, without loss in generality, from $\left[\widehat{\mathbf{Aa}}[n]\right]_1$, where $[.]_1$ denotes the first element of the vector.

$$SIR_{PE} = \frac{|A_1|^2(1 - \mathbf{s}_1^H\overline{\mathbf{S}}_e\overline{\mathbf{S}}_e^H\mathbf{s}_1)(1 - \mathbf{s}_1^H\overline{\mathbf{S}}_e\overline{\mathbf{S}}_e^H\mathbf{s}_1)}{\mathbf{s}_1^H(\mathbf{I} - \overline{\mathbf{S}}_e\overline{\mathbf{S}}_e^H)\overline{\mathbf{S}}_e\mathcal{P}\overline{\mathbf{S}}_e^H(\mathbf{I} - \overline{\mathbf{S}}_e\overline{\mathbf{S}}_e^H)\mathbf{s}_1} \tag{3.2.9}$$

where we have taken the expectation of the numerator and denominator w.r.t. the data, i.e. $E\{\mathbf{a}[n]\mathbf{a}[n]^H = \sigma_a^2\mathbf{I}\}$ and $\mathbf{S}_e = [\mathbf{s}1\ \overline{\mathbf{S}}_e]$; $\overline{\mathbf{A}} = diag\{A_2, \ldots, A_K\}; \mathcal{P} = \overline{\mathbf{A}}^H\overline{\mathbf{A}}$. Assuming that the spreading codes for all users consist of i.i.d. random variables $s_{k,l} \in \frac{1}{\sqrt{L}}\{+1, -1\}$, taking the expectation of the numerator and denominator of SIR_{PE}, over the spreading codes will give

$$SIR_{PE} = \frac{c}{w} \tag{3.2.10}$$

where we the numerator and denominator are given by

$$\begin{aligned} c &= |A1|^2(1 - \frac{2}{L}(K-1) + (K-1)(K-2)(Lm_4m_2^2 + L(L-1)m_2^4)) \\ w &= \sum_{k=2}^{K} |A_k|^2(1/L - 2((K-2)Lm_2^3 + L(L-1)m_2^3 + Lm_2m_4) \\ &\quad +\{Lm_2^4(K-2)(K-3) + (K-1)[m_2^4L(L-1)(L-2) + 3m_2^2m_4L(L-1) + m_2m_6L] \\ &\quad +3(K-2)[Lm_2^2m_4 + L(L-1)m_2^4]\} \end{aligned} \tag{3.2.11}$$

where m_x is the x-th moment of the random spreading code elements $s_{k,l}$. After substitution of the moments,m_x, for the spreading code elements $s_{k,l}$, and some algebraic simplifications, we obtain

$$m_x = \begin{cases} \frac{1}{L^{x/2}} & \text{if x even} \\ 0 & \text{if x odd} \end{cases}$$

$$SIR_{PE} = \frac{|A1|^2\{L^3 - (K-1)[2L^2 - L(K+1) + 2]\}}{(\sum_{k=2}^{K} |A_k|^2)\{K(K-5) + L(K-2) + 6\}} \tag{3.2.12}$$

If we furthermore take the expectation with respect to the amplitudes (where we assume A_k complex, with equally distributed real and imaginary parts and all A_k coming from the same distribution with finite second order moment) and then let $K, L \to \infty$ while keeping the loading factor $\beta = \frac{K}{L} = \frac{\text{no. users}}{\text{spreading factor}}$ constant, we can write an asymptotic large-system result for the SIR as

$$\begin{aligned} SIR_{PE;K,L\to\infty,\beta=const.} &= \left.\frac{(\beta-1)^2}{\beta^2(\beta+1)}\right|_{\beta\neq 0} \\ &\approx \frac{1}{\beta^2} \text{ for small } \beta \end{aligned} \tag{3.2.13}$$

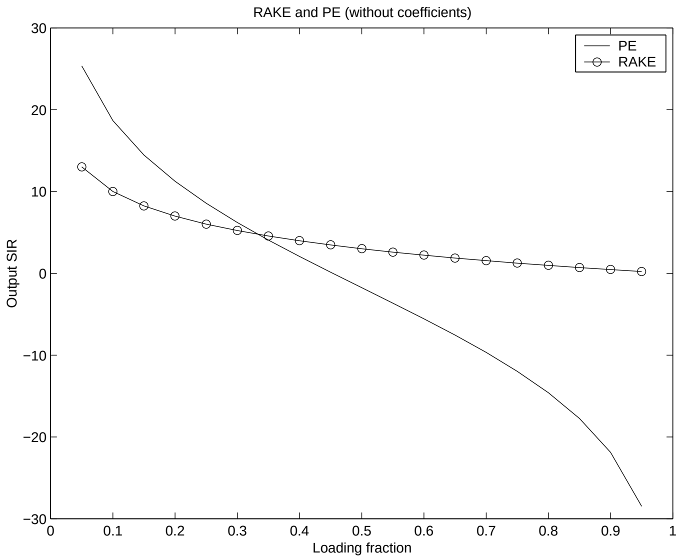

Figure 3.1: The large-system SIR of the RAKE and the PE (without coefficients) compared as a function of the loading factor, $\beta = K/L$, in the noiseless case.

In comparison, an equivalent analysis of the RAKE receiver is well known to give

$$SIR_{RAKE;K,L\to\infty,\beta=const.} = \left.\frac{1}{\beta}\right|_{\beta\neq 0} \tag{3.2.14}$$

In figure 3.1, the above expressions are plotted and it can be seen that a first-order polynomial expansion can only improve with respect to the RAKE for loading factors $\beta < \frac{1}{3}$, approximately. A more in-depth analysis leading to the same conclusion has recently been presented in [57]. The performance can be much improved by introducing scalar coefficients d_b according to some performance criterion in (3.2.7) as has been documented in various publications e.g. [47, 48, 51, 52, 58], i.e.

$$\mathbf{R}^{-1} \approx \tilde{\mathbf{R}}^{-1} = \sum_{b=0}^{B} d_b \overline{\mathbf{R}}^b \tag{3.2.15}$$

Note that with the introduction of scalar coefficients, d_b, the inverse will be exactly estimated with a finite number of stages, $B < L - 1$, by the Cayley-Hamilton theorem [56].

3.3 Polynomial Expansion using scalar coefficients

As mentioned in the introduction of this chapter, there are fundamentally two ways of applying polynomial expansion to linear interference cancellation: at the received signal directly or alternatively at the RAKE outputs. Those two variants correspond to the approaches introduced by Honig *et al.* and Moshavi *et al.* , respectively. We briefly introduce those two methods now.

3.3.1 Polynomial expansion applied to the RAKE outputs

Moshavi presented the original polynomial expansion receiver in 1996 [22,51] and applied it to the joint set of RAKE outputs for the various users. In this way, the polynomial expansion receiver involves only (de)spreading and channel (matched) filtering operations and hence is mostly parameterised in terms of the channel parameters (as opposed to the general coefficients of a general linear receiver). From the previous chapter (section 2.1.1, equation (2.1.5)), we can write the general, asynchronous received signal as

$$\mathbf{Y}[n] = \mathbf{E}\mathbf{a}_n + \mathbf{V}[n] \tag{3.3.1}$$

where the RAKE outputs are given by

$$\mathbf{E}^H\mathbf{Y}[n] = \mathbf{E}^H\mathbf{E}\mathbf{a}_n + \mathbf{E}^H\mathbf{V}[n] = \mathbf{R}\mathbf{a}[n] + \mathbf{E}^H\mathbf{V}[n] \tag{3.3.2}$$

where $\mathbf{R} = \mathbf{E}^H\mathbf{E}$. The LMMSE solution for the data estimate in this case is given by

$$\hat{\mathbf{a}}_n = \left(\sigma_a^2\mathbf{R} + \sigma_n^2\mathbf{I}\right)^{-1}\mathbf{E}^H\mathbf{Y}[n] \tag{3.3.3}$$

The aim is therefore to use a polynomial expansion in $\mathbf{R}$ to approximate the matrix inverse:

$$\left(\sigma_a^2\mathbf{R} + \sigma_n^2\mathbf{I}\right)^{-1} \approx \sum_{i=0}^{B}\mu_i\mathbf{R}^i \tag{3.3.4}$$

and therefore the symbol estimate is given by

$$\hat{\mathbf{a}}_{Moshavi} = \sum_{i=0}^{B}\mu_i\mathbf{R}^i\mathbf{E}^H\mathbf{Y}[n] \tag{3.3.5}$$

The coefficients can, for example, be obtained by solving

$$\mu_i^o = \min_{\mu_i \in \{0,1,\dots,B\}} E\|\mathbf{a}_n - \sum_{i=0}^{B} \mu_i \mathbf{R}^i \mathbf{E}^H \mathbf{Y}[n]\|^2 \tag{3.3.6}$$

other methods of computing the coefficients are possible [47, 48, 51, 58].

3.3.2 Polynomial Expansion applied to the received signal

Honig and coworkers apply the PE principle to the received signal directly. In this case, they were able to show [52] that PE is equivalent to the *Multistage Wiener Filter*. The multistage Wiener filter is a decomposition of the Wiener filter into multiple stages, based on orthogonal projections, allowing a nested implementation thereof. Its most notable feature is the fact that it does not require an estimate nor an inverse of the correlation matrix since only cross-correlations between vectors and scalars are required in determining the filters at each stage. Furthermore, this approach is suitable to reduced-rank Wiener filtering [54] by simply stopping the nested multistage decomposition at the Nth stage, where N is the rank required. For details, see [53].

Hence, working on the received signal directly, we can write the LMMSE estimate as

$$\hat{\mathbf{a}}_n = \mathbf{E}^H R_{YY}^{-1} \mathbf{Y}[n] \tag{3.3.7}$$

The polynomial expansion estimate for the data with $B+1$ stages is hence given by

$$\hat{\mathbf{a}}_{MSWF}[n] = \mathbf{E}^H \sum_{i=0}^{B} w_i \mathbf{R}_{YY}^i \mathbf{Y}[n] \tag{3.3.8}$$

Note that

$$\begin{aligned}
\mathbf{E}^H R_{YY}^{-1} \mathbf{Y}[n] &= \mathbf{E}^H (\sigma_a^2 \mathbf{E}\mathbf{E}^H + \sigma_n^2 \mathbf{I})^{-1} \mathbf{Y}[n] \\
&= \frac{1}{\sigma_n^2} \left[\mathbf{I} - \sigma_a^2 \mathbf{R} \left(\sigma_a^2 \mathbf{R} + \sigma_n^2 \mathbf{I} \right)^{-1} \right] \mathbf{E}^H \mathbf{Y}[n] \\
&= \frac{1}{\sigma_n^2} \left[\sum_{i=0}^{\infty} \left(-\frac{\sigma_a^2}{\sigma_n^2} \mathbf{R} \right)^i \right] \mathbf{E}^H \mathbf{Y}[n] \\
&= \left(\sigma_a^2 \mathbf{R} + \sigma_n^2 \mathbf{I} \right)^{-1} \mathbf{E}^H \mathbf{Y}[n]
\end{aligned} \tag{3.3.9}$$

where we have made use of the matrix inversion lemma and an infinite polynomial expansion. Hence, the LMMSE solution working on the received signal is equivalent to the LMMSE solution based on the RAKE outputs. Therefore, the two methods try to approximate the exactly same solution if the coefficients are obtained in the same fashion (e.g. LMMSE) for the same performance criterion.

3.3.3 Equivalence between PE at the RAKE output and PE applied to the received signal

To show the equivalence of the two approaches with the same, finite number of stages, we need to show a one-to-one correspondence. Assume that the two approaches are indeed the same for the same number of stages. Then we can write

$$\begin{aligned}
\sum_{i=0}^{B} \mu_i \mathbf{R}^i \mathbf{E}^H &= \mathbf{E}^H \sum_{i=0}^{B} w_i \left(\sigma_a^2 \mathbf{E}^H \mathbf{E} + \sigma_n^2 \mathbf{I}\right)^i && (3.3.10)\\
&= \mathbf{E}^H \sum_{i=0}^{B} w_i \sum_{j=0}^{i} \binom{i}{j} (\sigma_a^2 \mathbf{E}\mathbf{E}^H)^j (\sigma_n^2 \mathbf{I})^{i-j} \\
&= \sum_{i=0}^{B} w_i \sum_{j=0}^{i} \binom{i}{j} (\sigma_n^2)^{i-j} (\sigma_a^2)^j \underbrace{\mathbf{E}^H (\mathbf{E}\mathbf{E}^H)^j}_{\mathbf{R}^j \mathbf{E}^H} \\
&= \sum_{j=0}^{B} \underbrace{\sum_{i=j}^{B} w_i \binom{i}{j} (\sigma_n^2)^{i-j} (\sigma_a^2)^j}_{=\mu_j} \mathbf{R}^j \mathbf{E}^H && (3.3.11)\\
&= \sum_{j=0}^{B} \mu_j \mathbf{R}^j \mathbf{E}^H
\end{aligned}$$

where we have changed the summation order in (3.3.11). Hence, it can be seen that there is an exact one-to-one relationship between the two approaches for any arbitrary number of stages, B. For alternative proofs, see also [59, 60].

3.4 Pathwise Polynomial Expansion

In this section, we propose to introduce diagonal weighting matrices which corresponds to one weighting factor per signal component, as opposed to the scalar weighting introduced in the last sections. We propose to introduce polynomial expansion at the level of the pathwise RAKE outputs. As compared to Moshavi's approach, the PE is situated before the maximum ratio recombination of the path contributions and leads to pathwise interference cancellation which will allow to estimate the path parameters (amplitudes, or even angles in the spatio-temporal case) with improved SINR and hence with reduced estimation error. The diagonal weighting factors we introduce hence provide a weighting per path (or even possibly per antenna element per path in the spatio-temporal case).

3.4.1 Time Domain Filtering Notation

We shall now define the more general signal model that is used throughout the rest of this chapter. Recall from equation (1.3.4) that the general discrete-time received signal is given by

$$\mathbf{y}[n] = \sum_{i=-\infty}^{\infty} \mathbf{P}[n-i]\mathbf{SHAa}[i] + \mathbf{v}[n] \tag{3.4.1}$$

In order to avoid the FIR approximations inherent to a burst mode formulation like the one used in the last chapter (see section 2.1.1) we shall now introduce a time-domain filtering notation defined by the advance operator q, where $qy[n] = y[n+1]$ with respect to the symbol period. The q is equivalent to z in the *z-transform* domain but we prefer the use of q to emphasise the delay operator aspect and not the frequency domain interpretation. To this end, let us reformulate the received signal as given in (3.4.1) in the q-domain:

$$\begin{aligned} \mathbf{y}[n] &= \mathbf{P}(q)\mathbf{SHAa}[n] + \mathbf{v}[n] \\ &= \mathbf{E}(q)\mathbf{a}[n] + \mathbf{v}[n] \\ &= \mathbf{E}_k(q)a_k[n] + \sum_{i=1;i\neq k}^{K} \mathbf{E}_i(q)a_i[n] + \mathbf{v}[n] \end{aligned} \tag{3.4.2}$$

where we have decomposed the signal into user contributions and made use of

$$\mathbf{P}(q) = \sum_i \mathbf{P}[i]q^{-i} \tag{3.4.3}$$

Furthermore, note that we can also write

$$\underline{\underline{\mathbf{E}}}_k(q)\mathbf{H}_k\mathbf{A}_k \;=\; \sum_{m=1}^{M} \underline{\mathbf{E}}_{k,m}(q)\mathbf{h}_{k,m}A_{k,m} = \sum_{m=1}^{M} \mathbf{E}_{k,m}(q)A_{k,m} = \underline{\mathbf{E}}_k(q)\mathbf{A}_k = \mathbf{E}_k(q) \tag{3.4.4}$$

where the matrix dimensions are: $\underline{\underline{\mathbf{E}}}(q) = (JLQ \times KMQ)$, $\underline{\mathbf{E}}(q) = (JLQ \times KM)$, $\mathbf{E}(q) = (JLQ \times K)$. Applying pulse-shaped matched filtering, despreading and antenna recombining, we can define

$$\begin{aligned} \mathbf{x}[n] &= \mathbf{H}^H \underline{\underline{\mathbf{E}}}^\dagger(q)\mathbf{y}[n] &(3.4.5)\\ &= \underbrace{\mathbf{H}^H \underline{\underline{\mathbf{E}}}^\dagger(q)\underline{\underline{\mathbf{E}}}(q)\mathbf{H}}_{\mathbf{R}(q)=\mathbf{I}+\overline{\mathbf{R}}(q)} \mathbf{A}\mathbf{a}[n] + \mathbf{H}^H \underline{\underline{\mathbf{E}}}^\dagger(q)\mathbf{v}[n] \\ &= \underline{\mathbf{E}}^\dagger(q)\underline{\mathbf{E}}(q)\mathbf{A}\mathbf{a}[n] + \underline{\mathbf{E}}(q)^\dagger\mathbf{v}[n] \end{aligned}$$

where $\underline{\mathbf{E}}^\dagger(q) = \underline{\mathbf{E}}^H(1/q^*)$ is the *paraconjugate* and

$$\sum_i \underline{\mathbf{E}}^\dagger_{k,m}[i]\underline{\mathbf{E}}_{k,m}[-i] = 1, \forall\, k \in \{1 \ldots K\}, m \in \{1 \ldots M\}$$

Therefore, $\mathbf{x}[n] = [x_{1,1}[n] \ldots x_{K,M}[n]]^T$ are the pathwise RAKE outputs, spatially but not temporally recombined. Let us further define

$$\begin{aligned} \mathbf{R}(q) &= \underline{\mathbf{E}}^\dagger(q)\underline{\mathbf{E}}(q) \;\; (KM \times KM) &(3.4.6)\\ &= \sum_i \mathbf{R}[i]q^{-1} \\ diag\{\mathbf{R}[0]\} &= \mathbf{I} &(3.4.7) \end{aligned}$$

where the fact that the diagonal elements of $\mathbf{R}[0]$ are all unity, derives from the assumption of normalised spreading codes, i.e. $\mathbf{s}_k^H\mathbf{s}_k = 1$ and using the normalisation of the antenna array response vectors $\mathbf{h}_{k,m} : \|\mathbf{h}_{k,m}\| = 1$. From equation (3.4.5), it is clear that decorrelator to estimate the amplitude data product, $\mathbf{A}\mathbf{a}[n]$, is given by $\mathbf{R}^{-1}(q)$. We can now use the polynomial expansion introduced in section 3.2 to write the pathwise zero-forcing receiver by

$$\mathbf{R}^{-1}(q) \approx \tilde{\mathbf{R}}^{-1}(q) = \sum_{b=0}^{B}(-\overline{\mathbf{R}}(q))^b \tag{3.4.8}$$

where we have truncated the infinite series to $B+1$ terms. We now propose to introduce diagonal polynomial weighting matrices instead of scalar weighting coefficients, thereby increasing the degrees of freedom available to us. This corresponds to introducing a scalar coefficient *per path*. Let us define $\mathbf{D}_b = diag\{d_{b,1}, \ldots, d_{b,KM}\}$ and write

$$\tilde{\mathbf{R}}^{-1}(q) = \sum_{b=0}^{B}\mathbf{D}_b\overline{\mathbf{R}}^b(q) \tag{3.4.9}$$

or also

$$\tilde{\mathbf{R}}^{-1}(q) = \sum_{b=0}^{B} \mathbf{D}_b \mathbf{R}^b(q) \tag{3.4.10}$$

Note that we can also write the polynomial in terms of $\mathbf{R}(q)$ since there is a one-to-one relationship between the expansions in $\mathbf{R}(q)$ and $\overline{\mathbf{R}}(q)$. Explicitly,

$$\begin{aligned}
\sum_{b=0}^{B} \mathbf{D}_b \overline{\mathbf{R}}^b(q) &= \sum_{b=0}^{B} \mathbf{D}_b \left(\mathbf{R}(q) - \mathbf{I}\right)^b \\
&= \sum_{b=0}^{B} \mathbf{D}_b \sum_{j=0}^{b} \mathbf{R}^j(q)(-\mathbf{I})^{b-j} \binom{b}{j} \\
&= \sum_{j=0}^{B} \underbrace{\sum_{b=j}^{N} \binom{b}{j} (-1)^{b-j} \mathbf{D}_b}_{\Delta_j} \mathbf{R}^j(q) \\
&= \sum_{j=0}^{B} \Delta_j \mathbf{R}^j(q)
\end{aligned}$$

where Δ_j is another diagonal matrix.

Typically, we would only be interested in $B \in \{1,2\}$ stages after the RAKE in order to keep complexity at a reasonable level. Note that the additional complexity associated with every PE stage is about twice the complexity of the RAKE, as mentioned in section 3.2.

3.4.2 Pathwise Filter Design

A first possibility for a pathwise design is to let $\mathbf{D}_0$ be an identity matrix, and defining $\mathbf{z}[n] = \mathbf{R}(q)\mathbf{x}[n]$. We can write (3.4.9) for $B = 1$ as

$$\tilde{\mathbf{R}}^{-1}(q) = \mathbf{I} + (\mathbf{I} - \mathbf{D}\mathbf{R}(q))$$

which allows us to determine $\mathbf{D}$ blindly by minimising the following variance criterion.

$$\begin{aligned}
\mathbf{D}^o &= \arg\min_{\mathbf{D}} E\|(\mathbf{I} - \mathbf{D}\mathbf{R}(q))\mathbf{x}[n]\|^2 \\
&= diag\{\mathbf{R}_{xz}\}\left(diag\{\mathbf{R}_{zz}\}\right)^{-1}
\end{aligned} \tag{3.4.11}$$

where $\mathbf{R}_{xz} = E\{\mathbf{x}[n]\mathbf{z}^H[n]\}$ and $\mathbf{R}_{zz}$ correspondingly. The resulting performance will be evaluated by simulation. Note that no matrix inversions are required to compute the $d_{i,j}$'s in the above approach since the required correlation matrices are diagonal. An alternative is to extend the approach in (3.4.11) to a pilot-assisted scenario. In that case, we can solve for $\mathbf{D}$ using the following LMMSE criterion.

$$\begin{aligned} \mathbf{D}^o &= \arg\min_{\mathbf{D}} E\|\mathbf{A}\mathbf{a}[n] - (\mathbf{x}[n] - \mathbf{D}(\mathbf{R}(q) - \mathbf{I})\mathbf{x}[n])\|^2 \\ &= diag\{\mathbf{A}(\mathbf{R}_{ax} - \mathbf{R}_{az}) - \mathbf{R}_{xx} + \mathbf{R}_{xz}\}\left[diag\{\mathbf{R}_{xx} - 2\mathbf{R}_{xz} + \mathbf{R}_{zz}\}\right]^{-1} \end{aligned} \tag{3.4.12}$$

In the above examples, we have so far assumed $\mathbf{D}_0 = \mathbf{I}$ based on the polynomial expansion of $\mathbf{R}$. This is, however, not optimal in general and we can write the extension to an arbitrary number of stages as

$$\mathbf{D}_i^o = \arg\min_{\mathbf{D}_i: i\in 0\ldots B} E\|\mathbf{A}\mathbf{a}[n] - \sum_{b=0}^{B}\mathbf{D}_b\mathbf{R}^b(q)\mathbf{x}[n]\|^2 \tag{3.4.13}$$

This can be solved through a set of linear equations, satisfying

$$\mathbf{D}_u = \left[\mathbf{A}diag\{\mathbf{R}_{az_u}\} - \sum_{\substack{b=0\\ b\neq u}}^{B}\mathbf{D}_b diag\{\mathbf{R}_{z_b z_u}\}\right](diag\{\mathbf{R}_{z_u z_u}\})^{-1}\ \forall u \in \{0,\ldots,B\} \tag{3.4.14}$$

This is, however, not convenient to solve and we can proceed differently. Looking at any row j (corresponding to some path of some user) in equation (3.4.13), we can equivalently write

$$\begin{aligned} \mathbf{d}_j^o &= \arg\min_{\mathbf{d}_j} E|A_j a_l[n] - \mathbf{d}_j\mathbf{w}_j[n]|^2 \\ &= A_j E(a_l[n]\mathbf{w}_j^H[n])(E\mathbf{w}_j[n]\mathbf{w}_j^H[n])^{-1} \end{aligned} \tag{3.4.15}$$

where $j \in \{1\ldots KM\}$ is the path index, $l = \lceil \frac{j}{M} \rceil$ the corresponding data symbol and we have used the following definitions:

$$\begin{aligned} \mathbf{d}_j &= [d_{0,j}\ldots d_{B,j}] \\ \mathbf{z}_b[n] &= \mathbf{R}^b(q)\mathbf{x}[n] \\ &= [z_{b,1}[n]\ldots z_{b,KM}[n]]^T \\ \mathbf{w}_j &= [z_{0,j}\ldots z_{B,j}]^T \end{aligned}$$

and hence the problem decouples nicely into a path-by-path solvable problem. It is worth noting that this is not the case when the polynomial coefficient matrices $\mathbf{D}_b$ are replaced by scalars as the solution for the coefficients involves the summation over the paths j and hence there is no decoupling between paths nor users, i.e.

$$\begin{aligned} d_i^o &= \arg \min_{d_i : i \in 0 \dots B} E \|\mathbf{Aa}[n] - \sum_{b=0}^{B} d_b \mathbf{R}^b(q)\mathbf{x}[n]\|^2 \\ &= \sum_j E(A_j a_l[n] \mathbf{w}_j^H[n]) (\sum_j E\mathbf{w}_j[n]\mathbf{w}_j^H[n])^{-1} \end{aligned} \tag{3.4.16}$$

A variant of the approach in (3.4.13) is the sequential computation of the stages where each stage works on the error signal from the previous stage, i.e.

$$\begin{aligned} \mathbf{D}_b^o &= \arg \min_{\mathbf{D}_b} ||\mathbf{Aa}[n] - \left(\widehat{\mathbf{Aa}}_{b-1}[n] + \mathbf{D}_b\mathbf{R}^b(q)\mathbf{x}[n]\right)||^2 \\ &= \arg \min_{\mathbf{D}_b} ||\mathbf{e}_{b-1} - \mathbf{D}_b\mathbf{R}^b(q)\mathbf{x}[n]||^2 \\ &= diag\left(E\, \mathbf{e}_{b-1}[n]\mathbf{z}_b^H[n]\right)\left(diag(E\,\mathbf{z}_b[n]\mathbf{z}_b^H[n])\right)^{-1} \\ \mathbf{e}_b[n] &= \mathbf{Aa}[n] - \widehat{\mathbf{Aa}}_b[n] \end{aligned} \tag{3.4.17}$$

This approach is evidently suboptimal with respect to the more general approach given in (3.4.13) and in practise may be difficult to implement due to the necessity of obtaining an estimate of the error signal. We shall therefore concentrate on the approach in (3.4.13).

Given the amplitude data product after PE interference cancellation, we now need to recombine the path contributions to obtain the symbol estimate:

$$\hat{\mathbf{a}}[n] = \mathbf{K}^H\mathbf{F}(q)\left[\mathbf{R}(q)\mathbf{Aa}[n] + \underline{\mathbf{E}}^\dagger(q)\mathbf{v}[n]\right]$$

where $\mathbf{K}$ $(KM \times K)$ is a general recombination matrix of the same block diagonal structure as $\mathbf{A}$, namely $\mathbf{K} = diag\{\mathbf{K}_1, \dots, \mathbf{K}_K\}$. Maximum ratio combining is $\mathbf{K} = \mathbf{A}$. $\mathbf{F}(q)$ defines the linear filter corresponding to the PE approach above in (3.4.13). For the symbol estimate of user one, we have

$$\hat{a}_1[n] = \mathbf{K}_1^H\left[\mathbf{Z}_1(q)\mathbf{A}_1 a_1[n] + \overline{\mathbf{Z}}_1(q)\overline{\mathbf{A}}_1\overline{\mathbf{a}}_1[n] + \mathbf{X}(q)\mathbf{v}[n]\right]$$

where

$$\begin{aligned}
\mathbf{K} &= diag\{\mathbf{K}_1, \overline{\mathbf{K}}_1\} \\
[\mathbf{I}_M \mathbf{0}]\,\mathbf{F}(q)\mathbf{R}(q) &= [\mathbf{Z}_1(q)\overline{\mathbf{Z}}_1(q)] \\
\mathbf{X}(q) &= [\mathbf{I}_M \mathbf{0}]\,\mathbf{F}(q)\underline{\mathbf{E}}^{\dagger}(q) \\
\mathbf{a}[n] &= [a_1[n]\overline{\mathbf{a}}_1^T[n]]^T \\
\mathbf{A} &= diag\{\mathbf{A}_1, \overline{\mathbf{A}}_1\}
\end{aligned}$$

and $(.)_1$ is a signal model component acting on the useful signal contribution of user one whereas $\overline{(.)}_1$ defines the interfering terms. Hence, the output SINR of user one can be written as

$$SINR = \frac{\sigma_a^2|\mathbf{K}_1^H\mathbf{Z}_1[0]\mathbf{A}_1|^2}{\mathbf{K}_1^H\left(\sigma_a^2\sum_{i\neq 0}\mathbf{Z}_1[i]\mathbf{A}_1\mathbf{A}_1^H\mathbf{Z}_1^H[i] + \sigma_a^2\sum_i\overline{\mathbf{Z}}_1[i]\overline{\mathbf{A}}_1\overline{\mathbf{A}}_1^H\overline{\mathbf{Z}}_1^H[i] + \sigma_v^2\sum_i\mathbf{X}[i]\mathbf{X}^H[i]\right)\mathbf{K}_1}$$

Maximum ratio combining is, however, not optimal since the pathwise estimate is not determined with respect to a symbol optimality criterion (but the Amplitude-data product) whereas the SINR is computed for the symbol estimate. Hence, performance can be further improved by maximising the output SINR for the symbol estimate with respect to the recombining vector, $\mathbf{K}_1$. We can hence optimise the SINR with respect to the recombination vector, $\mathbf{K}_1$, by solving

$$\mathbf{K}_1^o = \arg\max_{\mathbf{K}_1} SINR = \arg\max_{\mathbf{K}_1}\frac{\sigma_a^2|\mathbf{K}_1^H\mathbf{Z}_1[0]\mathbf{A}_1|^2}{\mathbf{K}_1^H\mathbf{R}_1\mathbf{K}_1} \tag{3.4.18}$$

where we have defined

$$\mathbf{R}_1 = \sigma_a^2\sum_{i\neq 0}\mathbf{Z}_1[i]\mathbf{A}_1\mathbf{A}_1^H\mathbf{Z}_1^H[i] + \sigma_a^2\sum_i\overline{\mathbf{Z}}_1[i]\overline{\mathbf{A}}_1\overline{\mathbf{A}}_1^H\overline{\mathbf{Z}}_1^H[i] + \sigma_v^2\sum_i\mathbf{X}[i]\mathbf{X}^H[i] \tag{3.4.19}$$

The solution is of the generalised eigenvalue type and given by

$$\mathbf{K}_1^o = \mathbf{R}_1^{-1}\mathbf{Z}_1[0]\mathbf{A}_1 \tag{3.4.20}$$

and the resulting, maximised SINR, is given by

$$SINR_{max} = \sigma_a^2\mathbf{A}_1^H\mathbf{Z}_1^H[0]\mathbf{R}_1\mathbf{Z}_1[0]\mathbf{A}_1$$

One of the main advantages of applying pathwise polynomial expansion is the availability of the pathwise outputs *after* interference cancellation. Often, the complex amplitudes are estimated by correlating the pathwise RAKE outputs with a pilot signal to estimate the complex amplitudes. Compared to this approach, our method will provide us with an amplitude data product estimate at a higher SINR and therefore allow better estimation of fastly varying complex amplitude coefficients, $A_{k,m}$. Indeed, there are a number of ways on how we can interpret this fact: If the amount of data available for the estimation of the complex amplitudes is fixed, we will achieve a better SINR in our estimates which will allow faster adaptation of the receiver filters. Alternatively, we can take the point of view that our approach will require less data to obtain the same estimation quality, hence a shorter pilot. Yet another view is that we would require less power in the pilot to achieve the same estimation quality.

3.4.3 Joint filter and recombination design

Using maximum ratio recombining with $\mathbf{A}$, we can write the symbol estimate resulting from the filtering and combining from (3.4.13) as

$$\hat{\mathbf{a}}[n] = \mathbf{A}^H \sum_{b=0}^{B} \mathbf{D}_b \mathbf{R}^b(q)\mathbf{x}[n] = \sum_{b=0}^{B} \mathbf{W}_b \mathbf{R}^b(q)\mathbf{x}[n] \tag{3.4.21}$$

where $\mathbf{W}_b = \mathbf{A}^H \mathbf{D}_b = diag\{\mathbf{w}_{b,1}, \ldots, \mathbf{w}_{b,K}\}$, $\mathbf{w}_{b,k}$ is of dimension $M \times 1$. Therefore, $\mathbf{W}_b$ is another block diagonal matrix of the same structure and dimensions as $\mathbf{A}^H$. Note that stage $b = 0$ hence corresponds to a Generalised RAKE (G-RAKE). The G-RAKE is a RAKE where the path recombination vectors are optimised to maximise the symbol estimate SINR and was introduced in [61, 62]. Note however, that the direct application of the above approach would no longer provide the pathwise, SINR enhanced, outputs but the number of coefficients at our disposal remains at one scalar per path. Further, the performance of (3.4.21) in terms of output SINR at the symbol estimate is by construction equal or better than that of the approach in (3.4.13) since direct optimisation for the symbol estimate can only be better than the sequential optimisation of the amplitude data product, followed by max. SINR recombining. We can solve (3.4.21) per user:

$$\begin{aligned} \mathbf{w}_k^o &= \arg\min_{\mathbf{w}_k} ||a_k[n] - \mathbf{w}_k \mathbf{g}_k[n]||^2 \\ &= E(a_k[n]\mathbf{g}_k^H[n])(E\mathbf{g}_k[n]\mathbf{g}_k^H[n])^{-1} \end{aligned} \tag{3.4.22}$$

where $\mathbf{w}_k = [\mathbf{w}_{0,k} \ldots \mathbf{w}_{B,k}]$, $\mathbf{w}_{b,k}$ has dimensions $M \times 1$ and $\mathbf{g}_k[n] = [\mathbf{z}_{0,k}[n] \ldots \mathbf{z}_{B,k}[n]]^T$. $\mathbf{z}_{b,k}[n] = [\mathbf{0} \ldots \mathbf{0}\ \mathbf{I_M}\ \mathbf{0} \ldots \mathbf{0}]\mathbf{z_b}[\mathbf{n}]$ where $\mathbf{0}$ is $M \times M$ and $\mathbf{z}_{b,k}[n]$ is simply the contribution in $\mathbf{z}_b[n]$ for the paths of user k. Alternatively, (3.4.22) can be solved using the Linearly Constrained Minimum Variance (LCMV) approach, shown for user 1 to simplify notation and without loss of generality, as follows

$$\begin{aligned} \mathbf{w}_1^o &= \arg\min_{\mathbf{w}_1} \mathbf{w}_1 \mathbf{R}_{\mathrm{g}_1\mathrm{g}_1} \mathbf{w}_1^H \text{ subject to } \mathbf{w}_1 \Gamma_1[0] \mathbf{A}_1 = 1 \\ \mathbf{w}_1^o &= \mathbf{A}_1^H \Gamma_1^H[0] \mathbf{R}_{\mathrm{g}_1\mathrm{g}_1}^{-1} \end{aligned} \tag{3.4.23}$$

where

$$\begin{aligned} \Gamma_1[0] &= (\mathbf{I}_B \otimes [\mathbf{I}_M\ \mathbf{0}])[\mathbf{R}[0] \ldots \mathbf{R}^{B+1}[0]]^T [\mathbf{I}_M\ \mathbf{0}]^T \\ \mathbf{R}_{\mathrm{g}_1\mathrm{g}_1} &= E(\mathbf{g}_1[n]\mathbf{g}_1^H[n]) \end{aligned} \tag{3.4.24}$$

The constraint ensures that the contribution of the data $a_1[n]$ in $\mathbf{g}_1[n]$ remains constant under the application of the filter while minimising the estimate output variance.

While the two solutions (by LMMSE and LCMV) are equivalent when all the parameters are known, note that the computation of the LMMSE filter from (3.4.22) requires the desired data signal, $a_k[n]$ or an estimate thereof, whereas no information on the fastly varying amplitudes $\mathbf{A}_k$ is required. For the LCMV approach, the situation is the inverse and for both cases, the estimates of either $a_k[n]$ or $\mathbf{A}_k$ need to be provided. Hence, in practice, we would use an approach such as (3.4.13) to obtain the required estimates in conjunction with (3.4.21).

In an adaptive filtering setting, the LCMV approach would be expected to be more sensitive to estimation errors, partly because of the error introduced in the minimisation constraint, partly because the estimation of the data can be assumed to be more robust than the estimation of the amplitudes since the data originates from a strictly finite alphabet.

A natural extension to our proposal to introduce diagonal weighting coefficient matrices instead of scalars, as well as providing an interesting basis for comparison, is to introduce a symbolwise (joint) approach where we apply a single scalar coefficient per symbol per stage instead of per path, i.e.

$$\mathbf{D}_b^o = \arg\min_{\mathbf{D}_b} ||\mathbf{a}[n] - \sum_{b=0}^{B} \mathbf{D}_b (\mathbf{A}^H \mathbf{R}(q) \mathbf{A})^b \mathbf{A}^H \mathbf{x}[n]||^2 \tag{3.4.25}$$

where $\mathbf{D}_b = diag\{d_{b,1}, \ldots, d_{b,K}\}$ and $d_{b,k}$ are scalars. This can be solved in a user-by-user fashion, analogue to the procedure used in the LMMSE approach above. Note that this approach is a simple extension of the work in [51] which used a scalar coefficient per stage instead of a scalar per user.

3.4.4 Extension to spatio-temporal processing

The extension to spatio-temporal processing is straightforward. Considering equation (3.4.5)

$$\mathbf{x}[n] = \underbrace{\mathbf{H}^H \underline{\underline{\mathbf{E}}}^\dagger(q) \underline{\underline{\mathbf{E}}}(q) \mathbf{H}}_{\mathbf{R}(q)=\mathbf{I}+\overline{\mathbf{R}}(q)} \mathbf{A}\mathbf{a}[n] + \mathbf{H}^H \underline{\underline{\mathbf{E}}}^\dagger(q) \mathbf{v}[n] \tag{3.4.26}$$

where $\mathbf{R}(q)$ is defined so as to be situated before pathwise recombination takes place, i.e. to get pathwise polynomial expansion. Let us define

$$\mathbf{x}'[n] = \underbrace{\underline{\underline{\mathbf{E}}}^\dagger(q) \underline{\underline{\mathbf{E}}}(q)}_{\mathbf{R}'(q)=\mathbf{I}+\overline{\mathbf{R}}'(q)} \mathbf{H}\mathbf{A}\mathbf{a}[n] + \underline{\underline{\mathbf{E}}}^\dagger(q) \mathbf{v}[n] \tag{3.4.27}$$

To extend to the spatio-temporal case, we have defined $\mathbf{R}'(q) = \underline{\underline{\mathbf{E}}}^\dagger(q)\underline{\underline{\mathbf{E}}}(q)$ $(KMQ \times KMQ)$ in which case we would be situated before antenna recombination and the polynomial expansion would be path-antenna-wise. The techniques introduced above would directly apply and notably equation (3.4.13) would now read:

$$\mathbf{D}_i^o = \arg \min_{\mathbf{D}_i : i \in 0 \ldots B} E\|\mathbf{H}\mathbf{A}\mathbf{a}[n] - \sum_{b=0}^{B} \mathbf{D}_b (\mathbf{R}'(q))^b \mathbf{x}'[n]\|^2 \tag{3.4.28}$$

Further, consider the approach given in (3.4.21). Using the definitions above, the symbol estimate would be given by

$$\hat{\mathbf{a}}[n] = \mathbf{A}^H \mathbf{H}^H \sum_{b=0}^{B} \mathbf{D}_b \left(\mathbf{R}'(q)\right)^b \mathbf{x}'[n] = \sum_{b=0}^{B} \mathbf{W}'_b \left(\mathbf{R}'(q)\right)^b \mathbf{x}'[n] \tag{3.4.29}$$

where $\mathbf{W}'_b$ would be of the same structure as $\mathbf{A}^H \mathbf{H}^H$ which represents maximum ratio spatio-temporal recombining. Hence, the approaches proposed and their corresponding solutions remain fundamentally unchanged and can be modified easily to the spatio-temporal case. We will not pursue this any further at this point.

3.5 Numerical Simulation Results

In the following section, we will discuss the numerical results obtained from simulations. The spreading codes consist of i.i.d binary random variables such that $s_{k,l} \in \frac{1}{\sqrt{L}}\{+1,-1\}$ and therefore the spreading coded are normalised, $\mathbf{s}_k^H\mathbf{s}_k = 1$. We assume a single receiver antenna ($Q = 1$). First, we will show some results for the approaches providing pathwise outputs, followed by asynchronous scenarios where we compare with the approaches providing a symbol level output only. In order to keep complexity realistic we use only one extra stage after the rake, i.e. $B = 1$.

3.5.1 Pathwise Output Approaches

In this section, results will be shown comparing the results of the approaches providing pathwise outputs. All the simulations in figures 3.2, 3.3 and 3.4 show results for the output SINR (at symbol estimate level) obtained for user 1, averaged over 400 different channel realisations as a function of the SNR. SNR and SINR are calculated with respect to user 1. We will compare the following approaches to the RAKE receiver:

- PE from (3.4.8): $\widehat{\mathbf{Aa}}[n] = \sum_{b=0}^{B}(-\overline{\mathbf{R}}(q))^b\mathbf{x}[n]$
- PE-S from (3.4.16): $\widehat{\mathbf{Aa}}[n] = \sum_{b=0}^{B} d_b\mathbf{R}^b(q)\mathbf{x}[n]$
- PE-D from (3.4.11): $\widehat{\mathbf{Aa}}[n] = (\mathbf{I} + (\mathbf{I} - \mathbf{D}\mathbf{R}(q)))\,\mathbf{x}[n]$
- PE-DD from (3.4.12): $\widehat{\mathbf{Aa}}[n] = (\mathbf{I} - \mathbf{D}(\mathbf{R}(q) - \mathbf{I}))\,\mathbf{x}[n]$
- PE-DDD from (3.4.13): $\widehat{\mathbf{Aa}}[n] = \sum_{b=0}^{B} \mathbf{D}_b\mathbf{R}^b(q)\mathbf{x}[n]$

In figure 3.2, we are working in a relatively low load scenario ($\beta = K/L = 0.25$) and all the receivers can be seen to perform better than the RAKE with the PE-DDD approach doing best. It is notable, that in this case, even the unoptimised, i.e. truncated, polynomial expansion receiver (PE) provides some gain with respect to the RAKE. In the case of high loading($\beta = 0.75$), figure 3.3, it can be seen that the truncated PE receiver does no longer work whereas the optimised approaches still perform significantly better than the RAKE. Also note that the proposed approaches outperform the scalar PE (PE-S). In figure 3.4, the output SINR is shown as a function of the loading factor, β. We can see that while the proposed approaches are sensible to the loading factor, they degrade gracefully. Further note,

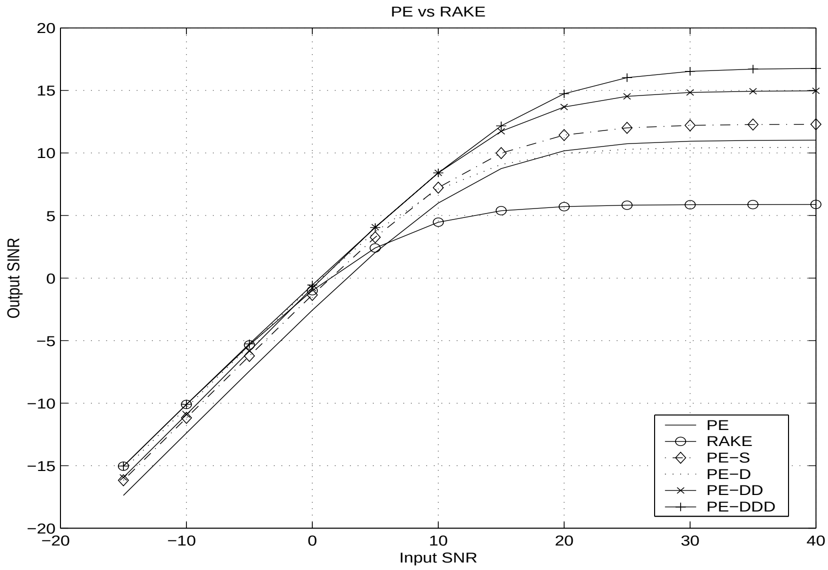

Figure 3.2: Polynomial expansion vs. RAKE: K=4, L=16, SIR = -10dB

that the PE result obtained corresponds and confirms the theoretical expression obtained in equation (3.2.13). In summary, we can see that the general multistage receiver, PE-DDD equation (3.4.13), performs best and since the complexity of the different approaches above is similar, the PE-DDD approach will be retained for the simulations comparing the approaches which provide a symbol level output only.

3.5.2 Asynchronous results

In this paragraph, we show extended numerical results obtained for the multipath case, including the approaches which provide the symbol estimate directly. We will use the following approaches:

- RAKE: $\hat{\mathbf{a}}[n] = \mathbf{A}^H \mathbf{x}[n]$
- Scalar PE (Moshavi) from (3.3.5): $\hat{\mathbf{a}}[n] = \sum_{b=0}^{B} d_b \left(\mathbf{A}^H \mathbf{R}(q) \mathbf{A}\right)^b \mathbf{A}^H \mathbf{x}[n]$
- Pathwise PE/PE-DDD from (3.4.13): $\hat{\mathbf{a}}[n] = \mathbf{K}^H \sum_{b=0}^{B} \mathbf{D}_b \mathbf{R}^b(q) \mathbf{x}[n]$
- Joint PE from (3.4.21): $\hat{\mathbf{a}}[n] = \mathbf{A}^H \sum_{b=0}^{B} \mathbf{D}_b \mathbf{R}^b(q) \mathbf{x}[n] = \sum_{b=0}^{B} \mathbf{W}_b \mathbf{R}^b(q) \mathbf{x}[n]$

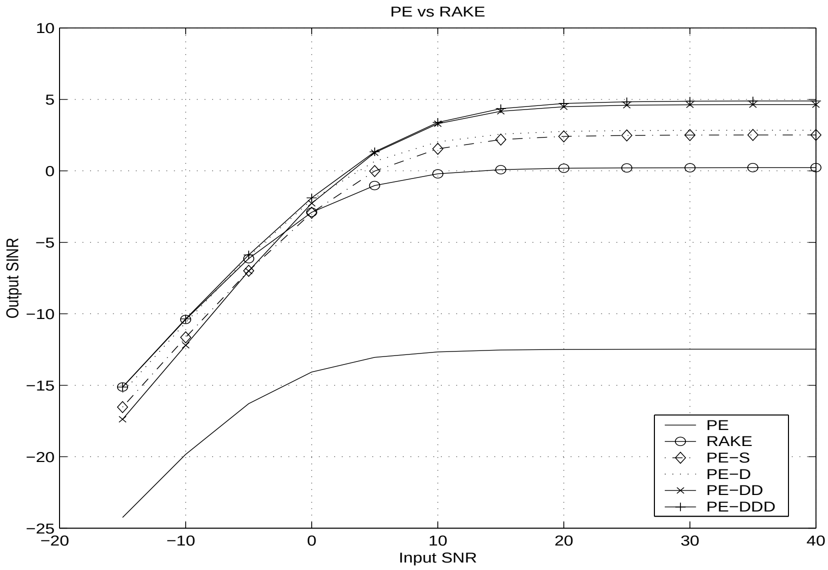

Figure 3.3: Polynomial expansion vs. RAKE: K = 12, L = 16, SIR = -10dB

We assume the maximum delay spread to be smaller than half a symbol period, T. In figure 3.5 we see the results of an asynchronous single path system ($M = 1,\ Q = 1$) where all the users have equal power. In this case, we can see that the scalar approach is performing practically equally well to the joint receiver while the pathwise is doing worse. If, however, the user powers are not equal, figure 3.6, then the scalar approach is performing only just better than the RAKE while the other approaches are not affected. When we introduce multipath, with $M = 2$ paths per user, figure 3.7, while maintaining equal power (that is, path powers are random but every user has an equal total power), we can see that the joint approach continues to outperform the scalar approach. However, the pathwise approach is only marginally better due to the small number of paths. In figure 3.8, finally, we have 4 paths per user. Whereas the scalar performs about the same as in the two path case, the pathwise approach and the joint approach now clearly outperform both the RAKE and the Scalar PE. Note that the Joint approach becomes zero-forcing (near-far resistant) in this configuration since the number of coefficients at its disposal (for user 1), $M \times (B+1) = 8$, is greater than the number of interfering users, $K - 1 = 7$. Clearly, the Joint approach is the most promising of the proposed receivers. However, it does require estimates of either

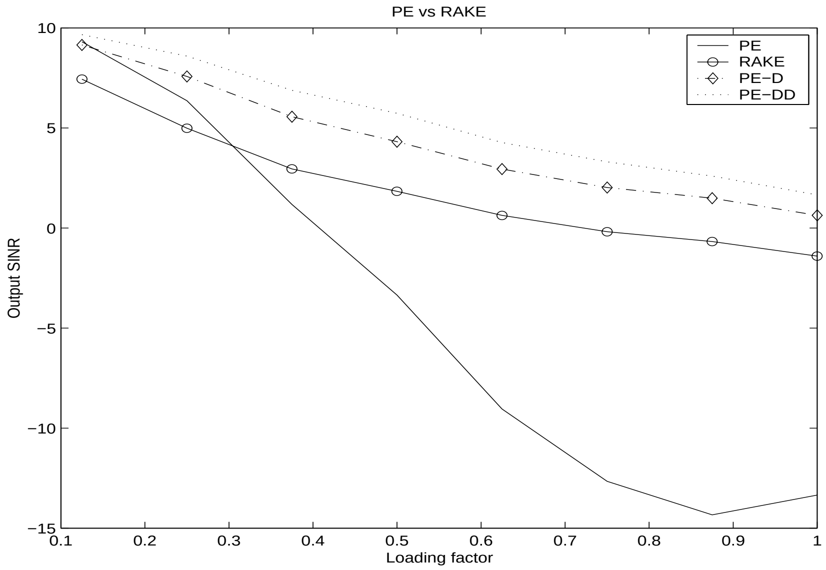

Figure 3.4: Polynomial expansion as a function of loading factor: L =16, SNR = 10dB, equal power users

the data or the amplitudes and therefore would in practice be used together with an approach that provides those estimates, such as the Pathwise/PE-DDD approach.

3.6 Conclusions

We have introduced the application of polynomial expansion receivers to pathwise interference cancellation. Polynomial expansion is an approximation technique for LMMSE and Decorrelating receivers and is particularly well suited for CDMA, due to the presence of a large number of small correlations. The method allows the approximation of the computationally costly matrix inverse required by both the LMMSE receiver and the decorrelator by expanding the matrix inverse as a polynomial. However, for polynomial expansion to work, polynomial weighting coefficients need to be introduced. We have shown, that giving each signal component a separate scaling factor allows for improved performance at a small cost. We have introduced polynomial expansion at path level, which allows for interference cancellation and hence improved parameter estimation. Also, we have shown that the extension

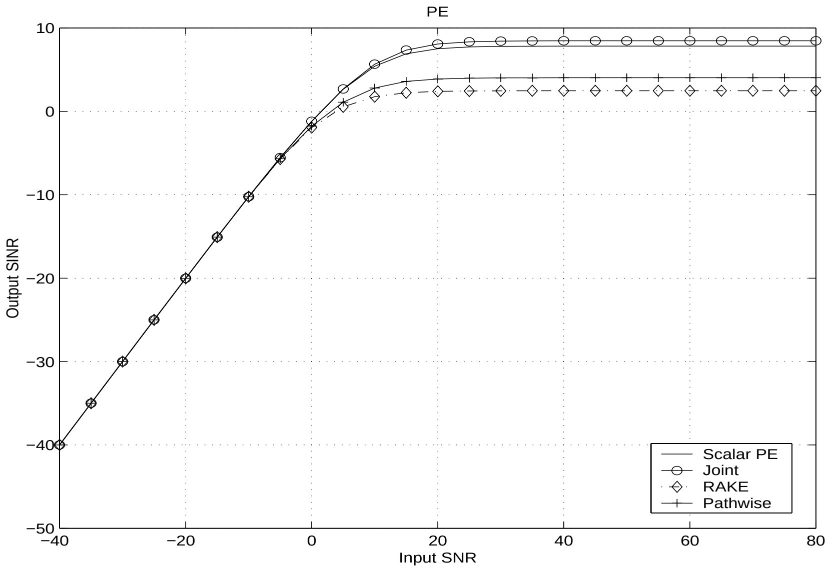

Figure 3.5: Polynomial expansion: L=16, K=8, M=1, equal power users

to spatio-temporal processing is straightforward for the proposed receivers. Furthermore, we introduced new approaches at the symbol level which provide more degrees of freedom by still allowing one scalar weighting coefficient per signal component. Compared to previous methods, we have demonstrated that significant performance gains can be achieved. These results have been published in [63, 64].

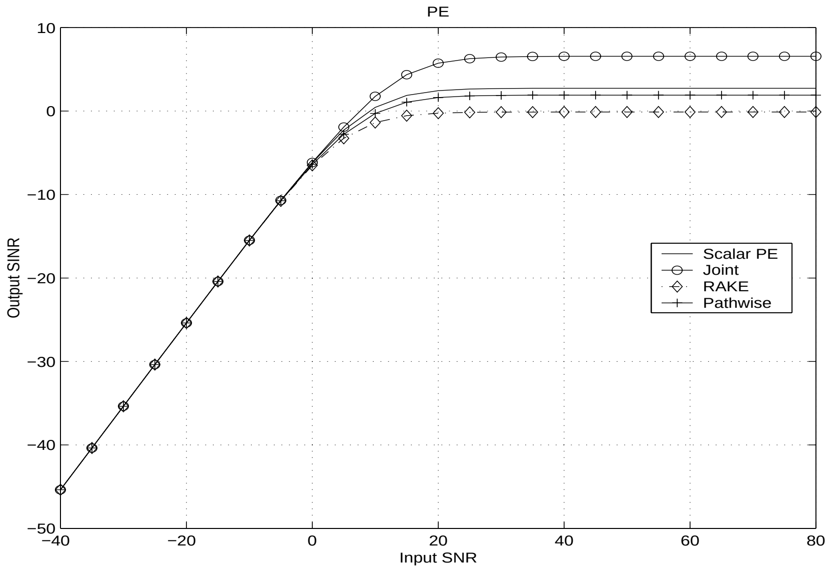

Figure 3.6: Polynomial expansion: L=16, K=8, M=1, unequal power users

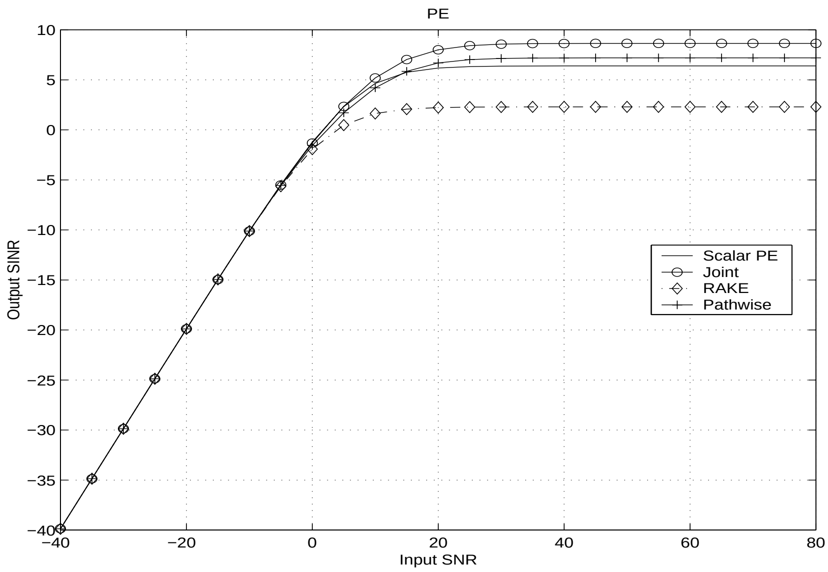

Figure 3.7: Polynomial expansion: L=16, K=8, M=2, equal power users

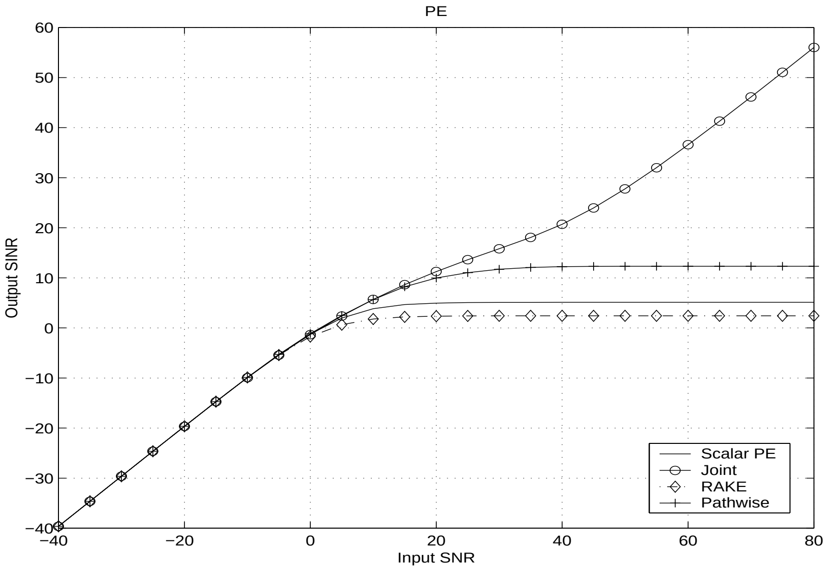

Figure 3.8: Polynomial expansion: L=16, K=8, M=4, equal power users

Chapter 4

Large System Analysis for Pathwise Polynomial Expansion

4.1 Introduction

We have shown in the last chapter how polynomial expansion can be applied to pathwise interference cancellation. However, it is very difficult to get any qualitative insight as to the behaviour of such a system. Simulations approaching more realistic scenarios with many users and long spreading codes are computationally too costly and the direct analysis of the expression for the SINR is firstly very complicated and secondly always a function of the particular spreading codes, amplitudes and delays for each realisation. For example, the LMMSE receiver, depends on the spreading codes and powers from *all* the users and it is therefore very difficult to make meaningful statements using standard analytical methodologies. In this chapter we will therefore make use of what is termed *large system analysis*. Since the realisation of the spreading codes affects the SINR which can be obtained, the spreading is assumed to be random in large system analysis. The principle then is to assume that the number of users, as well as the spreading factor, will tend to infinity while the ratio of the two, the loading factor, remains constant. This results in a system involving very large random matrices. Results from *random matrix theory* and *free probability theory* then allow us to obtain closed form expressions for the SINR, fundamentally based on the fact that the empirical eigenvalue distributions of such large random matrices converges to a non-random limit. Furthermore, it is then possible to obtain information about moments of functions of random matrices using only the limiting moments of the individual matrices involved, something which is generally not possible.

Random matrices have been studied for quite some time in mathematics and theoretical physics, for applications in quantum physics. Mostly, these studies were motivated by the need to find the eigenvalues of large random matrices, associated with energy levels. The results obtained by Wigner around 1955 for the limiting eigenvalue density (the semi-circle law) for random matrices generated a huge interest in the theoretical and nuclear physics communities [65–70].

Free probability theory, on the other hand, is a theory of non-commutative probability in which the concept of independence in classical probability is replaced by that of freeness. This theory was introduced around the mid-eighties by Voiculescu while studying problems in the theory of von Neumann algebras. It was, however, only around 1990 that the link between random matrix theory and free probability theory was made as Voiculescu recognised that certain large random matrices can be modelled as free random variables [71, 72].

To our knowledge, it was the papers by Silverstein and Combettes, which brought the techniques of random matrix theory and free probability first to the Communications community around 1992, analysing array processing problems [73, 74]. This was followed some time later by Tse and Hanly who introduced the application of large system analysis to CDMA and showed analytical results for the LMMSE and the decorrelating receivers [75]. It was demonstrated that the interference effectively decouples under the large system analysis and that the interferers provide a level of interference to the user of interest which is tractable. Furthermore, and probably most importantly, it was shown that the results derived from the analysis of infinite systems provide reasonable approximations to finite dimensional systems, with spreading gains as low $L = 32$. These results have triggered quite a number of publications where large system techniques were applied to various problems, mainly in the information theory community ([76–79] etc).

Motivated by the results in [49,52,80], we will in the following apply large system techniques to the receivers developed in chapter 3.

4.2 Asymptotic Analysis for Polynomial Expansion Receivers

We will begin the asymptotic analysis by analysing the case of a synchronous system. In particular, we will analyse the approach found in (3.4.21) and compare it to the extended Moshavi approach, i.e. (3.4.25) since this will provide the best comparison between pathwise weighting and user weighting. We shall model the synchronous system ($J = 1,\ Q = 1,\ M = 1$), as previously motivated in section 3.2 by considering the received discrete-time signal:

$$\mathbf{y}[n] = \mathbf{S}\mathbf{A}\mathbf{a}[n] + \mathbf{v}[n] \tag{4.2.1}$$

where

$$\begin{aligned} \mathbf{S} &= [\mathbf{s}_1 \ldots \mathbf{s}_K]\ (L \times K) \\ \mathbf{s}_k &= [s_{k,1} \ldots s_{k,L}]^T\ (L \times 1) \\ \mathbf{A} &= diag\{A_1, \ldots, A_K\}\ (K \times K) \\ \mathbf{a}[n] &= [a_1[n] \ldots a_K[n]]^T \end{aligned} \tag{4.2.2}$$

We further assume that the spreading codes consist of binary i.i.d. random variables such that $s_{k,l} \in \frac{1}{\sqrt{L}}\{+1, -1\}$. The signal after spreading matched filtering is therefore given by

$$\mathbf{x} = \mathbf{S}^H\mathbf{S}\mathbf{A}\mathbf{a} + \mathbf{S}^H\mathbf{v} = \mathbf{R}\mathbf{A}\mathbf{a} + \mathbf{S}^H\mathbf{v}$$

where we have omitted the time index and $\mathbf{R}$ is of dimensions $K \times K$.

4.2.1 Symbolwise Joint Approach

We shall begin by analysing the filter given in (3.4.25). The filter applied to $\mathbf{x}$, the pathwise RAKE outputs, is therefore given by

$$\mathbf{F} = \sum_{b=0}^{B} \mathbf{D}_b(\mathbf{A}^H\mathbf{R}\mathbf{A})^b\mathbf{A}^H \tag{4.2.3}$$

The symbol estimate is given by $\hat{\mathbf{a}} = \mathbf{F}\mathbf{x}$. We can write the output variance of the estimate by

$$
\begin{aligned}
E\{\hat{\mathbf{a}}^H\hat{\mathbf{a}}\} &= E\{tr(\hat{\mathbf{a}}\hat{\mathbf{a}}^H)\} \\
&= \sigma_a^2 tr\left(\mathbf{F}\mathbf{R}\mathbf{A}\mathbf{A}^H\mathbf{R}\mathbf{F}^H\right) + \sigma_v^2 tr\left(\mathbf{F}\mathbf{R}\mathbf{F}^H\right) \\
&= \sigma_a^2\left(\sum_{b=0}^{B}\sum_{i=0}^{B} tr\left(\mathbf{D}_b\mathbf{T}\Lambda^{b+i+2}\mathbf{T}^H\mathbf{D}_i^H\right)\right) \\
&\quad +\sigma_v^2\left(\sum_{b=0}^{B}\sum_{i=0}^{B} tr\left(\mathbf{D}_b\mathbf{T}\Lambda^{b+i+1}\mathbf{T}^H\mathbf{D}_i^H\right)\right)
\end{aligned} \tag{4.2.4}
$$

where we have substituted the the expression for $\mathbf{F}$ from (4.2.3) and used the eigendecomposition of $\mathbf{A}^H\mathbf{R}\mathbf{A} = \mathbf{T}\Lambda\mathbf{T}^H$. In order to investigate the behaviour of the SINR for user 1, we can look at element $(1,1)$ of the matrices under the trace operation in (4.2.4). Hence, we can write the total energy in the estimate for user one by

$$
\begin{aligned}
E\{|\hat{a}_1|^2\} &= \sigma_a^2\left(\sum_{b=0}^{B}\sum_{i=0}^{B}\sum_{l=1}^{K}\lambda_l^{b+i+2} d_{b,1} t_{l,1} t_{l,1}^* d_{i,1}^*\right) \\
&\quad +\sigma_v^2\left(\sum_{b=0}^{B}\sum_{i=0}^{B}\sum_{l=1}^{K}\lambda_l^{b+i+1} d_{b,1} t_{l,1} t_{l,1}^* d_{i,1}^*\right) \\
&= \sigma_a^2\left(\sum_{l=1}^{K}|\xi_l|^2|t_{l,1}|^2\right) + \sigma_v^2\left(\sum_{l=1}^{K}\lambda_l^{-1}|\xi_l|^2|t_{l,1}|^2\right)
\end{aligned} \tag{4.2.5}
$$

where $\xi_i = \sum_{b=0}^{B} d_{b,1}\lambda_i^{b+1}$. We can see that the power in the estimate not only depends on the eigenvalues, but also on the eigenvectors of the matrix $\mathbf{A}^H\mathbf{R}\mathbf{A}$. Note, that this is not the case when $\mathbf{D}_b$ is replaced by a scalar. We can find the useful signal part of user one in the total estimate power above from noting that

$$
\mathbf{F}\mathbf{R}\mathbf{A}\mathbf{a} = \sum_{b=0}^{B}\mathbf{D}_b(\mathbf{A}^H\mathbf{R}\mathbf{A})^{b+1}\mathbf{a} \quad = \quad \sum_{b=0}^{B}\mathbf{D}_b\sum_{i=1}^{K}\lambda_i^{b+1}\mathbf{t}_i\mathbf{t}_i^H\mathbf{a} \tag{4.2.6}
$$

and hence the useful signal part and power for user 1 can be written as

$$
Signal_1 = \sum_{b=0}^{B} d_{b,1}\sum_{i=1}^{K}\lambda_i^{b+1}|t_{i,1}|^2 a_1 \tag{4.2.7}
$$

$$
Power_1 = \sigma_a^2\sum_{i=1}^{K}\sum_{l=1}^{K}\xi_i\xi_l^*|t_{i,1}|^2|t_{l,1}|^2 \tag{4.2.8}
$$

Since the SINR is given by the ratio of the useful power over the interference and noise power, we can also write it as the ratio of useful power over total estimate power less the useful signal power, i.e.

$$SINR_1 = \frac{Power_1}{E\{|\hat{a}_1|^2\} - Power_1} = \frac{1}{\frac{E\{|\hat{a}_1|^2\}}{Power_1} - 1} \tag{4.2.9}$$

Hence, it suffices to study the ratio $Power_1/E\{|\hat{a}_1|^2\}$ which we shall call the Signal to Power ratio, SPR, to determine the SINR behaviour. Substituting for the useful signal power and the total estimate power from (4.2.8) and (4.2.5), respectively, we obtain

$$SPR_1 = \frac{\sigma_a^2 \sum_{i=1}^{K} \sum_{l=1}^{K} \xi_i \xi_l^* |t_{i,1}|^2 |t_{l,1}|^2}{\sigma_a^2 \left(\sum_{l=1}^{K} |\xi_l|^2 |t_{l,1}|^2 \right) + \sigma_v^2 \left(\sum_{l=1}^{K} \lambda_l^{-1} |\xi_l|^2 |t_{l,1}|^2 \right)} \tag{4.2.10}$$

We would now like to obtain the large system limit of the SPR by letting the number of users and the spreading gain tend to infinity while keeping the loading factor constant. That is to say, we let $K,\ L \to \infty$ while keeping $\beta = \frac{K}{L}$ constant. In order to do so, we make use of the following lemma to be able to deal with the eigenvector elements in the SPR:

Lemma 1

(Lemma 4, [80]) As $K \to \infty$ and $K = \beta N$ where all entries in S are real i.i.d. with all moments finite and the series $< \xi_\mu / k >$ be absolutely summable, then

$$\lim_{K\to\infty} \sum_{k=1}^{K} \xi_k |t_{k,m}|^2 = \lim_{K\to\infty} \frac{1}{K} \sum_{k=1}^{K} \xi_k \tag{4.2.11}$$

holds almost surely for any m.

This result is based on the fact that any inner product of a partial eigenvector with itself is proportional to its relative length in the limit [80], i.e. if we write some eigenvector in terms of subvectors, say $\mathbf{t} = [\mathbf{t}_1\ \mathbf{t}_2]^T$ where $\mathbf{t}$ is of length L and $\mathbf{t}_1$ of length L/c (c some constant), and by definition $\mathbf{t}^H \mathbf{t} = 1$, then in the limit $\lim_{L\to\infty} \mathbf{t}_1^H \mathbf{t}_1 = 1/c$. Using (4.2.11), we can now write the SPR for user one in the limit:

$$\lim_{K\to\infty} SPR_1 = \lim_{K\to\infty} \frac{\frac{\sigma_a^2}{K} \sum_{i=1}^{K} \xi_i \sum_{l=1}^{K} \xi_l^*}{\sigma_a^2 \left(\sum_{l=1}^{K} |\xi_l|^2 \right) + \sigma_v^2 \left(\sum_{l=1}^{K} \lambda_l^{-1} |\xi_l|^2 \right)} \tag{4.2.12}$$

Rewriting the summations over ξ_i in terms of the weighting coefficients and the eigenvalues gives, i.e.

$$\sum_{l=1}^{K} |\xi_l|^2 = \sum_{m=0}^{B}\sum_{b=0}^{B} d_{b,1} d^*_{m,1} \sum_{l=1}^{K} \lambda_l^{b+m+1} \tag{4.2.13}$$

and similarly for the other terms. We note, that these terms depend on the aysymptotic eigenvalue moments of the matrix $\mathbf{A}^H\mathbf{R}\mathbf{A}$ as $K,\ L \to \infty$. The results from large system analysis tell us that those empirical moments almost surely converge to a non-random limit. Hence, the sums of the eigenvalues need to be evaluated in the limit, i.e.

$$\lim_{K\to\infty} \frac{1}{K} tr \left(\mathbf{A}^H\mathbf{R}\mathbf{A}\right)^m = \lim_{K\to\infty} \frac{1}{K} \sum_{k=1}^{K} \lambda_k^m \tag{4.2.14}$$

where λ_k is an eigenvalue of $\mathbf{A}^H\mathbf{R}\mathbf{A}$. From [52, 75, 77] we have the following theorem, attributed to Silverstein [68]

Theorem 2

Let C_{ij} be an infinite matrix of i.i.d. complex-valued random variables with variance 1, and P_i be a sequence of real-valued random variables. Let $\mathbf{X}$ be an $N \times M$ matrix, whose (i, j)th entry is $C_{ij}/\sqrt{N}$. Let $\mathbf{P}$ be a $M \times M$ diagonal matrix with diagonal entries $P_1, \ldots, P_M$. As $M \to \infty$, we assume the empirical distribution, $F(P)$, of these entries to converge almost surely to a deterministic limit F. Let $G_N(\lambda)$ denote the empirical distribution of the eigenvalues of the Hermitian matrix $\mathbf{XPX}^H$, then, as $N, M \to \infty$, and for $M/N \to \beta > 0$, G_N converges almost surely to a deterministic limit G. Let us define

$$\begin{aligned} \gamma_m &= \mathbf{r}^H \mathbf{R}_I^m \mathbf{r} \\ \mathbf{R}_I &= \mathbf{XPX}^H + \sigma^2 \mathbf{I} \end{aligned} \tag{4.2.15}$$

where $\mathbf{r}$ is a vector of i.i.d. random elements, independent of $\mathbf{X}$ and $\mathbf{P}$, then

$$\lim_{K\to\infty} \gamma_m = \gamma_m^\infty(\beta, \sigma^2) \tag{4.2.16}$$

$$= \int (v + \sigma^2)^m dG(v) \tag{4.2.17}$$

where v denotes the eigenvalue random variable. Further, denote the Stieltjes transform *of $G(v)$ by*

$$m_G(z) = \int \frac{1}{v - z} dG(v) \tag{4.2.18}$$

for $z \in \mathcal{C}^+$*, i.e. IM*$(z) > 0$ *which in the* limit *satisfies a fixed-point equation given by*

$$m_G(z) = \frac{1}{-z + \beta \int \frac{\tau dF(\tau)}{1+\tau m_G(z)}} \tag{4.2.19}$$

Note also that

$$\begin{aligned}
\lim_{K\to\infty} \gamma_m &= \lim_{K\to\infty} \sum_i (v_i + \sigma^2)^m |\mathbf{r}^H \mathbf{u}_i|^2 && (4.2.20)\\
&= \lim_{K\to\infty} \frac{1}{K} \sum_i (v_i + \sigma^2)^m && (4.2.21)\\
&= \gamma_m^\infty(\beta, \sigma^2) && (4.2.22)
\end{aligned}$$

where $\mathbf{u}_i$ is the normalised eigenvector corresponding to v_i. In the limit the term $|\mathbf{r}^H \mathbf{u}_i|^2$ terms disappears [75, 80]. Since the effect of $\mathbf{r}$ vanishes in the limit, we can apply the above to write

$$\begin{aligned}
\lim_{K\to\infty} \frac{1}{K} tr\left(\mathbf{A}^H \mathbf{R} \mathbf{A}\right)^m &= \lim_{K\to\infty} \frac{1}{K} \sum_{k=1}^{K} \lambda_k^m && (4.2.23)\\
&= \lim_{K\to\infty} \mathbf{r}^H (\mathbf{SAA}^H \mathbf{S}^H)^m \mathbf{r} && (4.2.24)\\
&= \gamma_m^\infty(\beta, 0) = \int \lambda^m dG(\lambda) && (4.2.25)
\end{aligned}$$

where $G(\lambda)$ is the limiting empirical eigenvalue distribution of $\mathbf{A}^H\mathbf{RA}$ or $\mathbf{SAA}^H\mathbf{S}^H$, respectively. Hence, in principle, it's possible to find $m_G(z)$ (where $z \to -\sigma^2$, or in our case $z \to 0$) from (4.2.19) with respect to the power distribution $F(P)$, then find $G(\lambda)$ from the inverse function to the Stieltjes transform and then evaluate $\gamma_m^\infty(\beta, \sigma^2)$. Note that in general, no closed form solution is possible. However, in the special case of $\mathbf{P} = P\mathbf{I}$ in equation (4.2.15) and $\sigma^2 = 0$ an explicit solution is possible, given in [52]

$$\begin{aligned}
\gamma_m^\infty(\beta, 0) &= P^m \sum_{i=0}^{m-1} \binom{m}{i} \binom{m-1}{i} \frac{\beta^i}{i+1} && (4.2.26)\\
&= f(\beta, m) && (4.2.27)
\end{aligned}$$

This is directly applicable to our case when $\mathbf{AA}^H = P\mathbf{I}$. This would correspond to strict power control, equalising the received amplitudes. From the above development, it is clear that the determination of the limiting moments is not trivial.

Returning to our expression for the SPR and substituting for the sums over the eigenvalues, we can write from $\gamma_m^\infty(\beta,0) = f(\beta,m)$:

$$\lim_{K\to\infty} SPR_1 = \frac{\sigma_a^2\left(\sum_{b=0}^B d_{b,1} f(\beta,b+1)\right)\left(\sum_{b=0}^B d_{b,1}^* f(\beta,b+1)\right)}{\sigma_a^2\left(\sum_{m=0}^B\sum_{b=0}^B d_{b,1}d_{m,1}^* f\left(\beta,b+m+2\right)\right)+\sigma_v^2\left(\sum_{m=0}^B\sum_{b=0}^B d_{b,1}d_{m,1}^* f\left(\beta,b+m+1\right)\right)} \tag{4.2.28}$$

In the case of equal user powers,i.e. $\mathbf{A}\mathbf{A}^H = P\mathbf{I}$, equation (4.2.26) can be used directly. Ordering the coefficients $d_{b,1}$ and the functions $f(\beta,m)$ into vectors

$$\begin{aligned}\mathbf{d}_1 &= [d_{0,1}\ldots d_{B,1}]\\ \mathbf{f}_n &= [f(\beta,n)\ldots f(\beta,n+B)]^T\\ \mathbf{F}_n &= [\mathbf{f}_n\ldots\mathbf{f}_{n+B}]\end{aligned} \tag{4.2.29}$$

we can rewrite the signal to power ratio for user 1 as

$$\lim_{K\to\infty} SPR_1 = \frac{\sigma_a^2\mathbf{d}_1\mathbf{f}_1\mathbf{f}_1^H\mathbf{d}_1^H}{\sigma_a^2\mathbf{d}_1\mathbf{F}_2\mathbf{d}_1^H+\sigma_v^2\mathbf{d}_1\mathbf{F}_1\mathbf{d}_1^H} \tag{4.2.30}$$

$$= \frac{\mathbf{d}_1\mathbf{f}_1\mathbf{f}_1^H\mathbf{d}_1^H}{\mathbf{d}_1\left(\mathbf{F}_2+\frac{\sigma_v^2}{\sigma_a^2}\mathbf{F}_1\right)\mathbf{d}_1^H} \tag{4.2.31}$$

Maximising the asymptotic SINR for user one is equivalent to maximising $\lim_{K\to\infty} SPR_1$ with respect to $\mathbf{d}_1$ which can be seen to be a generalised eigenvalue problem. Let us define

$$\mathbf{F} = \mathbf{F}_2+\frac{\sigma_v^2}{\sigma_a^2}\mathbf{F}_1 \tag{4.2.32}$$

and reformulate the maximisation of the SPR as

$$\begin{aligned}\mathbf{d}_1^o &= \max_{\mathbf{d}_1}\frac{\mathbf{d}_1\mathbf{f}_1\mathbf{f}_1^H\mathbf{d}_1^H}{\mathbf{d}_1\mathbf{F}\mathbf{d}_1^H}\\ \mathbf{d}_1^o &= \mathbf{f}_1^H\mathbf{F}^{-1}\end{aligned} \tag{4.2.33}$$

Note that since $\mathbf{F}$ is a matrix of dimensions equal to the number of stages, $B+1\times B+1$, which is generally very small, the optimal asymptotic solution is very simple to compute. Furthermore, note that the solution is independent from the power of user one. This implies that the solution for the optimal weighting coefficients will asymptotically be the same for all users and therefore, there is no benefit in applying diagonal weighting matrices. Hence, asymptotically, we can replace $\mathbf{D}_b$ by a simple scalar d_b to obtain the same result.

The practical difficulty lies in the determination of the scalars $f(\beta, n)$ which we require in order to find the asymptotically optimal weighting. In [52], a recursive method based on a combinatorial argument is shown which allows the computation of the $f(\beta, n)$s. It is based on the following idea: Note that

$$\frac{d\gamma_m^\infty(\beta, x)}{dx} = m\gamma_{m-1}^\infty(\beta, x) = m \int (\lambda + x)^{m-1} dG(\lambda) \tag{4.2.34}$$

and it can also be seen that $\gamma_0^\infty(\beta, \sigma^2) = 1$ and hence $\gamma_1^\infty(\beta, \sigma^2) = \sigma^2 + c_1$ where c_1 is some constant. In the appendix of [52], it's also shown that

$$\begin{aligned} \gamma_1^\infty(\beta, 0) &= E(P)\beta \\ \gamma_2^\infty(\beta, 0) &= [\beta E(P)]^2 + \beta E(P^2) \\ \gamma_3^\infty(\beta, 0) &= \beta E\left[P^3\right] + 3\beta^2 E\left[P^2\right] E\left[P\right] + \beta^3 E^3\left[P\right] \end{aligned} \tag{4.2.35}$$

where P is the power random variable. There is also a method shown to compute higher moments of $\gamma_m^\infty(\beta, 0)$, for details see in [52]. Combining (4.2.35) and (4.2.34), it can be seen that the expressions for $\gamma_m^\infty(\beta, 0)$ provide the constants needed in $\gamma_m^\infty(\beta, \sigma^2)$, e.g $\gamma_1^\infty(\beta, \sigma^2) = \sigma^2 + \beta E\left[P\right]$ or $\gamma_2^\infty(\beta, \sigma^2) = \gamma_2^\infty(\beta, 0) + \sigma^4 + 2\beta E\left[P\right] \sigma^2$ etc. However, for our problem, we only need the values of $\gamma_m^\infty(\beta, 0) = f(\beta, m)$.

We propose an alternative way to compute the $f(\beta, n)$ using results from free probability theory:

Proposition 3
As $K,\ L \to \infty$, the matrices $\mathbf{R}$ and $\mathbf{A}\mathbf{A}^H$ are asymptotically free non-commutative random variables (NCRV) with respect to the trace functional (see appendix 4.A).

This allows us, to compute the eigenvalue moments of the product of $\mathbf{R}$ and $\mathbf{A}\mathbf{A}^H$ using only the moments of the individual product terms. For example, $\lim_{K\to\infty} \frac{1}{K} tr\left(\mathbf{A}^H\mathbf{R}\mathbf{A}\right)^m$

for $m = 1, 2$ are given by

$$\lim_{K\to\infty} \frac{1}{K} tr\left(\mathbf{A}^H\mathbf{R}\mathbf{A}\right) = \lim_{K\to\infty} \frac{1}{K} tr\left(\mathbf{R}\right) \frac{1}{K} tr\left(\mathbf{A}^H\mathbf{A}\right) \quad (4.2.36)$$

$$\lim_{K\to\infty} \frac{1}{K} tr\left(\mathbf{A}^H\mathbf{R}\mathbf{A}\right)^2 = \lim_{K\to\infty} \left\{\frac{1}{K^2} tr^2(\mathbf{R}) \frac{1}{K^2} tr^2(\mathbf{A}\mathbf{A}^H) + \frac{1}{K^2} tr^2(\mathbf{R}) \frac{1}{K} tr(\mathbf{A}\mathbf{A}^H\mathbf{A}\mathbf{A}^H) + \frac{1}{K} tr(\mathbf{R}^2) \frac{1}{K^2} tr^2(\mathbf{A}\mathbf{A}^H)\right\} \quad (4.2.37)$$

see appendix 4.B for computation details. Note that we have the expressions for the moments in $\mathbf{R}$ explicitly in (4.2.26) with $P = 1$ and there is no requirement for equal user power ($\mathbf{A}\mathbf{A}^H$ is allowed to be different from a multiple of identity). Also, since $\mathbf{A}$ is diagonal,

$$tr\left(\mathbf{A}\mathbf{A}^H\right)^m = tr\left(\mathbf{A}^H\mathbf{A}\right)^m = \sum_{k=1}^{K} P_k^m \quad (4.2.38)$$

where P_k^m is simply the user power. We shall now follow a similar analysis for the approach in equation (3.4.21)

4.2.2 Pathwise Joint Approach

Consider again the synchronous single path per user system with the symbol estimate given by

$$\hat{\mathbf{a}} = \mathbf{A}^H \sum_{b=0}^{B} \mathbf{D}_b \mathbf{R}^b \mathbf{x} = \mathbf{F}\mathbf{x} \quad (4.2.39)$$

with the total power in the symbol estimate given by

$$E\{\hat{\mathbf{a}}^H\hat{\mathbf{a}}\} = \sigma_a^2 tr\left(\mathbf{A}^H \sum_{b=0}^{B}\sum_{i=0}^{B} \mathbf{D}_b \mathbf{R}^{b+1} \mathbf{A}\mathbf{A}^H \mathbf{R}^{i+1} \mathbf{D}_i^H \mathbf{A}\right) + \sigma_v^2 tr\left(\mathbf{A}^H \sum_{b=0}^{B}\sum_{i=0}^{B} \mathbf{D}_b \mathbf{R}^{b+i+1} \mathbf{D}_i^H \mathbf{A}\right) \quad (4.2.40)$$

The power in the estimate for user one, $E\{|\hat{a}_1|^2\}$, is hence given by element (1,1) from the above expressions

$$\begin{aligned} E\{|\hat{a}_1|^2\} &= \sigma_a^2 \sum_{b=0}^{B}\sum_{i=0}^{B} A_1^* d_{b,1} \sum_{l=1}^{K}\sum_{m=1}^{K} \lambda_m^{i+1}\lambda_l^{b+1}\mathbf{u}_l^H\mathbf{A}\mathbf{A}^H\mathbf{u}_m u_{l,1}u_{m,1}^* d_{i,1}^* A_1 \\ &\quad +\sigma_v^2 \sum_{b=0}^{B}\sum_{i=0}^{B} A_1^* d_{b,1} \sum_{l=1}^{K} \lambda_l^{b+i+1} u_{l,1}u_{l,1}^* d_{i,1}^* A_1 \\ &= \sigma_a^2 |A_1|^2 \sum_{n=1}^{K}|A_n|^2 \sum_{l=1}^{K}\xi_l u_{l,1}u_{l,n}^* \sum_{m=1}^{K}\xi_m^* u_{m,n}u_{m,1}^* \\ &\quad +\sigma_v^2|A_1|^2\sum_{l=1}^{K}|\xi_l|^2\lambda_l^{-1}u_{l,1}u_{l,1}^* \end{aligned} \tag{4.2.41}$$

where λ_l is the l-th eigenvalue of $\mathbf{R}$, $\mathbf{u}_l$ is the corresponding eigenvector such that $\mathbf{u}_l = [u_{l,1}\ldots u_{l,K}]^T$ and ξ_l is defined as in the last section. The signal component in the estimated data is given, analogue to the last section by

$$\mathbf{FRAa} = \mathbf{A}^H \sum_{b=0}^{B}\mathbf{D}_b \sum_{i=1}^{K}\lambda_i^{b+1}\mathbf{u}_i\mathbf{u}_i^H\mathbf{Aa} \tag{4.2.42}$$

and the useful signal and signal power in the estimate $\hat{a}_1$ is given by

$$\begin{aligned} Signal_1 &= |A_1|^2 d_{b,1}\sum_{i=1}^{K}\lambda_i^{b+1}|u_{i,1}|^2 a_1 \\ &= |A_1|^2\sum_{i=1}^{K}\xi_i|u_{i,1}|^2 a_1 \\ Power_1 &= \sigma_a^2|A_1|^4\left|\sum_{i=1}^{K}\xi_i u_{i,1}u_{i,1}^*\right|^2 \end{aligned} \tag{4.2.43}$$

Using the same reasoning as in the last section regarding the $SINR_1$, we can hence form the SPR_1 as

$$SPR_1 = \frac{\sigma_a^2|A_1|^2\left|\sum_{i=1}^{K}\xi_i u_{i,1}u_{i,1}^*\right|^2}{\sigma_a^2\left(\sum_{n=1}^{K}|A_n|^2\left|\sum_{l=1}^{K}\xi_l u_{l,1}u_{l,n}^*\right|^2\right)+\sigma_v^2\left(\sum_{l=1}^{K}|\xi_l|^2\lambda_l^{-1}u_{l,1}u_{l,1}^*\right)}$$

Note that the interference term in this case involves eigenvector elements $u_{l,n}$ for n different from unity, in contrast to the approach of (4.2.28). We shall therefore look at this term first. We have

$$\begin{aligned} E\{|\hat{a}_1|^2\} &= \sigma_a^2|A_1|^2\left(\sum_{n=1}^{K}|A_n|^2\left|\sum_{l=1}^{K}\xi_l u_{l,1}u_{l,n}^*\right|^2\right) && (4.2.44)\\ &= \sigma_a^2|A_1|^2\sum_{n=1}^{K}|A_n|^2\sum_{l=1}^{K}\xi_l u_{l,1}u_{l,n}^*\sum_{m=1}^{K}\xi_m^* u_{m,n}u_{m,1}^* && (4.2.45)\end{aligned}$$

The key to this problem lies with the eigenvector elements. We are not aware of a solution to render the above independent from the eigenvectors for a general set of spreading sequences. However, there is a way out by imposing the spreading codes to be made up of Gaussian random variables.

Lemma 4
[72] Consider a random matrix $\mathbf{S}$ *of dimension* $L \times K$ *whose elements* $[S]_{i,j}$ *are i.i.d Gaussian random variables with zero mean and variance* $1/L$*. The matrix* $\mathbf{R} = \mathbf{S}^H\mathbf{S}$ *allows the eigendecomposition* $\mathbf{R} = \mathbf{U}\Lambda\mathbf{U}^H$*, with* $\mathbf{U}$ *and* Λ *asymptotically independent. Furthermore,* $\mathbf{U}$ *is then* Haar *distributed.*

Hence, asymptotically the eigenvector elements are i.i.d random variables from a Haar distribution and most of the mixed moments are zero (for details, consult [72]). We know already that

$$\lim_{K\to\infty}\sum_{l=1}^{K}\xi_l|u_{l,1}|^2 = \lim_{K\to\infty}\frac{1}{K}\sum_{l=1}^{K}\xi_l \tag{4.2.46}$$

which means that

$$E\left(|u_{l,1}|^2\right) = \frac{1}{K} \tag{4.2.47}$$

We therefore need to look at all the different combinations of the indices which have non-vanishing moments in the limit. We have the following cases [72]

$$\begin{aligned} l \neq m,\ n \neq 1 &= E\left(u_{l,1}u_{l,n}^{*}u_{m,n}u_{m,1}^{*}\right) = 0 \\ l \neq m,\ n = 1 &= E\left(\left|u_{l,1}\right|^2\left|u_{m,1}\right|^2\right) = \frac{1}{K(K+1)} \\ l = m,\ n \neq 1 &= E\left(\left|u_{l,1}\right|^2\left|u_{l,n}\right|^2\right) = \frac{1}{K(K+1)} \\ l = m,\ n = 1 &= E\left(\left|u_{l,1}\right|^4\right) = \frac{2}{K(K+1)} \end{aligned} \tag{4.2.48}$$

After substituting these moments of the eigenvector elements and some algebraic manipulation, we can write the SPR for user one:

$$\lim_{K\to\infty} SPR_1 = \lim_{K\to\infty} \frac{\sigma_a^2|A_1|^2\left|\frac{1}{K}\sum_{i=1}^{K}\xi_i\right|^2}{\sigma_a^2\left(\frac{1}{K}\sum_{n=1}^{K}|A_n|^2\right)\left(\frac{1}{K}\sum_{l=1}^{K}|\xi_l|^2\right) + \sigma_a^2|A_1|^2\left|\frac{1}{K}\sum_{l=1}^{K}\xi_l\right|^2 + \sigma_v^2\frac{1}{K}\sum_{l=1}^{K}\lambda_l^{-1}|\xi_l|^2} \tag{4.2.49}$$

Substituting for the ξ_l in terms of $d_{b,i}$ and λ_l to obtain an expression suitable to determine the weighting coefficients, we can write

$$\lim_{K\to\infty} SPR_1 = \lim_{K\to\infty} \frac{num}{den} \tag{4.2.50}$$

where the numerator and denominator are defined by

$$\begin{aligned} num &= \sigma_a^2|A_1|^2\left|\frac{1}{K}\sum_{b=0}^{B} d_{b,1}\sum_{i=1}^{K}\lambda_i^{b+1}\right|^2 \\ den &= \sigma_a^2|A_1|^2\left|\frac{1}{K}\sum_{b=0}^{B} d_{b,1}\sum_{i=1}^{K}\lambda_i^{b+1}\right|^2 + \frac{\sigma_a^2}{K}\sum_{n=1}^{K}|A_n|^2\sum_{b=0}^{B}\sum_{i=0}^{B} d_{b,1}d_{i,1}^{*}\frac{1}{K}\sum_{l=1}^{K}\lambda_l^{b+i+2} \\ &\quad + \frac{\sigma_v^2}{K}\sum_{b=0}^{B}\sum_{i=0}^{B} d_{b,1}d_{i,1}^{*}\sum_{l=1}^{K}\lambda_i^{b+i+1} \end{aligned} \tag{4.2.51}$$

Further substituting the limiting functions for the sums of the eigenvalues in the above expression, i.e. $f(\beta, b) = \frac{1}{K}\sum_{i=1}^{K}\lambda_i^b$, we can rewrite the numerator and the denominator as

$$
\begin{aligned}
num &= \sigma_a^2 |A_1|^2 \left| \sum_{b=1}^{B} d_{b,1} f(\beta, b+1) \right|^2 \\
den &= \sigma_a^2 |A_1|^2 \left| \sum_{b=1}^{B} d_{b,1} f(\beta, b+1) \right|^2 + \sigma_a^2 \tilde{P} \sum_{b=0}^{B} \sum_{i=0}^{B} d_{b,1} d_{i,1}^* f(\beta, b+i+2) \\
&\quad + \sigma_v^2 \sum_{b=0}^{B} \sum_{i=0}^{B} d_{b,1} d_{i,1}^* f(\beta, b+i+1) \qquad (4.2.52)
\end{aligned}
$$

where we have defined the mean power, $\tilde{P}$, by

$$
\tilde{P} = \frac{1}{K} \sum_{n=1}^{K} |A_n|^2 \qquad (4.2.53)
$$

Finally, by rewriting everything in the vector notation introduced in (4.2.29) we obtain:

$$
\lim_{K \to \infty} SPR_1 = \frac{|A_1|^2 \mathbf{d}_1 \mathbf{f}_1 \mathbf{f}_1^H \mathbf{d}_1^H}{\mathbf{d}_1 \left(\tilde{P} \mathbf{F}_2 + |A_1|^2 \mathbf{f}_1 \mathbf{f}_1^H + \frac{\sigma_v^2}{\sigma_a^2} \mathbf{F}_1 \right) \mathbf{d}_1^H} \qquad (4.2.54)
$$

This again can be seen to be a generalised eigenvalue problem. For the optimal solution, we hence obtain

$$
\mathbf{d}_1^o = \mathbf{f}_1^H \mathbf{F}^{-1} \qquad (4.2.55)
$$

where $\mathbf{F}$ is defined by the denominator terms on which $\mathbf{d}_1$ operates, that is

$$
\mathbf{F} = \tilde{P} \mathbf{F}_2 + |A_1|^2 \mathbf{f}_1 \mathbf{f}_1^H + \frac{\sigma_v^2}{\sigma_a^2} \mathbf{F}_1 \qquad (4.2.56)
$$

Therefore, again, we see that the asymptotic solution is indeed independent from the user power (since $\mathbf{d}_1$ is determined up to a scalar factor) and therefore there is no benefit in employing diagonal weighting matrices asymptotically.

4.3 Asymptotic Analysis extended to Multipath Propagation

We would now like to extend the results of the previous sections to a large system analysis in the multipath case. Most asymptotic analyses to date have treated the synchronous system case, and indeed, a fully general extension to the asynchronous model is difficult. We will therefore introduce certain approximations in order to make the problem tractable. Our fully asynchronous system description is given by

$$\begin{aligned} \mathbf{y}[n] &= \mathbf{P}(q)\mathbf{SHAa}[n] + \mathbf{v}[n] \\ \mathbf{x}[n] &= \mathbf{S}^H\mathbf{P}^\dagger(q)\left(\mathbf{P}(q)\mathbf{SHAa}[n] + \mathbf{v}[n]\right) \end{aligned} \tag{4.3.1}$$

where $\mathbf{y}[n]$ is the sampled, received signal and $\mathbf{x}[n]$ is the pulse-shape matched filtered and despread signal, i.e. the RAKE finger outputs prior to combining. We will assume that the delay spread $\max_{k,m}(\tau_{k,m})$ is much smaller than the symbol period T so that the effect of Intersymbol Interference (ISI) can be neglected and we can look at a one-shot detector, i.e.

$$\mathbf{y}[n] = \mathbf{P}[n]\mathbf{SHAa}[0] + \mathbf{v}[n] \tag{4.3.2}$$

$$\rightarrow \mathbf{y} = \mathbf{PSHAa} + \mathbf{v} \tag{4.3.3}$$

Assuming that the delays are multiples of the chip-period and chip-rate sampling (synchronised to the chip-rate), the pulse-shaped matched filtering can be assumed to be perfect and we are left with S essentially containing spreading sequences shifted by a number of chips equivalent to the delays. Since the delays and therefore the shifts are random and the spreading codes are made of i.i.d random variables, we assume the spreading matrix S to be modelled by

$$\mathbf{S} = [\mathbf{s}_{1,1} \dots \mathbf{s}_{k,m} \dots \mathbf{s}_{K,M}] \tag{4.3.4}$$

where the $\mathbf{s}_{k,m}$ are the column vectors of length L, consisting of Gaussian i.i.d. random variables for user k and path m. $\|\mathbf{s}_{k,m}^H\mathbf{s}_{k,m}\| = 1$, i.e. the spreading codes are normalised. The received signal model ($J = 1,\ M = 1,\ Q = 1$) and the pathwise RAKE outputs are therefore given by

$$\mathbf{y} = \mathbf{SAa} + \mathbf{v} \tag{4.3.5}$$

$$\mathbf{x} = \mathbf{RAa} + \mathbf{S}^H\mathbf{v} \tag{4.3.6}$$

$\mathbf{a}$ as defined for one symbol, i.e. $\mathbf{a}[0]$, $\mathbf{A}$ as usual block diagonal. To further justify the above model, note that it was found in [78] that a symbol asynchronous but chip synchronous system is asymptotically equivalent to a symbol synchronous model for the purpose of an SINR analysis. Also, if the pulse-shape is an ideal sinc, the fully asynchronous system is asymptotically equivalent to the symbol synchronous system [82]. In the case of multipath, we assume independence between paths, as in [77].

4.3.1 Symbolwise Joint approach

The problem setting in this case is exactly the same as the one given for single path case as can be seen from inspecting equations (4.2.3) and (4.2.4). The only difference is the change in the eigenvalues of the matrix $\mathbf{A}^H\mathbf{R}\mathbf{A}$, i.e. we need to find

$$\begin{aligned}\lim_{K\to\infty}\frac{1}{K}tr(\mathbf{A}^H\mathbf{R}\mathbf{A})^m &= \lim_{K\to\infty}\frac{1}{K}tr(\mathbf{R}\mathbf{A}\mathbf{A}^H)^m \\ &= \lim_{K\to\infty}\frac{1}{K}tr(\mathbf{S}\mathbf{A}\mathbf{A}^H\mathbf{S}^H)^m \end{aligned} \tag{4.3.7}$$

First, note that $\mathbf{A}\mathbf{A}^H = diag(\mathbf{A}_1\mathbf{A}_1^H \ldots \mathbf{A}_K\mathbf{A}_K^H)$ is block diagonal. By taking the expectation with respect to the amplitudes, $E\{\mathbf{A}\mathbf{A}^H\}$ we get:

- if $E\{A_{k,m}A^*_{k,n}\} = 0 \;\forall\; m \neq n \;\forall\; k$, i.e. the path amplitudes of every user k are assumed to be uncorrelated, then the distribution $F(P)$ is the limiting distribution of the path powers and we can use the identical techniques of the last section to find a solution to

$$\lim_{K\to\infty}\frac{1}{K}tr(\mathbf{R}E\{\mathbf{A}\mathbf{A}^H\}) \tag{4.3.8}$$

  since $E\{\mathbf{A}\mathbf{A}^H\}$ is diagonal. Furthermore, if the average power in all the paths of all the users is equal, we can again use (4.2.26).

- If $E\{A_{k,m}A*_{k,n}\} = \rho_{k,m,n} \neq 0 \;\forall\; m \neq n \;\forall\; k$, i.e. the amplitudes are correlated then the situation is more complicated since then the matrix $\mathbf{A}\mathbf{A}^H$ is not diagonal under the expectation operation and the correlation coefficients will influence the eigenvalues of $\mathbf{A}\mathbf{A}^H$. The technique involving the Stieltjes transform in the last section can therefore not be used either since $\mathbf{A}\mathbf{A}^H$ is not diagonal, which is required according to theorem 2.

However, in appendix 4.A, we show that $\mathbf{R}$ and $\mathbf{A}\mathbf{A}^H$ are asymptotically free, noncommutative random variables. Therefore, the moments of the eigenvalues can be found by knowing the limiting empirical distributions of $\mathbf{R}$ and $\mathbf{A}\mathbf{A}^H$. Note that we have the moments of the eigenvalues of $\mathbf{R}$ explicitly from (4.2.26). For the amplitudes, note that

$$\lim_{K\to\infty} tr\left[(\mathbf{A}\mathbf{A}^H)^m\right] = \lim_{K\to\infty} tr\left[(\mathbf{A}^H\mathbf{A})^m\right] \tag{4.3.9}$$

$$= \lim_{K\to\infty}\frac{1}{K}\sum_{k=1}^{K}P_k^m \tag{4.3.10}$$

Hence, the solution is exactly equivalent to the single path solution of section 4.2.1 and furthermore, the solution is independent of the power distribution. Also, we notice that the correlation between the path amplitudes of user k seems to be irrelevant in the limit and performance is the same with or without correlation.

Hence, using the expression obtained for the moments using free probability theory, it is possible to obtain explicit expressions of the SINR for the Symbolwise Joint PE approach. Asymptotically, there is no benefit in using a coefficient per user in this model, even under power imbalance between the users and/or the paths.

4.3.2 Pathwise Joint Approach

In this section, the multipath scenario is analysed for the pathwise joint approach, following the same procedure as used for the synchronous case. The signal model assumptions are those introduced above. The total power in the symbol estimate for user 1, $E\{|\hat{a}_1|^2\}$, needs to be recomputed from

$$\begin{aligned} E\{\hat{\mathbf{a}}\hat{\mathbf{a}}^H\} &= \sigma_a^2 tr\left(\mathbf{A}^H \sum_{b=0}^{B}\sum_{i=0}^{B} \mathbf{D}_b \mathbf{R}^{b+1}\mathbf{A}\mathbf{A}^H\mathbf{R}^{i+1}\mathbf{D}_i^H\mathbf{A}\right) \\ &\quad + \sigma_v^2 tr\left(\mathbf{A}^H \sum_{b=0}^{B}\sum_{i=0}^{B} \mathbf{D}_b \mathbf{R}^{b+i+1}\mathbf{D}_i^H\mathbf{A}\right) \end{aligned} \tag{4.3.11}$$

where we need the first element in the matrices above (i.e. the first element in the sum for the trace). Using the eigendecomposition for $\mathbf{R} = \mathbf{U}\Lambda\mathbf{U}^H$, we can write the variance from the symbol estimate of user one as:

$$\begin{aligned} E\{|\hat{a}_1|^2\} &= \sigma_a^2 \mathbf{A}_1^H \sum_{b=0}^{B}\sum_{i=0}^{B} \mathbf{D}_{b,1} \underbrace{\mathbf{u}_1\Lambda^{b+1}\mathbf{U}^H\mathbf{A}\mathbf{A}^H\mathbf{U}\Lambda^{i+1}\mathbf{u}_1}_{=\mathbf{J}_{b,i}} \mathbf{D}_{i,1}\mathbf{A}_1 \\ &\quad + \sigma_v^2 \mathbf{A}_1^H \sum_{b=0}^{B}\sum_{i=0}^{B} \mathbf{D}_{b,1}\mathbf{u}_1\Lambda^{b+1}\mathbf{u}_1^H\mathbf{D}_{i,1}\mathbf{A}_1 \end{aligned} \tag{4.3.12}$$

where we have defined the eigenvector quantities by

$$\begin{aligned} \mathbf{U} &= [\mathbf{u}_1^H \dots \mathbf{u}_K^H]^H \\ \mathbf{u}_1 &= [\mathbf{I}_M \ \mathbf{0}]\mathbf{U} \\ \mathbf{u}_k &= [\mathbf{u}_{k,1}^H \dots \mathbf{u}_{k,M}^H]^H \end{aligned}$$

Hence, the vectors $\mathbf{u}_{k,m}$ are the rows of $\mathbf{U}$ and $\mathbf{u}_k$ is therefore of dimensions $M \times MK$. We can write the matrix $\mathbf{J}$ by

$$\begin{aligned}\mathbf{J} &= \sum_{k=1}^{K} \mathbf{u}_1 \Lambda^{b+1} \mathbf{u}_k^H \mathbf{A}_k \mathbf{A}_k^H \mathbf{u}_k \Lambda^{i+1} \mathbf{u}_1^H \\ &= \mathbf{u}_1 \Lambda^{b+1} \mathbf{u}_1^H \mathbf{A}_1 \mathbf{A}_1^H \mathbf{u}_1 \Lambda^{i+1} \mathbf{u}_1^H + \sum_{k=2}^{K} \mathbf{u}_1 \Lambda^{b+1} \mathbf{u}_k^H \mathbf{A}_k \mathbf{A}_k^H \mathbf{u}_k \Lambda^{i+1} \mathbf{u}_1^H\end{aligned} \tag{4.3.13}$$

Looking at the term for $k = 1$, we can write the (m, n)th element as follows:

$$\begin{aligned}\left[\mathbf{u}_1 \Lambda^{b+1} \mathbf{u}_1^H \mathbf{A}_1 \mathbf{A}_1^H \mathbf{u}_1 \Lambda^{i+1} \mathbf{u}_1^H\right]_{m,n} &= \mathbf{u}_{1,m} \Lambda^{b+1} \left(\sum_{l \neq m=1}^{M} \mathbf{u}_{1,l}^H A_{1,l} + \mathbf{u}_{1,m}^H A_{1,m} \right) \\ &\quad \times \left(\sum_{p \neq m=1}^{M} A_{1,p}^* \mathbf{u}_{1,p} + A_{1,n}^* \mathbf{u}_{1,n} \right) \Lambda^{i+1} \mathbf{u}_{1,n}^H\end{aligned}$$

Since

$$\begin{aligned}\mathbf{u}_1^H \mathbf{A}_1 \mathbf{A}_1^H \mathbf{u}_1 &= \left(\sum_{l=1}^{M} \mathbf{u}_{1,l}^H A_{1,l} \right) \left(\sum_{p=1}^{M} \mathbf{u}_{1,p} A_{1,p}^* \right) \\ \mathbf{u}_1 &= \begin{bmatrix} \mathbf{u}_{1,1} \\ \vdots \\ \mathbf{u}_{1,M} \end{bmatrix}\end{aligned} \tag{4.3.14}$$

i.e. $\mathbf{u}_{k,m}$ are the rows of $\mathbf{u}_k$ and of dimensions $1 \times KM$. Recall that asymptotically, the elements in the matrix $\mathbf{U}$ are Haar distributed due to the Gaussian spreading codes, obeying (4.2.48) under expectation (see also appendix 4.A). Therefore,

$$\begin{aligned}E\{\mathbf{u}_{1,m} \mathbf{u}_{1,l}^H \mathbf{u}_{1,p} \mathbf{u}_{1,n}^H\} &= \lim_{K \to \infty} \mathbf{u}_{1,m} \mathbf{u}_{1,l}^H \mathbf{u}_{1,p} \mathbf{u}_{1,n}^H \\ &= 0 \; \forall m \neq n\end{aligned}$$

Hence, if $m \neq n$, then asymptotically

$$\begin{aligned}\lim_{K \to \infty} \left[\mathbf{u}_1 \Lambda^{b+1} \mathbf{u}_1^H \mathbf{A}_1 \mathbf{A}_1^H \mathbf{u}_1 \Lambda^{i+1} \mathbf{u}_1^H\right]_{m,n:\, m \neq n} &= \lim_{K \to \infty} \left(\mathbf{u}_{1,m} \Lambda^{b+1} \mathbf{u}_{1,m}^H\right) A_{1,m} A_{1,n}^* \left(\mathbf{u}_{1,n} \Lambda^{i+1} \mathbf{u}_{1,n}^H\right) \\ &= \frac{A_{1,m} A_{1,n}^*}{(KM)^2} \left(\sum_{l=1}^{KM} \lambda_l^{b+1} \right) \left(\sum_{p=1}^{KM} \lambda_p^{i+1} \right)\end{aligned} \tag{4.3.15}$$

when $m = n$ note that

$$E\{\mathbf{u}_{1,m}\mathbf{u}_{1,l}^H\mathbf{u}_{1,p}\mathbf{u}_{1,m}^H\} = 0 \;\forall l \neq p \neq m \tag{4.3.16}$$

Therefore,

$$\begin{aligned}\lim_{K\to\infty}\left[\mathbf{u}_1\Lambda^{b+1}\mathbf{u}_1^H\mathbf{A}_1\mathbf{A}_1^H\mathbf{u}_1\Lambda^{i+1}\mathbf{u}_1^H\right]_{m,n:\, m=n} &= \lim_{K\to\infty}\mathbf{u}_{1,m}\Lambda^{b+1}\sum_{l\neq m=1}^{M}\mathbf{u}_{1,l}^H|A_{1,l}|^2\mathbf{u}_{1,l}\Lambda^{i+1}\mathbf{u}_{1,m}^H \\ &\quad +|A_{1,m}|^2\mathbf{u}_{1,m}\Lambda^{b+1}\mathbf{u}_{1,m}^H\mathbf{u}_{1,m}\Lambda_{i+1}\mathbf{u}_{1,m}\end{aligned} \tag{4.3.17}$$

and in the limit we obtain

$$\begin{aligned}\lim_{K\to\infty}\left[\mathbf{u}_1\Lambda^{b+1}\mathbf{u}_1^H\mathbf{A}_1\mathbf{A}_1^H\mathbf{u}_1\Lambda^{i+1}\mathbf{u}_1^H\right]_{m,n:\, m=n} &= \frac{1}{KM}\left(\sum_{l\neq m=1}^{M}|A_{1,l}|^2\right)\frac{1}{KM}\left(\sum_{p=1}^{KM}\lambda_p^{b+i+2}\right) \\ &\quad +\frac{|A_{1,m}|^2}{(KM)^2}\sum_{l=1}^{KM}\sum_{p\neq l=1}^{KM}\lambda_l^{b+1}\lambda_p^{i+1} \\ &\quad +\frac{2|A_{1,m}|^2}{KM(KM+1)}\sum_{l=1}^{KM}\lambda_l^{b+i+2}\end{aligned} \tag{4.3.18}$$

Looking at the second term in equation (4.3.13) involving $k \neq 1$ we can write

$$\lim_{K\to\infty}\sum_{k=2}^{K}\mathbf{u}_1\Lambda^{b+1}\mathbf{u}_k^H\mathbf{A}_k\mathbf{A}_k^H\mathbf{u}_k\Lambda^{i+1}\mathbf{u}_1^H = \frac{1}{KM}\sum_{k=2}^{K}\left(\sum_{l=1}^{M}|A_{k,l}|^2\right)\frac{1}{KM}\left(\sum_{m=1}^{KM}\lambda_m^{b+i+2}\right)\mathbf{I}_M$$

since

$$\begin{aligned}\lim_{K\to\infty}\mathbf{u}_k^H\mathbf{A}_k\mathbf{A}_k^H\mathbf{u}_k &= \frac{\mathbf{I}}{KM}\sum_{l=1}^{M}|A_{k,l}|^2 \\ \lim_{K\to\infty}\mathbf{u}_1\Lambda^{b+i+2}\mathbf{u}_1^H &= \frac{\mathbf{I}}{KM}\sum_{m=1}^{KM}\lambda_m^{b+i+2}\end{aligned} \tag{4.3.19}$$

For the second term in (4.3.11), note that

$$\lim_{K\to\infty}\mathbf{u}_1\Lambda^{b+i+1}\mathbf{u}_1^H = \frac{\mathbf{I}_M}{KM}\sum_{k=1}^{KM}\lambda_k^{b+i+1}$$

Using the following notation introduced earlier: $f(\beta M, l) = \frac{1}{KM}\sum_{m=1}^{KM}\lambda_m^l$, and using the above results, we can now write the matrix $\mathbf{J}$ as

$$\begin{aligned}\mathbf{J} &= \left(\frac{1}{KM}\sum_{k=2}^{K}\sum_{l=1}^{M}|A_{k,l}|^2\right) f(\beta M, b+i+2)\mathbf{I}_M + f(\beta M, b+1) f(\beta M, i+1)\mathbf{A}_1\mathbf{A}_1^H \\ &\quad - f(\beta M, b+1) f(\beta M, i+1) diag\left(\mathbf{A}_1\mathbf{A}_1^H\right) + f(\beta M, b+1) f(\beta M, i+1) diag\left(\mathbf{A}_1\mathbf{A}_1^H\right) \\ &\quad + \left(\frac{2}{KM+1} - \frac{1}{KM}\right) f(\beta M, b+i+2) diag\left(\mathbf{A}_1\mathbf{A}_1^H\right) \\ &\quad + \frac{1}{KM} f(\beta M, b+i+2)\left(\|\mathbf{A}_1\|^2\mathbf{I} - diag\left(\mathbf{A}_1\mathbf{A}_1^H\right)\right) \\ &= \left(\frac{1}{KM}\sum_{k=1}^{K}\|\mathbf{A}_k\|^2\right) f(\beta M, b+i+2)\mathbf{I}_M + f(\beta M, b+1) f(\beta M, i+1)\mathbf{A}_1\mathbf{A}_1^H \end{aligned} \quad (4.3.20)$$

We can now write the output variance of the symbol estimate from (4.3.11) as

$$\begin{aligned} E\{|\hat{a}_1|^2\} &= \sigma_a^2\sum_{b=0}^{B}\sum_{i=0}^{B} f(\beta M, b+i+2)\mathbf{A}_1^H\mathbf{D}_{b,1}\mathbf{D}_{i,1}^H\mathbf{A}_1 + \sigma_a^2\left(\sum_{b=0}^{B} f(\beta M, b+1)\mathbf{A}_1^H\mathbf{D}_{b+1}\mathbf{A}_1\right)^2 \\ &\quad + \sigma_v^2\sum_{b=0}^{B}\sum_{i=0}^{B} f(\beta M, b+i+1)\mathbf{A}_1^H\mathbf{D}_{b,1}\mathbf{D}_{i,1}^H\mathbf{A}_1 \end{aligned} \quad (4.3.21)$$

where the signal part is given by

$$Power_1 = \sigma_a^2\left(\sum_{b=0}^{B} f(\beta M, b+1)\mathbf{A}_1^H\mathbf{D}_{b+1}\mathbf{A}_1\right)^2 \quad (4.3.22)$$

Note here that due to multiple paths, we obtain an effective load of $\beta' = KM/L$, due to the dimensions of $\mathbf{S}$, which is $L \times KM$.

Using vector notation, we can now write

$$\mathbf{K}_1^H = [\mathbf{A}_1^H\mathbf{D}_{0,1}\ldots\mathbf{A}_1^H\mathbf{D}_{B,1}] \quad (4.3.23)$$

$$\underline{\mathbf{A}}_1 = \begin{bmatrix} f(\beta M, 1)\mathbf{A}_1 \\ \vdots \\ f(\beta M, B+1)\mathbf{A}_1 \end{bmatrix} \quad (4.3.24)$$

Writing the output variance and minimising it under the constraint that $\mathbf{K}_1^H\underline{\mathbf{A}}_1 = 1$ is equivalent to maximising the SINR, i.e.

$$\min_{\mathbf{K}_1:\ \mathbf{K}_1^H\underline{\mathbf{A}}_1=1} \mathbf{K}_1^H\mathbf{F}\mathbf{K}_1 \quad (4.3.25)$$

where

$$\mathbf{F} = \left(\sigma_a^2 \mathbf{F}_2 + \sigma_v^2 \mathbf{F}_1\right) \otimes \mathbf{I}_M \tag{4.3.26}$$

with the variables defined as previously in equation (4.2.29) with the optimal solution given by

$$\mathbf{K}_1^o = \left(\underline{\mathbf{A}}_1^H \mathbf{F}^{-1} \underline{\mathbf{A}}_1\right)^{-1} \mathbf{F}^{-1} \underline{\mathbf{A}}_1 \tag{4.3.27}$$

and therefore

$$\mathbf{K}_1 = \mathbf{F}^{-1} \underline{\mathbf{A}}_1 = \mathbf{F}^{-1} \underbrace{\begin{bmatrix} f(\beta M, 1)\mathbf{I}_M \\ \vdots \\ f(\beta M, B+1)\mathbf{I}_M \end{bmatrix}}_{\mathbf{f}_1 \otimes \mathbf{I}_M} \mathbf{A}_1 \tag{4.3.28}$$

and

$$\begin{aligned} \mathbf{F}^{-1}\left(\mathbf{f}_1 \otimes \mathbf{I}_M\right) &= \left(\left(\sigma_a^2 \mathbf{F}_2 + \sigma_v^2 \mathbf{F}_1\right)^{-1} \underbrace{\begin{bmatrix} f(\beta M, 1) \\ \vdots \\ f(\beta M, B+1) \end{bmatrix}}_{= \mathbf{f}_1} \right) \otimes \mathbf{I}_M \\ &= \left[\mathbf{D}_{0,1}^H \ldots \mathbf{D}_{B,1}^H\right]^H \\ \rightarrow \mathbf{D}_{b,1}^H &= \alpha_{b,1}^* \mathbf{I}_M = \left\{ \left[\left(\sigma_a^2 \mathbf{F}_2 + \sigma_v^2 \mathbf{F}_1\right)^{-1}\right]_{b+1,:} \mathbf{f}_1 \right\} \otimes \mathbf{I}_M \end{aligned}$$

where $[.]_{j,:}$ denotes the j-th row. Therefore, it can be seen that the optimal solution is achieved using only a scalar coefficient which is user and path independent and varies only from stage to stage. Hence, also in this case, asymptotically there is no benefit in diagonal weighting matrices.

Note that we can also treat the userwise PE using the above approach since $\mathbf{S}_1 \mathbf{A}_1 = \sum_{m=1}^{M} A_{1,m} \mathbf{s}_{1,m} = A_1' \mathbf{s}_1'$ is also Gaussian ($|A_1|^2 = 1$). The only difference is in the loading we need to apply, notably, $\beta M \rightarrow \beta$.

4.3.3 Note on Implementation

The result above suggests that there is no benefit in using diagonal weighting matrices. Since the information of the amplitudes are not included in the polynomial expansion in $\mathbf{R}$, the approach can at best do equally well to the original approach by Moshavi where the polynomial expansion is in $\mathbf{A}^H\mathbf{R}\mathbf{A}$. Hence, the Moshavi approach imposes itself as a better solution in the limit. However, due to the fact that the expansion involves the amplitudes, the approach will be more sensitive to estimation error between the amplitudes and the amplitude estimates. Consider the case where strict power control is employed, i.e. $||A_k||^2 = 1$. Then, the term in the polynomial expansion will be approximated by

$$\hat{\mathbf{A}}^H\mathbf{R}\mathbf{A} \tag{4.3.29}$$

which may no longer be close to identity and therefore may not work that well using polynomial expansion. A pathwise approach with an expansion in $\mathbf{R}$, on the other hand, only uses the amplitudes to recombine for the final symbol estimate and will therefore avoid any propagation of the estimation error. Therefore, in the case where the amplitude estimates are unreliable, for example through very fast fading, it may still be advantageous to use an expansion in $\mathbf{R}$.

The above results suggest yet another paradigm shift. Notably, the obtained results suggest a distinction based on the amplitude knowledge available. In the case where amplitudes are available or reliable, respectively, it is advantageous to use this information and apply userwise polynomial expansion in the term $\mathbf{A}^H\mathbf{R}\mathbf{A}$, i.e. to use the approach of Moshavi. This approach allows to efficiently make use of all the available information while amplitude estimation can be made part of this approach. Consider a filter following the approach due to Moshavi where the filter for the symbol estimate is given by

$$\begin{aligned}
\hat{\mathbf{a}}[n] &= \mathbf{F}(q)\mathbf{x}[n] = \sum_{b=0}^{B} d_b \left(\mathbf{A}^H\mathbf{R}(q)\mathbf{A}\right)^b \mathbf{A}^H\mathbf{x}[n] \\
&= \left[d_0\mathbf{I} + d_1\mathbf{A}^H\left\{\mathbf{R}(q)\mathbf{A}\right\} + d_2\mathbf{A}^H\left\{\mathbf{R}(q)\mathbf{A}\mathbf{A}^H\mathbf{R}(q)\mathbf{A}\right\} + \ldots\right]\mathbf{A}^H\mathbf{x}[n]
\end{aligned}$$

clearly, at each term the spreading and despreading operation (essentially $\mathbf{R}(q)$) is followed by amplitude recombination. Therefore, we can combine those signals to obtain an amplitude estimate, i.e.

$$\widehat{\mathbf{A}\mathbf{a}}[n] = \sum_{i=0}^{B} d_i \left(\mathbf{R}(q)\mathbf{A}\mathbf{A}^H\right)^i \mathbf{x}[n]$$

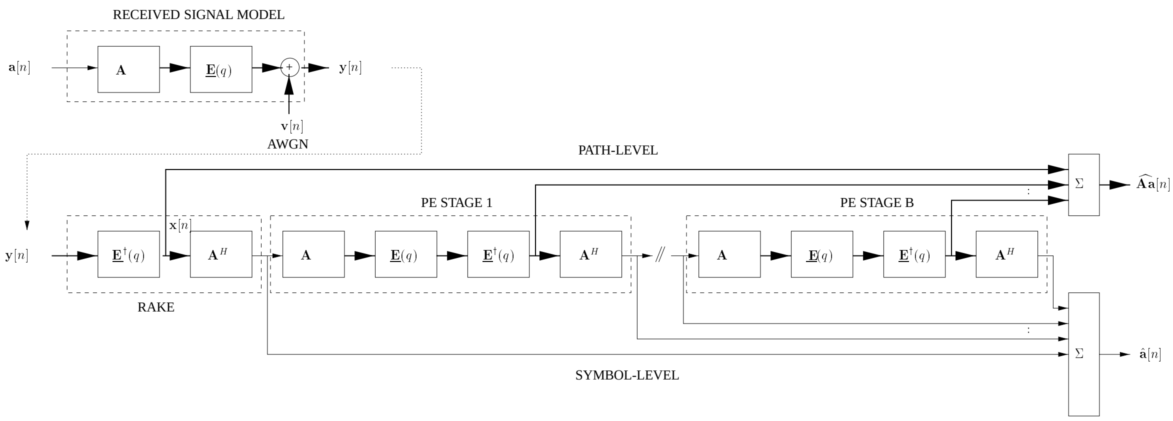

Figure 4.1: Amplitude and symbol estimation suggested by LS results when amplitude knowledge is reliable

This should allow us to obtain a polynomial receiver with minimum complexity in a large system, while also being able to estimate amplitudes. This proposition is shown in figure 4.1. From this we can easily see the fact that every PE stage after the RAKE is twice the complexity of the RAKE. Also, the structure shows how the symbol level signal is spread again to path level and despread back to symbol level in every PE stage.

In the case where the amplitudes are not available or cannot be estimated reliably (in fast fading, for example), we suggest to use pathwise polynomial expansion with the expansion being in $\mathbf{R}$, if possible together with differential modulation. Differential modulation modulates the data based on the phase difference to the last transmitted symbol. Consider

$$a_k[n] = b_k[n]a_k[n-1]$$

where we restrict b_k to $|b_k|^2 = 1$. To obtain the amplitude-data product estimate, we write the estimate as the true value plus some interference plus noise term:

$$\begin{aligned}\widehat{A_i a_k}[n] &= A_i a_k[n] + v_{i,k}[n] = b_k A_i a_k[n-1] + v_{i,k} \\ &= b_k \widehat{A_i a_k}[n-1] + v_{i,k}[n] - b_k v_{i,k}[n-1]\end{aligned}$$

Let us define

$$\mathbf{Z}_k = [\widehat{A_1 a_k}[n], \ldots, \widehat{A_M a_k}[n]]^T$$

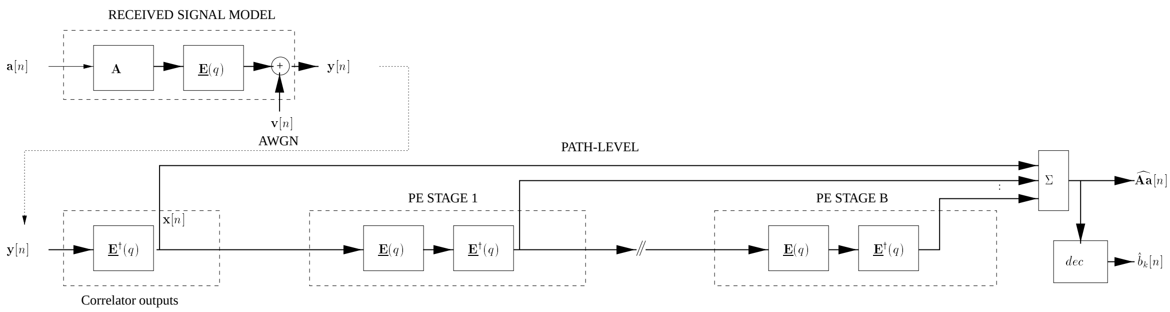

Figure 4.2: Symbol estimation employing differential modulation that requires no knowledge of fastly varying amplitudes

We can then solve for b_k by solving

$$\hat{b}_k[n] = \min_{b_k \in \text{ Alphabet}} ||\mathbf{Z}_k[n] - b_k \mathbf{Z}_k[n-1]||^2$$

If b_k is constant modulus, i.e. $b_k = e^{j\phi_k}$, the solution is given by estimating the angle ϕ_k such that

$$\phi_k^o = dec\{-\arg(\mathbf{Z}_k^H[n]\mathbf{Z}_k[n-1])\}$$

This can be seen as a kind of noisy maximum ratio combining. Note that this allows the recombination of the paths without knowledge of the fast parameters, i.e. the path amplitudes. This structure can be seen in figure 4.3.3.

4.4 Conclusions

In this chapter we derived analytical expressions for two polynomial expansion approaches under large system assumptions. Interestingly, it was found that there is no benefit, asymptotically, to use a scalar weighting per user or per path even under power imbalances between users and paths. Furthermore, it was shown that the asymptotically optimal solutions for the weighting coefficients are easy to compute, given the relevant eigenvalue moments. While the asymptotic analysis proves that there is no benefit in using weighting coefficients per path for large systems, the simulation results obtained in chapter 3 clearly showed the benefits obtained by introducing such coefficients. Basically, we attribute those evidently differing results to a number of factors. Firstly, the results of the asymptotic analysis are large system results which allow to introduce certain simplifications (through the averaging processes) which do not hold in finite dimensions and therefore, the results are approximative in nature for finite systems. As can be seen from the simulation results provided in chapter 3, the simulations we have shown were of small dimensions, typically with a spreading gain of only $L = 16$. Also, whereas we have run simulations using a truly asynchronous system, the analysis is based on a simplified, synchronous model (assuming no ISI, perfect pulse-shaped matched filtering and especially independent codes between paths, binary vs. Gaussian codes). Also, in a finite system, the power of any one user may be significant with respect to the total, finite power of all users. In an asymptotic system, on the other hand, it is essentially assumed that the power of any one user is asymptotically a vanishing fraction of the total power. While there are good indications that such a system may indeed be valid asymptotically (e.g. [77, 81, 82]), the formal proof is still an open issue at this point, in particular when moving away from chip synchronous to fully asynchronous models. In addition, the correlation function of the pulse shape employed impacts on the large system signal model and deviations from the large system results would be expected to increase with increasing deviation of the pulse shape frequency spectrum from an ideal low-pass filter. Another point which has been scarcely covered, is the impact of using periodic spreading codes as opposed to aperiodic ones in large system analysis. While, given the nature of large system analysis, it may be desirable to have aperiodic codes, in our simulations we have employed periodic codes throughout. While there are a substantial number of open issues, we do not see the asymptotic results as contradictory to what we have obtained in earlier chapters but instead it does provide an idea of what might be a good solution.

We have to distinguish between two aspects introduced, namely, the issue of using diagonal weighting matrices and the estimation of the amplitude data product, required for the amplitude estimation. From the results obtained in this chapter, the consequence is that for larger spreading gains, it is advantageous to implement the symbol estimate by using an approach involving the polynomial expansion in $\mathbf{A}^H\mathbf{R}(q)\mathbf{A}$. In this way, the receiver can make use of the maximum of information available (due to the inclusion of the amplitudes in the polynomial expansion) and therefore provide the best symbol estimate. However note, that in a situation of fast fading where the estimation of the amplitudes may become very unreliable or if no amplitude information is available, it may still be useful to consider a PE in $\mathbf{R}(q)$ only, together with differential modulation.

Considering the estimation of the amplitudes, we do require the pathwise outputs and this, indeed, remains the main point of a pathwise treatment. This will still allow us to estimate the amplitudes at an improved SINR, even in the case of applying the Moshavi approach, as was shown in the last section.

4.A Appendix: Asymptotic freeness of R and $\mathbf{A}\mathbf{A}^H$

We are interested in finding the limiting behaviour of the following expression:

$$\begin{aligned}\lim_{K\to\infty}\frac{1}{K}tr(\mathbf{A}^H\mathbf{R}\mathbf{A})^m &= \lim_{K\to\infty}\frac{1}{K}tr(\mathbf{R}\mathbf{A}\mathbf{A}^H)^m \\ &= \lim_{K\to\infty}\frac{1}{K}tr(\mathbf{S}\mathbf{A}\mathbf{A}^H\mathbf{S}^H)^m \qquad (4.A.1)\end{aligned}$$

Assume the general model as motivated in section 4.3, i.e.

$$\begin{aligned}\mathbf{S} &= [\mathbf{s}_{1,1}\ldots\mathbf{s}_{k,m}\ldots\mathbf{s}_{K,M}] \\ \mathbf{R} &= \mathbf{S}^H\mathbf{S} \qquad (4.A.2)\\ \mathbf{A} &= diag\{\mathbf{A}_1,\ldots,\mathbf{A}_K\} \qquad (4.A.3)\\ \mathbf{A}_k &= [A_{k,1}\ldots A_{k,M}]^T \qquad (4.A.4)\end{aligned}$$

and the spreading codes, $\mathbf{s}_k$ are normalised and and consist of i.i.d random elements such that $s_{k,l}\in\frac{1}{\sqrt{L}}\{+1,-1\}$. Note that $\mathbf{A}\mathbf{A}^H = diag(\mathbf{A}_1\mathbf{A}_1^H\ldots\mathbf{A}_K\mathbf{A}_K^H)$ is block diagonal in the multipath case and diagonal in the single path case.

In order to show that $\mathbf{R}$ and $\mathbf{A}\mathbf{A}^H$ are asymptotically free (Proposition 3) with respect to the trace operator, we introduce a number of definitions required from free probability theory.

Definition 5 (Non-commutative probability spaces and random variables)
[72]:if $\mathcal{A}$ is a unital algebra on the complex number field $\mathbb{C}$, and φ is a linear functional of $\mathcal{A}$ such that $\varphi(\mathbf{1}) = 1$, with $\mathbf{1}$ the unit element of $\mathcal{A}$, then the pair $(\mathcal{A},\varphi)$ is called a noncommutative probability space *and the elements of $\mathcal{A}$ are called noncommutative random variables (NCRV). The complex number $\varphi(a^n)$ is called the nth moment of $a\in\mathcal{A}$*

Definition 6 (Algebra properties)
*[72]: Consider the probability space of $n\times n$ matrices $(\mathcal{A}_n,\varphi_n)$ where $\mathcal{A}_n$ is a unital *-algebra (unit, product, sum, involution defined) and φ_n is the state/linear functional such that $\varphi_n(\mathbf{A}_n) = \frac{1}{n}E\left[tr(\mathbf{A}_n)\right]$, $\mathbf{A}_n\in\mathcal{A}_n$. If as $n\to\infty$, φ_n converges to φ, then the*

expectation is defined w.r.t. this probability measure. Sum and product are defined in the normal way for matrices, involution is defined by the Hermitian transpose and the unit is given by the identity matrix $\mathbf{I}_n$.

Definition 7

A $n \times n$ random matrix $\mathbf{A}_n$ is called unitarily invariant *if the probability measure of $\mathbf{A}_n$ as a random matrix/noncommutative random variable is the same as that of the matrix $\mathbf{V}_n\mathbf{A}_n\mathbf{V}_n^H$ for any unitary matrix $\mathbf{V}_n$*

Theorem 8

If the distribution of $\mathbf{A}_n$ is unitarily invariant, it admits the following eigenvalue decomposition $\mathbf{A}_n = \mathbf{U}_n\Lambda_n\mathbf{U}_n^H$, where $\mathbf{U}_n$ and Λ_n are independent.

Returning to the problem at hand, writing the trace of $\mathbf{R}$ using the eigendecomposition

$$tr(\mathbf{V}\mathbf{R}\mathbf{V}^H) = tr(\mathbf{V}\mathbf{U}\Lambda\mathbf{U}^H\mathbf{V}^H) = tr(\mathbf{Q}\Lambda\mathbf{Q}^H) \tag{4.A.5}$$

$$= \sum_{i=1}^{K} \lambda_i \tag{4.A.6}$$

$$\mathbf{Q} = \mathbf{V}\mathbf{U} \tag{4.A.7}$$

shows that $\mathbf{R}$ is unitarily invariant to any unitary $\mathbf{V}$ since the product of two unitary matrices, here $\mathbf{Q}$, is also unitary. Since $\mathbf{R}$ is hermitian, it is also self-adjoint and due to the fact that it is a random matrix, $\mathbf{U}$ and Λ are independent. Further note that the elements in $\mathbf{U}$ are asymptotically i.i.d., Haar distributed random variables [72].

Theorem 9 (Theorem for free random matrices)

[71, 72] Let

- *$\mathbf{A}_n(s)$ be an independent family of $n \times n$ Hermitian deterministic or random matrices, $s \in \mathcal{S}$ in some index set $\mathcal{S}$*
- *$\mathbf{A}_n(s)\mathbf{A}_n^H(s)$ admit a limit distribution compactly supported*
- *$\mathbf{B}_n(t) = \mathbf{U}(t)\mathbf{B}'_n(t)\mathbf{U}_n(t)^H$ with $\mathbf{U}_n(t)$ independent on $\mathbf{A}_n(s)$ and $\mathbf{B}'_n(t)$ with eigenvalues $\lambda_1(n,t), \ldots, \lambda_n(n,t)$ such that*
    - *$\sup_n \max_i \lambda_i(n,t) < \infty \; \forall \, t \in \mathcal{T}$ where $\mathcal{T}$ is some index set*

– *and* $(\mathbf{B}_n(t), \mathbf{B}_n(t))_{t\in\mathcal{T}}$ *has a limit distribution*

Then as $n \to \infty$, *the family* $\left(\{\mathbf{A}_n(s)\}_{s\in\mathcal{S}}, \{\mathbf{B}_n(t), \mathbf{B}_n^H(t)\}_{t\in\mathcal{T}}\right)$ *is asymptotically free.*

If we let $(\mathbf{A}\mathbf{A}^H)^{1/2} = \mathbf{A}_n$, $\mathbf{R} = \mathbf{B}_n$, $\mathbf{U} = \mathbf{U}_n$ and $\Lambda = \mathbf{B}'_n$ we can see that hence $\mathbf{R}$ and $\mathbf{A}\mathbf{A}^H$ are asymptotically free.

4.B Appendix: Computation of NCRV moments

Having established that $\mathbf{R}$ and $\mathbf{A}\mathbf{A}^H$ are asymptotically NCRVs, we are now interested in finding the moments.

Definition 10 (Definition of freeness)
[72] Let $(\mathcal{A}, \varphi)$ *be a noncommutative probability space and let* $\mathcal{A}_i$ *be subalgebras of* $\mathcal{A}$ $(i \in I)$. *We say that the family* $(A_i)_{i\in I}$ *is in* free relation *(or* free*) with respect to* φ *if, for every* $n \in \mathbb{N}$ *and* $i(1), \ldots, i(n) \in I$ *such that* $i(k) \neq i(k+1) (1 \leq k \leq n-1)$,

$$\varphi(a_1 a_2 \ldots a_n) = 0 \text{ if and only if } a_k \in \mathcal{A}_{i(k)},\ \varphi(a_k) = 0,\ 1 \leq k \leq n \tag{4.B.1}$$

This basically means that every $\varphi(a_k) = 0$ for all elements and that neighbouring ncrv's from the same subalgebra are not allowed to have consecutive indices. e.g. $\varphi(a_1 a_3) = 0$ where $\varphi(a_1) = \varphi(a_3) = 0$ but $\varphi(a_1 a_2) \neq 0$ because the two neighbours have consecutive indices even though $\varphi(a_1) = \varphi(a_3) = 0$

Theorem 11 (Moments of NCRVs)
[72,83] For free noncommutative random variables $a_1, \ldots, a_n$ *the following holds:*

$$\varphi\left[(a_1 - \varphi(a_1)\mathbf{1})\,(a_2 - \varphi(a_2)\mathbf{1}) \ldots (a_n - \varphi(a_n)\mathbf{1})\right] = 0 \tag{4.B.2}$$

which allows the computation of the moments.

As an example how this can be solved, here is an example from [83]. Let $\mathcal{B}, \mathcal{C} \in \mathcal{A}$ be two free subalgebras and $b \in \mathcal{B}$ and $c \in \mathcal{C}$ then we can write $b = b' + \overline{b}$ where ç$\overline{b} = \varphi(b)\mathbf{1}$, so that $\varphi(b') = 0$. Similarly we have $c = c' + \overline{c}$. Using the definition of freeness, we see that

$\varphi(b'c') = 0$, thus

$$\begin{aligned}\varphi(bc) &= \varphi\left[(b' + \overline{b})(c' + \overline{c})\right] \\ &= \varphi\left[b'c' + b'\overline{c} + \overline{b}c' + \overline{b}\overline{c}\right] \\ &= \varphi(b)\varphi(c) \end{aligned} \tag{4.B.3}$$

where we have used $\varphi(\overline{b}c') = \varphi(\varphi(b)\mathbf{1}.c') = \varphi(b)\varphi(c') = 0$ and similarly for $\varphi(b'\overline{c}) = 0$.

Definition 12 (moments of a product of two ncrvs)
Given the free random variables $a = a' + \overline{a}$ and $b = b' + \overline{b}$ we can compute the moments of their product by:

$$\varphi\left[(ab)^m\right] = \varphi(a)\varphi(b)\varphi\left[(ab)^{m-1}\right] + \varphi\left[a'b'(ab)^{m-1}\right] + \varphi(a)\varphi\left[b'(ab)^{m-1}\right] + \varphi(b)\varphi\left[a'(ab)^{m-1}\right]$$

using this, e.g. the second moment is given by:

$$\varphi\left[(ab)^2\right] = \varphi^2(a)\varphi^2(b) + \varphi^2(a)\varphi(b^2) + \varphi(a^2)\varphi^2(b) \tag{4.B.4}$$

The direct application of this formula gives the result in equation (4.2.36)

Conclusions

In chapter 2 we have established the concept of user-wise distortionless pathwise interference cancellation which is independent of the fastly varying complex amplitude coefficients. This could be achieved through the separation of the received signal into fastly and slowly varying components. Furthermore, we have alleviated the problem of signal cancellation that occurs in the original pathwise approach when there is strong correlation between the amplitudes of different paths of the same user. The advantage of the approaches introduced is the relaxed adaptation requirements due to the filter's independence from the fastly varying coefficients. This allows the scarce training data to be used in the estimation of the fastly varying parameters while the whole signal can be used to estimate the slowly varying parameters over a much larger interval. Since the interference cancellation takes place between paths, the signal thus obtained contains the desired parameters at an improved SINR compared to the received signal and hence allows improved channel estimation. However, the approaches of chapter 2 are computationally costly to implement and we have therefore considered pathwise polynomial expansion as a low complexity approach in chapter 3. Polynomial expansion allows the approximation of the computationally intensive matrix inverse required by both the LMMSE receiver and the decorrelator by expanding the matrix inverse as a polynomial. However, for polynomial expansion to work, weighting coefficients need to be introduced. We have shown, that giving each signal component a scalar weighting factor allows for improved interference cancellation and therefore improved parameter estimation. Also, we have shown that the extension to spatio-temporal processing is straightforward. Furthermore, we have also introduced new polynomial expansion approaches which work at symbol level and provide more degrees of freedom by still allowing a scalar coefficient per signal component. Unfortunately, it is very difficult to characterise the performance behaviour of a polynomial expansion receiver analytically using standard techniques, not least due to the fact that the output SINR is a function of the particular set of spreading codes, delays and amplitudes used. We have therefore resorted to what is known as large system analysis in chapter 4. This method lets the dimensions of the system grow to infinity and assumes the spreading codes to be made up of i.i.d. random variables. The resulting SINR, involving large random matrices, can then be simplified based on the fact that the empirical eigenvalue distributions of certain classes of asymptotically infinite matrices converge to a deterministic distribution. Interestingly, it was found that there is no benefit asymptotically in using a weighting coefficient per multipath component or per user, even under power imbalances. Furthermore, it was shown that the asymptotically optimal solution for the weighting coefficients can be found easily, given the relevant moments of the eigenvalues of the large random matrices. While the asymptotic analysis proves that there is no benefit attained by the introduction of weighting coefficients per signal component, the simulations in the preceding chapter have clearly shown that performance can be improved by increasing the number of coefficients. We attribute this discrepancy to a number of open issues which remain in the large system analysis. Notably, the asymptotic analysis is by its very nature only approximate for finite systems. Since the simulations presented are all with relatively low spreading factor, a certain amount of disagreement between the results can be expected. Furthermore, the simulations have been run using a truly asynchronous system whereas the large system analysis is based on a simplified, symbol-synchronous system. While there are good indications that such a system may asymptotically hold for the asynchronous model, the formal proof at this point in time is still an open issue. Also, the correlation function of the pulse-shaping filter is of importance in the large system signal model and deviations from the large system results would be expected with increasing deviation of the pulse shape frequency spectrum from and ideal low-pass filter. Finally, the impact of using periodic spreading codes versus aperiodic ones in large system analysis remains unclear. It is, however, important to distinguish between two aspects of polynomial expansion receivers introduced in this document, the issue of using diagonal weighting matrices and the estimation of the amplitude data product, respectively. In consequence of the results obtained from the large system analysis, it is advantageous to estimate the symbols from an approach following the original polynomial expansion receiver, that is, to use a polynomial expansion involving the amplitudes. Due to the extra amplitude information which such an approach utilises, any approach which does not make use of this information can only perform worse. It is worth mentioning, however, that in the case where amplitude estimates are very unreliable due to very fast fading, the application of purely pathwise polynomial expansion may still be advantageous, particularily in conjunction with differential modulation. Considering the issue of amplitude estimation, we continue to require the pathwise outputs and this, indeed, remains the main point of a pathwise treatment. It is shown that even using an approach providing symbol outputs, it is still possible to obtain pathwise signals and combine pathwise with symbolwise polynomial expansion in order to profit from the benefits of both approaches.

Bibliography

[1] Raymond Steele. *Mobile Radio Communications*. Pentech Press Limited, 1992.

[2] Flavio Muratore. *UMTS Mobile Communications for the Future*. John Wiley and Sons, Inc., 2001.

[3] R. Prasad, W. Mohr, and W.Konhauser. *Third Generation Mobile Communication Systems*. Artech House, 2000.

[4] T.S. Rappaport. *Wireless Communications - Principles and Practice*. Prentice Hall, 1996.

[5] K.S. Gillhausen et al. On the Capacity of a Cellular CDMA System. *IEEE Trans. on Vehicular Tech.*, 40(2), May 1991.

[6] Editor Francis Swarts. *CDMA techniques for Third Generation Mobile Systems*. Kluwer Academic Publishers, 1999.

[7] J.G. Proakis. *Digital Communications*. McGraw-Hill, Inc., 3 edition, 1995.

[8] B. Sklar. *Digital Communications - Fundamentals and Applications*. Prentice Hall, 1988.

[9] R. Prasad and T. Ojanpera. An Overview of CDMA Evolution toward Wideband CDMA. *IEEE Communications Surveys*, 1998.

[10] R.L. Peterson, R.E. Ziemer, and D.E. Borth. *Introduction to Spread Spectrum*. Prentice Hall, 1995.

[11] A. Viterbi. *CDMA: Principles of Spread Spectrum Communications*. Addison-Wesley, 1995.

[12] K. Feher. *Wireless digital communications: Modulation and Spread Spectrum Applications*. Prentice Hall, 1995.

[13] H.V. Poor. Signal detection in multiple access channels. *US Army Research Office Proposal*, 1980.

[14] R. Lupas and S. Verdu. Optimum near-far resistance of linear detectors for code division multiple access channels. In *Proc. IEEE Int. Symposium on Information Theory*, Kobe, Japan, June 1988.

[15] R. Lupas and S. Verdu. Near-Far Resistance of Multiuser Detectors in Asynchronous Channels. *IEEE Trans. Information Theory*, 35, Jan 1989.

[16] S. Verdu. Minimum probability of error for asynchronous multiple access comuunuication systems. In *Proc. IEEE MILCOM Conf*, Washington D.C., USA, Nov 1983.

[17] S. Verdu. Optimum sequence detection of asynchronous multiple-access communications. In *Proc. IEEE Int. Symposium on Information Theory*, St. Jovite, Canada, Sep 1983.

[18] S. Verdu. Maximum Likelihood Sequence Detection for Intersymbol Interference Channels: A New Upper Bound on Error Probability. *IEEE Trans. on Information Theory*, 33, Jan 1987.

[19] U. Madhow and M.L. Honig. MMSE Interference Suppression for Direct Sequence Spread Spectrum CDMA. *IEEE Trans. on Communications*, Dec 1994.

[20] D.S. Chen and S. Roy. An adaptive Multiuser Receiver for CDMA systems. *IEEE Journal on Selected Areas of Communications*, 12, 1994.

[21] A. Duel-Hallen, J. Holtzman, and Z. Zvonar. Multiuser Detection for CDMA Systems. *IEEE Personal Communications*, pages 46–58, April 1995.

[22] S. Moshavi. Multi-User Dectection for DS-CDMA Communications. *IEEE Communications Magazine*, pages 124–136, Oct. 1996.

[23] M. Honig and M.K. Tsatsanis. Multiuser CDMA Receivers. *IEEE Signal Processing Magazine*, May 2000.

[24] A. Duel-Hallen. Decorrelating Decision-Feedback Multiuser Detector for Synchronous Code-Division Multiple Access. *IEEE Trans. on Communications*, 41, Feb 1993.

[25] M.K. Varanasi and B. Aazhang. Multistage Detection in Asynchronous Code Division Multiple Access Communications. *IEEE Trans. on Communications*, 38, Apr 1990.

[26] M.K. Varanasi and B. Aazhang. Near Optimum Detection in Synchronous Code Division Multiple Access Systems. *IEEE Trans. on Communications*, 39, May 1991.

[27] B. Sklar. Rayleigh Fading Channels in Mobile Communications, Part I/II. *IEEE Comm. Magazine*, 16, 1997.

[28] Y. Okumura, E. Ohmori, and K. Fukuda. Field Strength and its Variability in VHF and UHF Land Mobile Radio Service. *Rev. Elec. Commun. Lab*, 16, 1968.

[29] M. Hata. Empirical Formulae for Propagation Loss in land Mobile Radio Services. *IEEE Trans. Vehic. Tech.*, 29, 1980.

[30] H. Suzuki. A Statistical Model for Urban Radio Propagation. *IEEE Trans. on Communications*, 25, July 1977.

[31] G.L. Turin et al. A Statistical Model of Urban Multipath Propagation. *IEEE Trans. Vehic. Tech.*, Feb 1972.

[32] P.A. Bello. Characterization of Randomly Time-Variant Linear Channels. *IEEE Trans. Commun. Sys.*, 11, Dec 1963.

[33] G. L. Stüber. *Principles of Mobile Communication*. Kluwer Academic Publishers, 1996.

[34] P. Van Rooyen, M. Lötter, and D. Van Wyk. *Space-Time Processing for CDMA Mobile Communication*. Kluwer Academic Publishers, 2000.

[35] William C. Jakes. *Microwave Mobile Communications*. IEEE Press, 1974.

[36] Spyros J. Papantoniou. *Modelling the Mobile-Radio Channel*. PhD thesis, Swiss Federal Institute of Technology Zurich, 1989.

[37] A. Duel-Hallen, S. Hu, and H. Hallen. Long-Range Prediction of Fading Signals. *IEEE Sig. Proc. Mag.*, May 2000.

[38] P. Hoeher. A Statistical Discrete-Time Model for the WSSUS Multipath Channel. *IEEE Trans. Vehic. Tech.*, 41(4), Nov 1992.

[39] T.S. Rappaport, S.Y. Seidel, and K. Takamizawa. Statistical Channel Impulse Response Models for Factory and Open Plan Building Radio Communication System Design. *IEEE Trans. on Communications*, 39, May 1991.

[40] Matti Latva-aho. *Advanced Receivers for Wideband CDMA Systems*. PhD thesis, Oulu University, Finland, September 1998.

[41] Matti Latva-aho and Markus Juntti. LMMSE Detection for DS-CDMA Systems in Fading Channels. In *IEEE Trans. Commun.*, February 2000.

[42] Matti Latva-aho, Markus Juntti, and Kimmo Kansanen. LMMSE Receivers for DS-CDMA Systems in Frequency-Selective Channels. In *FRAMES Workshop*, January 1999.

[43] M. Latva-aho and M.J. Juntti. LMMSE Detection for DS-CDMA Systems in Fading Channels. *IEEE Trans. Communications*, 48(2), February 2000.

[44] M.J. Juntti and M. Latva-aho. Bit-Error Probability Analysis of Linear Receivers for CDMA Systems in Frequency-Selective Fading Channels. *IEEE Trans. Communications*, 47(12), December 1999.

[45] Matti Latva-aho, Markus Juntti, and Ian Oppermann. Reconfigurable Adaptive RAKE Receiver for Wideband CDMA Systems. In *Proc. IEEE Vehicular Technology Conference*, May 1998.

[46] C. Fischer and D.T.M. Slock. Userwise Distortionless Pathwise Interference Cancellation for the DS-CDMA Uplink. In *Proc. PIMRC 2000 Conf*, London, UK, September 2000.

[47] Ralf R. Mueller. Polynomial expansion equalizers for communication via large antenna arrays. In *Proc. EPMCC 2001*, Vienna, February 2001.

[48] C. Boulanger. Simplified multistage linear DS-CDMA receivers. In *Electronics Letters*, April 1999.

[49] W. Xiao and M.L. Honig. Convergence analysis of adaptive full-rank and multi-stage reduced-rank interference suppression. In *Proc. CISS 2000*, Princeton, NJ, March 2000.

[50] M.L. Honig and W. Xiao. Large system performance of reduced-rank linear filters. In *Proc. Allerton Conf. on Commun., Control, and Computing*, Monticello, IL, September 1999.

[51] S.Moshavi, E.G.Kanterakis, and D.L.Schilling. Multistage Linear Receivers for DS-CDMA Systems. *Int. Journal of Wireless Information Networks*, 3(1), March 1996.

[52] M.L. Honig and W. Xiao. Performance of reduced-rank linear interference suppression for DS-CDMA. *IEEE Trans. Inform. Theory*, 47, Jul 2001.

[53] J.S. Goldstein, I.S. Reed, and L.L Scharf. A Multistage Representation of the Wiener Filter Based on Orthogonal Projections. *IEEE Trans. Inform. Theory*, 44(7), November 1998.

[54] L. L. Scharf. *Statistical Signal Processing - Detection, Estimation, and Time Series Analysis*. Addison-Wesley Publishing, 1991.

[55] S.M. Kay. *Fundamentals of Statistical Signal Processing Estimation Theory*. Prentice-Hall, Englewood Cliffs, NJ, 1993.

[56] R. A. Horn and C. R. Johnson. *Matrix Analysis*. Cambridge University Press, 1985.

[57] D.R. Brown, M. Motani, V.V. Veeravalli, H.V. Poor, and C.R. Johnson. On the Performance of Linear Parallel Interference Cancellation. *IEEE Trans. Inform. Theory*, 47(5), July 2001.

[58] C. Boulanger, L. Ouvry, and M. Bouvier des Noes. Multistage linear DS-CDMA receivers. In *Proc. IEEE Symp. Spread Spectrum Tech. and Appl.*, 1998.

[59] W. Chen, U. Mitra, and P. Schiter. Reduced Rank Detection Schemes for DS-CDMA Communication Systems. *submitted to IEEE Trans. Inform. Theory*, 2001.

[60] M.L. Honig and J. S. Goldstein. Adaptive Reduced-Rank Interference Suppression Based on the Multistage Wiener Filter. *submitted to IEEE Trans. Communications*, 2000.

[61] G. Bottomley, T. Ottoson, and Y.P.E. Wang. A Generalized RAKE Receiver for Interference Suppression. *IEEE Journal Seleted Areas on Communications*, 18, Aug 2000.

[62] M. Lenardi and D.T.M. Slock. SINR Maximizing Equalizer Receiver for DS-CDMA. In *Proc. EUSIPCO 2000*, Tampere, Finland, Sep 2000.

[63] C. Fischer and D.T.M. Slock. Pathwise Polynomial Interference Cancellation for DS-CDMA. In *Proc. ASILOMAR 01 Conf.*, Nov 2001.

[64] C. Fischer and D.T.M. Slock. Multistage DS-CDMA Receivers with Pathwise Interference Mitigation. In *Proc. Int. Zurich Seminar*, Feb 2002.

[65] L. Arnold. On the Asymptotic Distribution of the Eigenvalues of Random Matrices. *Journal of Mathematical Analysis and Applications*, 20, 1967.

[66] R. Wegmann. The Asymptotic Eigenvalue-Distribution for a Certain Class of Random Matrices. *Journal of Mathematical Analysis and Applications*, 56, 1976.

[67] D. Jonsson. Some Limit Theorems for the Eigenvalues of a Sample Covariance Matrix. *Journal of Multivariate Analysis*, 12, 1982.

[68] J. W. Silverstein and Z.D. Bai. On the Empirical Distribution of Eigenvalues of a Class of Large Dimensional Random Matrices. *Journal of Multivariate Analysis*, 54, 1995.

[69] J. W. Silverstein and S. Choi. Analysis of the limiting spectral distribution of Large Dimensional Random Matrices. *Journal of Multivariate Analysis*, 54, 1995.

[70] V.L. Girko. *Theory of Random Determinants*. Kluwer Academic Publishers, 1990.

[71] D. V. Voiculescu. *Free Probability Theory*. American Mathematical Society, 1997.

[72] F. Hiai and D. Petz. *The Semicircle Law, Free Random Variables and Entropy*. American Mathematical Society, 2000.

[73] J. W. Silverstein and P. L. Combettes. Large dimensional Random Matrix Theory for Signal Detection and Estimation in Array Processing. In *Proc. SSAP*, 1992.

[74] J. W. Silverstein and P. L. Combettes. Signal detection via Spectral Theory of large dimensional Random Matrices. *IEEE Trans. Sig. Proc*, 40, Aug 1992.

[75] D. N. C. Tse and S. V. Hanly. Linear Multiuser Receivers: Effective Interference, Effective Bandwidth and User Capacity. *IEEE Trans. Inf. Theory*, 45, Mar 1999.

[76] M. Debbah, W. Hachem, P. Loubaton, and M. de Courville. MMSE Analysis of Certain Large Isometric Random Precoded System. In *Proc. IEEE Inf. Th. Workshop*, 2001.

[77] J. Evans and D. N. C. Tse. Large System Performance of Linear Multiuser Receivers in Multipath Fading Channels. *IEEE Trans. Inf. Theory*, 46, Sep 2000.

[78] Kiran and D. N. C. Tse. Effective Interference and Effective Bandwidth of Linear Multiuser Receivers in Asynchronous CDMA Systems. *IEEE Trans. Inf. Theory*, 46, Jul 2000.

[79] R. R. Muller and P. Schramm. Spectral Efficiency of CDMA systems with linear MMSE interference suppression. *IEEE Trans. Communications*, 47, May 1999.

[80] R. R. Muller and S. Verdu. Design and Analysis of low-complexity Interference Mitigation on Vector Channels. *IEEE Journal Selected Areas in Communications*, 19, Aug 2001.

[81] A. Mantravadi and V.V. Veeravalli. Asynptotic Analysis of MMSE detection in asynchronous CDMA systems: an equivalence result. In *Proc. Int. Symp. Inf. Theory*, 2001.

[82] A. Mantravadi and V.V. Veeravalli. MMSE detection in asynchronous CDMA systems: An equivalence result. *submitted to IEEE Trans. Inf. Theory*, 2001.

[83] P. Baine. Free Probability for Probabilists. In *http://www.dma.ens.fr/˜biane/articles/biane-QPC-Grenoble.ps*, École Normale Supérieure, Paris, France, 2001.